THE DIURNAL CYCLE OF CLOUD COVER OVER SOUTHERN AND CENTRAL AFRICA

by

LISA JANE COOP

CPXLIS001

A dissertation submitted to the Faculty of Science, University of Cape Town, in fulfilment of the requirements for the degree of **Masters of Science in Environmental and Geographical Science** through the Department of Environmental and Geographical Science.

February 2008

Supervisors: Prof. Bruce Hewitson, Department of Environmental and Geographical Science, UCT

Dr. Mark Tadross, Department of Environmental and Geographical Science, UCT

ABSTRACT

The current understanding of the temporal and spatial distribution of clouds over southern and central Africa is poor and the regional processes governing cloud occurrence is only weakly understood. This study seeks to improve the current understanding of cloud diurnal variability over this region by providing a base-line diurnal climatology of low-level, mid-level and high-level cloud cover. Diurnal variations of cloudiness are examined using ten years of cloud data from latest version of the International Satellite Cloud Climatology Project (ISCCP-D1). The broad seasonal average diurnal variability is explored across the region. Thereafter a more detailed analysis of regionally specific variability is made using a Self-Organising Map.

The findings of this study are in broad agreement with previous work. Cloud over the southern and central African region shows clear spatial organisation, most significantly associated with the location of the Intertropical Convergence Zone. The diurnal variation of high-level cloud is large, closely correlated to its mean and is enhanced by orographic features. Minimum high-level cloud occurs at 1100 LST and maximum extent is reached during the evening around 1800 LST, except in locations experiencing deep convection which displayed a redevelopment of cloud in the early morning (0300 LST). This redevelopment of HLCA is hypothesised to be due to the destabilization of the upper troposphere through nighttime cloud radiative cooling. Mid-level cloud exhibits smaller diurnal variations, reaching maximum coverage at approximately 0300 LST. Clouds at this level are severely obscured by higher clouds and therefore the detected diurnal variation is due to both real and artificial signals and care needs to be taken in interpreting the results. Low-level cloud shows strong diurnal variations when not obscured by higher clouds, reaching a maximum just after midday.

The results of this study are interpreted in terms of the life-cycle of deep convective cloudiness. A number of mechanisms are suggested to explain the regional differences in diurnal variations with land surface heating being the primary mechanism.

This present-day diurnal large-scale cloud climatology is valuable in that it provides a base upon which higher resolution studies can be founded, as well as assisting in the validation of climate simulations.

ACKNOWLEDGEMENTS

I have benefited from the help of many people over this period of research. I would like to thank my two supervisors, Bruce Hewitson and Mark Tadross, for their advice, guidance and assistance. I would also like to thank my colleagues in the Climate Systems Analysis Group. In particular I would like to thank Chris Jack, Jeremy Main and Sepo Hachigonta for assisting me with my many computer programming problems.

I am very obliged to the University of Cape Town International Office and the Norwegian Centre for International Cooperation in Higher Education for giving me the opportunity to spend a semester attending the University of Bergen, Norway on a Masters Student Exchange Programme.

I would like to acknowledge and thank my family for their continued love and support. I would specifically like to thank my dad for his support, encouragement and persistent motivation and for his unwavering belief in me, especially in the last few months before submission.

Dad, this thesis is dedicated to you.

LIST OF FIGURES

TABLE OF CONTENTS

CHAPTER 1

INTRODUCTION

This thesis investigates the diurnal cycle of cloud cover over southern and central Africa. Cloud is a critical component of the climate system, with special impact on the energy balance. However, current understanding of the temporal and spatial distribution is poor, the regional processes governing cloud occurrence is weakly understood, and this lack of climatological baseline knowledge limits the development of climate models.

The diurnal cycle is a key periodicity found in a number of important climatic variables and plays a crucial role in governing the radiative budget. Thus the aim of this study is to improve the current understanding of cloud cover over southern and central African by focussing on the diurnal variation of these clouds.

The thesis first characterises the broad spatial differences found in seasonal mean diurnal variations of high-level, mid-level and low-level cloud cover. It then investigates the regionally averaged diurnal life-cycle of each of these cloud levels. The results are interpreted in terms of convective processes and the principal mechanisms responsible for the diurnal variability of continental cloud cover.

The southern and central African region represents a significant landmass extending from 10° north to 34° south and is therefore influenced by tropical, subtropical and mid-latitude circulation systems. The region is characterised by differing climatic zones due largely to topography and latitudinal location. The Inter-tropical Convergence Zone (ITCZ) migrates latitudinally with the seasons and is broadly responsible for the strong seasonality of rainfall and convective cloud cover over the study area.

Clouds are extremely complex three-dimensional atmospheric features. They occur over a wide range of horizontal, vertical and temporal scales. At the macrophysics scale, the

annual and diurnal cycles of clouds are very strong, especially over low-latitude continental locations like southern and central Africa. Clouds further play a vital role in the hydrological cycle, acting both as a source and sink of water vapour. They are closely tied to atmospheric convection, precipitation and latent energy release (Stephens, 2005). Cloud cover strongly influences both the short-wave radiation from the sun and the long-wave radiation from the Earth's surface and atmosphere. This radiative effect of clouds influences the distribution of surface and atmospheric heating, thereby both driving and responding to atmospheric motion. Clouds are also involved in a number of important feedback loops within the climate system, including the water vapour, ice-albedo and cloud-surface temperature feedbacks.

In the energy balance at the top of the atmosphere, clouds have a net cooling effect when averaged over the globe. However this effect is highly variable depending on location, height, type and optical properties of the cloud. Any future change in the climate has the potential to alter the character, distribution and frequency of cloudiness, thereby changing the net radiative effect of clouds. The strong radiative effect of clouds also has the potential to modulate and drive future regional change in the climate.

For these reasons, it is important to establish a baseline understanding of the regional cloud climatology. Moreover, as climate change becomes more evident, a present-day climatology becomes even more critical to understand and detect change, as well as assessing model simulations of the regional climate. Climate models are able to provide credible simulation of the large-scale distribution of primary climate variables such as temperature and pressure. However the parameterisation of clouds, convection and precipitation, and the representation of the interactions between the land-surface and these hydrologic processes present significant outstanding problems (Gates et al., 1999). Traditionally, models are evaluated by comparing the output of General Circulation Models (GCMs) against that of observed mean fields at monthly, seasonal, and annual timescales. However, there is an apparent limitation to this approach since it is possible for GCMs to produce realistic climate states for the wrong reasons (Lin et al., 2000).

As mentioned above, the diurnal cycle represents a key mode of externally forced, periodic variability in the climate system (Slingo et al., 2004). A number of important variables, including cloud cover and other related variables such as surface temperature, convection, precipitation and water vapour, all show strong variability at this periodicity. The large amplitude, coherent phase and short time scale of the diurnal cycle makes it an excellent test-bed for the evaluation of climate model physics (Dai and Trenberth, 2004). This periodicity also allows the model to be tested on a timescale much closer to that of many important atmospheric physical processes (Slingo et al., 2004).

The diurnal cycle of cloud cover has been the focus of numerous global and large-scale studies. These studies identified clear differences in the diurnal variation of cloud cover over oceans versus continental locations, as well as over convective and non convective location (Konragunta and Grubbber, 1994, 1996). Low-, mid- and high-level clouds have been found to exhibit clear differences in the amplitude and phase of their diurnal variations (Cairns, 1995). The diurnal variation of these different cloud types has been shown to be closely linked to different climatological variables which also exhibit clear diurnal variations (Bergen and Salby (1996).

Smaller regional-scale studies, making use of higher-resolution data, have shown that the diurnal variation of cloudiness is influenced by orographic features. Also, the mesoscale circulation associated with complicated topography can significantly alter the diurnal variations. Coastal regions and large inland water bodies also appear to have an impact on the diurnal cycle of cloud cover. The studies by Ba and Nicholson (1998) and Desbois et al. (1989) showed that the complicated topography associated with the Lake Victoria region induced strong local circulation which influenced the amplitude and phase of the diurnal cycle of clouds.

The Central American region has been the focus of significant research into clouds, convection and precipitation and has benefited from the availability of a numerous complementary data sources. The diurnal cycle over this region is therefore quite well studied and understood in relation to the underlying convective process and other climatic

variables (Meisner and Arkin, 1987; Garreaud and Wallace, 1997; Soden, 2000; Machado et al., 2002; Wylie and Woolf, 2002; Rickenbach, 2004) In contrast with the central American region, southern and central Africa have not benefited from scope and magnitude of these types of collaborative programmes.

The African continent has been included in a number of global studies which have shown strong diurnal variations evident over this continent. However, these studies have been relatively coarse and only a few have focussed specifically on the diurnal variation of cloud cover over this particular region (Desbois et al., 1989; Ba and Nicholson, 1998; Chung et al., 2007). Of these, the majority focussed on mesoscale convective complexes over Central and West Africa (Martin and Schreiner, 1981; Machado et al., 1992; Laing and Fritsch, 1993; Hodges and Thorncroft, 1997; Laing et al., 1999).

There is a growing body of literature on the diurnal variations of other related climatic variables over the African region. These include: precipitation (Geerts and Dejene, 2005), Upper-tropospheric humidity (Chung et al.,2007) and outgoing longwave radiation (Comer et al.,2007) which are all strongly linked to cloud cover and provide valuable supplementary data.

It is clear that clouds are a key component of the climate and that their diurnal variations play an important role in modulating the energy balance and hydrological cycle of the earth. Although there is a significant body of literature in this field, there are still gaps and weaknesses in our knowledge, especially that which is concerned with the southern and central African region.

These gaps and weaknesses include factors such as that the majority of base-line climatologies compiled for this region were created in the 1990's and were based on outdated cloud datasets such as the ISCCP-C series. Further, these large-scale climatologies provided only a few descriptive of the diurnal cycle, such as amplitude and phase and made little or no attempt to describe the more subtle rates of cloud growth and decay or sub-diurnal variation.

Also, the large climatological datasets provide sufficient spatial and temporal resolution to determine cloud diurnal climatologies at subcontinent or even regional scales but were not often use for this purpose. These datasets may therefore be able to detect the more subtle variations due to orographic and breeze-type circulations.

1.1. Objectives of the Study

In light of the discussion above, the core objectives of the thesis can be summarised as:

- To create a base-line cloud diurnal-cycle climatology using the most recent and appropriate data available for the southern and central African region. This climatology could provide a qualitative assessment of the spatial variability of clouds at each of the three vertical levels. Moreover, this climatology would allow the diurnal cycle to be revealed, separated from the strong seasonal variation due to the migration of the Inter-tropical Convergence Zone across the region. Finally, it may uncover more subtle influences arising from orographic and breeze-type circulation on the diurnal cycle of cloud cover.

- To provide a more detailed regional analysis of the diurnal cycle of cloud cover. These more detailed studies would be able to resolve the rate of cloud growth and decay within each of the vertical levels, highlight any sub-diurnal variability in the cloud cover and would suggest how clouds at each of the levels may interact. This regional-scale study would also be able to identify slight differences in the amplitude or phase of the diurnal cloud variation over different location. These results could then be interpreted in terms of differing convective processes or underlying driving mechanisms.

- This latter objective requires the study area to be subdivided into smaller regions. The study makes user of a Self-Organising Map (SOM) to separate the study areas into non-discrete regions according to the similarity of each location's cloud

climatologies. Therefore a secondary objective of the study is to test the skill and suitability of this regionalisation methodology.

- The final objective is to explain the seasonal and regional differences in the diurnal variation in terms of convective processes and differing underlying forcing-mechanisms. A related objective is to determine the validity of the cloud results by attempting to separate the true diurnal signal from the signals introduced by changing levels of obscuration, misdetection, or misclassification of cloud levels.

This chapter provides an introduction to the thesis topic and lists the main objectives. The following chapter offers further background information and a review of the available literature whilst Chapter 3 describes the data and the ISCCP project from which they were taken. The different methods used to analyze the data are also presented in chapter 3, whilst Chapter 4 presents the results from the large-scale analysis of cloud variability. Chapter 5 presents the results from the regionalization procedure as well as the cloud diurnal cycle results obtained for each of the specific geographic regions Chapter 6, the final chapter, discusses the results, the limitations of the present study and further potentially fruitful avenues of investigation.

CHAPTER 2

LITERATURE REVIEW

This chapter reviews the literature pertinent to this thesis. It first provides a brief overview of the physical setting and climate of the study area which both play leading roles in modulating the diurnal variation of cloud cover. It then discusses the role of clouds in the climate system, specifically their effect on the earth's radiative balance and hydrological cycle. This is followed by a discussion on the spatial and temporal distribution and variability of clouds.

Once the background information is presented, the chapter then reviews the body of literature on the diurnal cycle of cloud cover. It begins by summarising global-scale studies since they provide an important backdrop against which the results of this study can be compared and contrasted. A number of regional-scale studies are then presented, specifically those concerned with the diurnal cycle over Central America. These studies highlight the limitation of using a single data source. The Central American studies also provide valuable insights into the finer-scale variation of cloud cover which can be compared and contrasted to the results found in our study. Finally, the results from regional studies of southern and central Africa are reviewed. These results provide varying levels of spatial and temporal detail but none provides a suitable base-line climatology which is the aim of this study.

The results found in this study are placed into context using an idealised description of the growth and decay of deep convective cloud and the primary mechanisms which drive their diurnal variability. Therefore a short review of convective cloud development is presented.

Finally, the relevance and importance of a diurnal-scale observational study such as this one, to modelled climate studies, is presented.

2.1. Study Area

The study area seen in Figure 2.1 below encompasses the continental locations of southern and central Africa as well as the island of Madagascar (10° N - 40° S and 0° E - 50° E). The study does not include regions further north, firstly to limit the scale of the study, but also because West Africa has been the focus of a number of previous studies (Machado et al., 1993; Mathon and Laurent, 2001; Fink and Reiner, 2003). The eastern boundary at 50° E was chosen to exclude the swath of less reliable data over the central Indian Ocean which lacked geostationary satellite coverage (Kondragunta and Grubber, 1996). This study restricts itself to cloud cover over land since the diurnal cycles of continental and marine clouds are quite dissimilar and are driven by different factors.

2.1.1. Physical Setting

The southern and central African region represents a large landmass extending across the tropics and southern hemisphere subtropics. Much of the study area is located more than 1000 m above sea level in the low-relief interior plateau of South Africa and the Angolan and East African Highlands (Figure 2.1). The subcontinent lacks large mountain ranges, with the exception of the Drakensberg and Ruwenzori ranges (peaks > 5000m), the peaks in the Ethiopian highlands, and the mountains associated with the East African Rift System and those along the length of Madagascar. The high plateaus are broken by a few significant river basins, most notably the Congo, Niger and Zambezi River basins. There are several large lakes in the study area that have significant influences on their local climates and cloud cover, most notably Lake Victoria and the lakes associated with the African Rift Valley. The West Coast of southern and central Africa has a very narrow coastal plain, while the east coast (north of South Africa) has a wider coastal plain.

Figure 2.1 The Southern and Central Africa Study Area.

The two oceans bordering the study region, the South Atlantic and Indian Oceans, influence the temperature and moisture content of the air masses which are advected over the region (Lindesay, 1998). The east coast of southern Africa is influenced by the warm waters of the Mozambique and Agulhas currents of the Indian Ocean. Although the warm Angolan current of the South Atlantic flows southwards along the tropical west coast, it seldom penetrates further south of 10° or 15° South (Lindesay, 1998). South of the Angolan current, the west coast is influenced by strong upwelling of cold deep water in what is known as the Benguela Upwelling Region.

2.1.2. Atmospheric Circulation Patterns over Study Area

The principal components of the atmospheric circulation over this region include the circumpolar westerly winds polewards of 25° S. These winds dominate throughout the depth of the troposphere in the midlatitudes and extend as far north as 10° S in the upper troposphere (Lindesay, 1998). Near the surface, the subtropics are dominated by the two large semi-permanent high pressure cells, the South Indian and South Atlantic anticyclones which are centred to the east and west of the region respectively. The South Atlantic anticyclone produces strong subsidence along the west coast of southern Africa, while the South Indian anticyclone brings moist onshore easterly flow over the eastern half of the subcontinent especially during austral summer.

The tropical latitudes have lower surface pressures and the winds are generally easterly. The surface winds converge forming a region of pronounced uplift and convection referred to as the Inter-Tropical Convergence Zone (ITCZ). A second region of surface air convergence over southern Africa, called the Zaire Air Boundary (ZAB), separates airflow originating from the South Atlantic and South Indian Oceans (Tyson and Preston-Whyte, 2000).

The summer (DJF) conditions over the study area are characterized by the interplay of converging airstreams with the ITCZ located over the eastern half of the subcontinent and the ZAB over the western parts (See figure 2.2 below). These regions of convergence are formed by three primary airstreams: the north-east airflow from the East African Monsoon, which crosses the equator and pushes southwards from east Africa; tropical easterlies from the Indian Ocean and the re-curved westerlies that move in over southern Africa from the Atlantic ocean around 12° South (Tyson and Preston-Whyte, 2000).

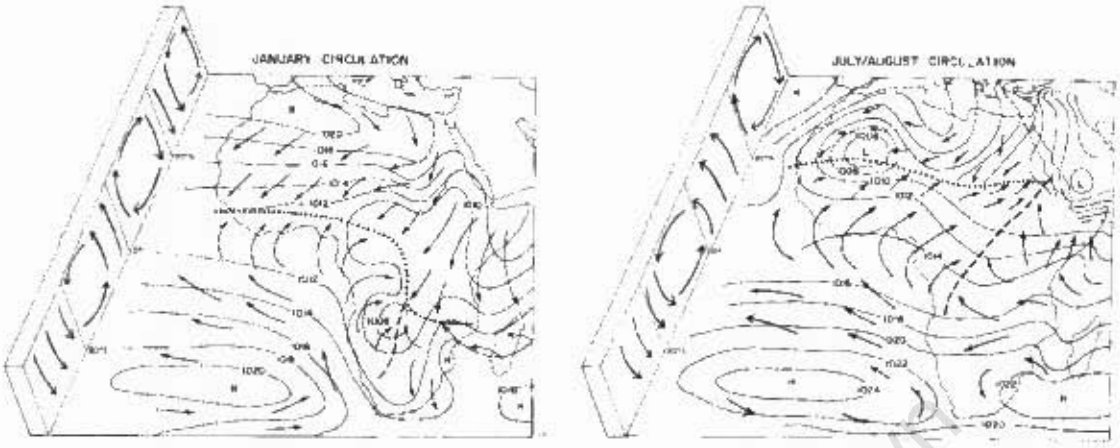

Figure 2.2 Schematic of the general patterns of winds, pressure, and convergence over Africa (from Nicholson, 1996). Dotted lines indicate the Intertropical Convergence Zone; dashed lines represent the Zaire Air Boundary (ZAB) convergence zones.

The winter (JJA) conditions differ from those of summer mainly in the location of the ITCZ and strength of the subtropical high pressure system (see figure 2.2 above). During this season the low pressure trough associated with the thermal equator is found north of the study area. The southern hemisphere circumpolar westerlies move northwards and expand and the southern African subcontinent is dominated by a high-pressure system and general subsidence and stability. The northward movement of the ITCZ results in the recurved westerlies from the southern Atlantic pushing deeper into the western half of central Africa. The eastern parts of central Africa show a clear seasonal reversal in wind direction with southwesterly winds prevailing.

Tropical-Temperate Troughs (TTT) form when an easterly wave or low in the tropical circulation over southern Africa becomes linked with a temperate westerly disturbance to the south. TTT are an important combined system associated with strong convection, cloud cover and precipitation over southern Africa (Lindsay, 1998).

2.1.3. Climate Regions of Southern and Central Africa

The climates of southern and central Africa are often classified primarily by their rainfall patterns; the majority of the study area can be characterized as being found within three distinct climatic zones: Wet Tropical Climates, Wet-Dry Tropical Climate and Dry Tropical Climate (Huq et al., 1996). The western half of central Africa has a wet tropical climate, with high temperatures and copious precipitation throughout the year, with maximum rainfall occurring shortly after the two equinoxes. The eastern half of southern Africa shows a large seasonal shift in precipitation with a single wet season during the summer, lasting 3 to 5 months and rainfall being rare outside of this season. The western half of southern Africa has a dry climate with little precipitation and a large range in daily temperatures. The far southwestern parts of South Africa is unique in that it has a Mediterranean climate with clear dry summers and cool wet winters.

2.2. The Role of Clouds in the Global Climate System

Clouds play a leading role in the climate system. They influence the radiative energy balance both at the surface and at the top of the atmosphere. They effect the distribution of surface and atmospheric heating which in turn helps drive atmospheric motion. This atmospheric motion itself plays a strong role in the development and distribution of clouds.

Clouds are closely linked to atmospheric convection, precipitation and latent energy release. They fulfil an important role in the hydrological cycle, being the intermediate stage between water vapour that evaporates from and cools the surface, and the precipitation that heats the atmosphere as it condenses and returns the water back to the surface (Rossow and Schiffer, 1999). Clouds are integral to many feedbacks, such as those relating to snow/ice albedo, water vapour, soil moisture, and lapse rate (Stephens, 2005).

Clouds influence the Earth's global mean radiative budget at the Top of the Atmosphere (TOA) both in the shortwave and longwave parts of the spectrum. In the visible spectrum clouds are highly reflective and therefore their presence increases the globally averaged reflectance of shortwave (SW) radiation back to space by 50 W m^{-2} (cooling effect). The strong greenhouse effect of clouds results in a longwave (LW) warming of 30 W m^{-2}. Thus clouds produce a global net cooling effect of 20 W m^{-2} at the TOA (Wielicki et al., 1995).

The extent to which clouds warm or cool the atmosphere, relative to clear sky conditions, is further influenced by a number of cloud features including: cloud height, thickness, horizontal extent, horizontal variability, water content, phase (liquid or ice) and the size of droplets and crystals (Warren et al., 2007). High, optically thin ice-clouds tend to warm the atmospheric column relative to surrounding clear skies, particularly in low latitudes. Conversely, low thick water-clouds enhance the cooling effect on the atmosphere (Stephens, 2005).

During the day, clouds reduce the amount of solar radiation reaching the surface, reducing the diurnal variation in surface temperature, while at night the land surface is kept warmer than it would be in the absence of clouds due to their almost perfect absorption of terrestrial radiation (Stephens, 2005). Therefore the time of day or night at which clouds are most prevalent dictates whether the influence is one of warming or cooling.

This section has revealed the complex relationships between clouds and the climate system, and shown how sensitive the radiative balance of the earth is to a number of cloud characteristics. Therefore a complete understanding of the climate system requires a detailed knowledge of the spatial and temporal distribution of the clouds.

2.3. Cloud Studies

There is a long and rich history of observational cloud studies which fall into two broad groups; those obtained from surface observations and those that infer cloud cover from satellite-recorded data. Both surface- and satellite-based studies have their strengths and weaknesses and differ in the descriptives they use to classify clouds. Surface studies characterise clouds as viewed from below, providing information on low-level clouds and mid- and high-level clouds not obscured by lower clouds. Satellite-based studies on the other hand, provide good information on high-clouds but in turn can only sense mid- and low-level clouds that are not obscured by high-clouds. Most satellite-based cloud data are obtained from radiometers, which measure the reflected, scattered, and emitted radiation from the earth's surface, atmosphere, and clouds. Radiative transfer models are then used to convert the measured radiances into cloud properties. For example the International Satellite Cloud Climatology Project (ISCCP) data only makes use of two broad spectral bands and can therefore only classify clouds by their cloud-top pressure and cloud optical depth (daytime only). A number of other satellite-based sensors are able to provide results on other cloud variables due to higher spatial, temporal or spectral resolution.

2.3.1. Cloud Geographic Distribution

Stubenrauch et al. (2006) compared the results from two different satellite-based 8-year cloud climatologies (1987-95). The time-averaged results showed that roughly 70% of the earth's surface is covered by clouds. The Television Infrared Observation Satellite-N (TIROS-N) Observational Vertical Sounder (TOVS) detected slightly more cloudiness over oceans than continents, 74% and 69% respectively. Similarly ISCCP-D2 found the proportions to be 71% and 58%. The slightly higher values of TOVS compared to ISCCP may be due to differences in spectral resolution or the temporal sampling of the two datasets. Both of these datasets recorded higher values than those obtained from surface observations, which found 65% cloud cover over oceans (Warren et al., 1988) and 52%

over land (Warren et al., 1986). These differences are probably due to the superior spatial coverage, especially over the ocean, provided by the satellite-based observations.

Cloud cover is most extensive over the Tropics (15°N-15°S) followed by the mid-latitudes between 50°-60° and least extensive over the subtropics (Peixoto and Oort, 1992). Stubenrauch et al. (2006) found that over the Tropics, high opaque clouds showed very small horizontal extent, covering only 2.5% or 3.5% for TOVS and ISCCP data respectively. The finer infrared spectral resolution of the TOVS data compared to ISCCP provided superior cirrus identification and showed 45% of the tropics covered by cirrus clouds in contrast to the 24.9% detected by ISCCP. Very little mid-level cloud was detected by TOVS (4.1%) with larger values detected by ISCCP (13.4%) though this may be due to ISCCP's well-publicised misclassification of cirrus as mid-level cloud (Rossow et al., 2005). Low-level cloud was found to be more extensive over the oceans than continents (35.1% and 20.5% respectively).

Dessler et al. (2006) analysed cloud-top heights using the Geoscience Laser Altimeter System (GLAS) in order to get a better picture of the horizontal and vertical distribution of tropical clouds. They separated cloud-top heights for thick and thin clouds by time and by surface type. Results showed two main peaks in the cloud-top distribution, one maximum in the upper troposphere (12-17 km) and one in the lower troposphere generally below 4 km. Both thick and thin clouds showed the same basic peaks and had the same shape, though thin clouds predominated. A less prominent maximum was also found between 6 and 8 km.

Clouds at different vertical levels often co-occur. Wang et al. (2000) showed that slightly less than half of all clouds were multi-layered, with most consisting of two layers. They also found that multilayered clouds were most common in the tropics and least common in the subtropics and that generally, multilayered clouds included a low-level cloud layer.

This section demonstrated that cloud cover is clearly organised both geographically as well as vertically. It suggested that the southern and central African parts of the study

area may show quite dissimilar cloud distributions. The review above also highlighted our incomplete understanding of the spatial distribution of clouds. It showed that even when averaged over both space and time, large differences are found in the results obtained from different sources and therefore care needs to be taken when interpreting results from a single source

2.4. Diurnal Cycle of Cloud Cover

The section above discussed the spatial variations of cloud cover both horizontally and vertically through the atmosphere. Clouds also show strong temporal variations, especially at the annual and diurnal periodicities. The primary objective of this study is to create a regional climatology of the diurnal cycle of cloud cover over southern and central Africa. It is therefore useful to review the existing body of literature pertinent to this topic in order to determine what is known and to identify any key gaps in our current knowledge.

2.4.1. Large-Scale Studies of Cloud Diurnal Variation

The release of the ISCCP dataset in the 1990's resulted in a number of global (or near global) cloud studies being produced. Konragunta and Gruber, in their preliminary examination (Konragunta and Gruber, 1994) and more comprehensive study (Konragunta and Gruber, 1996), looked at the large-scale features of the diurnal variation of total cloud amount over the globe. They used Empirical Orthogonal Function (EOF) analysis on the hourly monthly mean total cloud amount from ISCCP-C2. They found that the first EOF mode represented the contrast between diurnal variations of cloud cover over land versus ocean and accounted for 58.5% of the normalized variance. This mode displayed a maximum at 0500 local solar time (LST) over oceans, and 1500 LST over continental regions. The second EOF mode picked out the diurnal cycle associated with deep convection over both oceanic and continental regions and explained 25% of the

normalized variance. This mode showed that these convective regions had a minimum cloudiness at 1000 LST and maximum cloudiness around 2000 LST over convective regions. Broadly speaking they found that the first mode explained the diurnal cycle of low-level cloudiness, while the second mode explained the diurnal variation of high-level cloudiness (Konragunta and Gruber, 1996).

Cairns (1995) also used the ISCCP-C2 data to study the diurnal variation of high-, mid- and low-level cloud amount over the whole globe. The results found that low-level cloud showed a significant diurnal cycle with a maximum around 1330 LST over almost all continental locations. The diurnal maximum of mid-level cloud was found in the early morning or late at night, while the maximum in high-level clouds tended to occur in the evening or night. They found that over tropical land masses, maximum mid-level cloud tended to peak 9-hours after the peak in high cloud.

Bergman and Salby (1996) went slightly further and used the ISCCP-C2 data to investigate the relationship between climatological conditions and diurnal variations of cloud cover. They separated the data into four cloud categories: Maritime high-cloud, Maritime low-cloud, Continental high-cloud and Continental low-cloud. Their results showed that the diurnal variation of continental high-cloud cover was strong, with maximum cloud persisting through the night and a minimum found at 1100 LST. Continental low-cloud cover also showed strong diurnal variation with a maximum at 1300 LST.

The diurnal amplitude was most strongly associated with mean cloud cover. For continental high-cloud, the strongest correlation for mean high-cloud amount was with total cloudiness and was anti-correlated with the diurnal amplitude of surface temperature (areas with little surface temperature diurnal variability showed largest high-cloud). They also found that it was correlated with precipitable water and the noontime solar zenith angle (Bergman and Salby, 1996). The diurnal amplitude of continental high-cloud was strongly correlated with its mean amount but the phase showed considerable scatter,

however maximum cloud fraction was rarely found during daylight hours (Bergman and Salby, 1996).

Continental low-cloud amount showed the strongest diurnal variation of the four categories. They found a nearly linear relationship between the diurnal amplitude and the mean low-cloud amount. The phase was very uniform, occurring between 1200-1500 LST almost everywhere. The amplitude was most strongly related to the moisture content and the diurnal amplitude of surface temperature, but this can partly be explained by the surface temperature bias of the data (Bergman and Salby, 1996).

These preliminary global studies provided valuable insight into the large-scale patterns found in the diurnal variation of cloudiness. They showed that marine and continental clouds display quite different variations, as well as convective and non-convective locations. These studies also verified that over continental location, high- and low-level clouds display strong but different diurnal variations, and that the diurnal cycle of mid-level clouds is less significant. These preliminary studies have provided a base from which many subsequent studies have grown. The studies which follow make use of other satellite-based data, many of which are able to provide additional information on the diurnal variations of cloud cover and are able to validate and explain the results found in the initial ISCCP global studies.

The study by Yang and Slingo (2001) explored the diurnal cycle of convection, cloudiness and surface temperature in the tropics using high-resolution (0.5° lat-lon, 3-hourly resolution, 11-12 μm) brightness temperature (T_b) data from the European Union Archive User Service (CLAUS) project. Their results showed strong amplitude in T_b over clear sky continental regions such as the Namib Desert and Antarctica during DJF, and the Sahara and Kalahari Desert in JJA. This is reportedly due to the response of the surface to daytime solar heating. Continental convective regions also showed large diurnal amplitudes of T_b, which were linked to the forcing of convection by the diurnal cycle of land surface heating. The study calculated an equivalent precipitation rate from the brightness temperature data, which suggested that convective precipitation tended to

occur in the late afternoon and evening. The results also found interesting regional variations due to orography and the lifecycle and movement of Mesoscale Convective Complexes, which may not have been discernable in the lower-resolution global studies.

Luo and Rossow (2004) attempted to characterise the life cycle and evolution of cirrus clouds and their interaction with upper-tropospheric water vapour. They used the split-window method to detect cirrus cloud, where two radiance channels (roughly 11μm and 12μm) provided continuous coverage through the day and night. The study found that the decay of deep convection was immediately followed by the growth of cirrostratus and cirrus, and cirrus continued to grow even while cirrostratus decayed.

The study found that the decay of deep convection by convective detrainment was rapid and the transition from convection to cirrostratus was about 6 hours. The decay of cirrostratus was then accompanied by the continued growth of cirrus indicating the decay of cirrostratus into cirrus also took roughly 6 hours (though it could be shorter since the data were recorded at a 6-hour time interval). They also stated that decay of cirrostratus may be complex and probably not due to a simple loss of water through evaporation. Instead it could be due to a combination of rapid sedimentation to lower levels (which is opposed by a dynamical supply of water vapour from below) and a dispersal of water as the area expands, since cirrostratus typically cover 2-3 times the area of convective towers (Luo and Rossow, 2004). Cirrostratus was found at lower pressure levels (higher altitude) than cirrus which also suggests that the transition is accompanied by a decrease in cloud-top height. Cirrus tends to thin out and move to lower levels as air moves away from convective regions. These results provide important supplementary information on cloud type and lifecycle to studies relying on ISCCP data. However, these studies do not provide the required temporal resolution, spatial coverage or length of record as that of the ISCCP data and are therefore not able to provide a suitable climatology of the diurnal cycle of cloud cover.

A number of studies investigated the diurnal cycle of cloud cover over tropical America (Meisner and Arkin, 1987; Garreaud and Wallace, 1997; Soden, 2000; Machado et al.,

2002; Wylie and Woolf, 2002; Rickenbach, 2004). The study by Machado et al. (2002) investigated the diurnal variation of convection using radiosonde, satellite, and radar data along with rainfall data collected from the WETAMC-LBA experiment over the Amazon region. They also used Geostationary Operational Environmental Satellite (GOES 8) images to describe the diurnal cycle of total, high and convective cloud fraction. Their study found that both deep convective cloud and high cloud fraction increased strongly from 1130 LST with maximum growth occurring around 1330 LST. Deep convective cloud fraction peaked at 1630 LST, one hour earlier than high cloud fraction (1730 LST). Both deep convective and high clouds showed a rapid decrease from their maximum until 2030 LST after which they decreased more slowly, though high cloud decreased more slowly from 2030 LST. Total cloud fraction showed a very different diurnal variation peaking at 0330 LST and reaching a minimum at 1230 LST. The study showed that maximum rain rate occurs a few hours before maximum cloud faction, and corresponded to the time at which convective systems were small and growing most rapidly.

The diurnal cycle of upper tropospheric water vapour over the tropical Americas was compared to that of convection and cloud cover (Soden, 2000). Results showed significant diurnal variations in water vapour over both land and oceans and that there was a coherent diurnal relationship between convection, clouds and water vapour over continental locations, where water vapour lagged clouds by around 2 hours. (1800 - 2000 LST). This result was consistent with the formation of cirrus anvil clouds and their subsequent evaporation. He found that the relationship between the diurnal variations in upper tropospheric clouds, water vapour and convection was in phase over land, but was out of phase over the oceans (Soden, 2000).

The use of many different types of data allowed the Central American studies to distinguish between different types of cloud and to relate these different clouds to convection and precipitation and water vapour. Central America and central Africa have relatively similar climates and therefore these results could prove useful in the interpretation of the results for central African diurnal cycle of cloudiness.

2.4.2. Diurnal Variation of Cloud Cover over Africa

Relatively few diurnal cloud studies have focussed specifically on the African Continent. Of these, most concentrated on the West African region (Arnaud et al., 1992; Machado et al., 1993 and Mathon and Laurent, 2001; Fink and Reiner, 2003) and were concerned with the diurnal cycle of convective cloud clusters and their relation to the tropical easterly circulation.

Desbois et al. (1989) used water vapour and infrared data from the original 30 km pixel resolution ISCCP dataset to investigate the diurnal cycle of convective clouds over tropical Africa. Their study highlighted the association between the diurnal cycle of convective clouds and orographic features. Maximum diurnal variations were found to occur over mountainous areas and areas where breeze-type circulations occurred. The time of maximum cloud cover was found to be earlier over these mountainous locations, becoming progressively later downwind (westwards). The relatively flat Sahel region showed large diurnal variations associated with propagating convective systems, which were tracked by following their development over a series of satellite images (Desbois et al., 1989).

The study also found that the sharp and complicated orography associated with the Lake Victoria area and the East Africa regions induced strong local circulation. On Lake Victoria itself, a strong cycle related to a lake-breeze effect was evident. West of the main volcanic range, the phase of maximum cloudiness was shifted towards later hours, up till midnight, indicating a progressive advection of the upper level clouds by the easterly upper level flow. The study found that the amplitude of the cycle was enhanced over the full domain during wetter years, and the phase remains approximately the same over the main convective areas (Desbois et al. 1989). This study may be relatively old, but the fine resolution of the data allowed the influence of orographic features on the diurnal cycle of cloud cover to be detected. This study attempt to detect these subtle influences on the diurnal variation in the much coarser-scale 280 km ISCCP-D1 data.

A number of diurnal studies of other, related variables have provided information over the African region and their finding provide useful insight on the diurnal variation of cloud cover. The study by Yang and Slingo (2001) mentioned in the previous section, also evaluated the diurnal cycle over three Africa regions. They demonstrated that for the Clear Sky regions of northern Africa (0°-30°C, 10°N-30°N) during JJA, and southern Africa (15°E-35°E, 5°S-30°S) during DJF, maximum brightness temperatures (related to minimum total cloudiness) occurred just after noon and that the minimum T_b (related to maximum total cloudiness) occurred between 0400 and 0600 LST. They also showed that for the Convective region of Central Africa (15°E-35°E, 0°-15°N) during JJA, deep convection developed in the late afternoon and reached a maximum in the evening, after which clouds decayed during the early hours of the morning before dawn.

Geerts and Dejene (2005) used 5 years of extreme-season TRMM Precipitation Radar data to determine whether the vertical structure of precipitation systems and their diurnal variations were different in the distinct climatic zones of African, and if they differed from that found over the Amazon Region. The study found a strong diurnal cycle with maximum heavy precipitation occurring in the afternoon and evening (1500-1800 LST) over most regions in Africa. The morning hours showed the lowest rain rate and rainfall amount in all regions. The diurnal variation in rate and amount was strongest over East Africa (JJA) and the desert regions and was weakest in the western Tropical region. This western tropical region also showed a second nocturnal peak in rain rate and rain amount in the early morning, while the timing of maximum precipitation was earlier (1200-1500) over the central parts of southern Africa. This second nocturnal peak in precipitation over the western tropical region is interesting and our study will investigate whether it is linked to an increase in cloudiness at this hour.

This same study found that precipitating systems over tropical Africa tended to be deeper and more intense than those over the Amazon and that shallow warm-rain events were less common (Geerts and Dejene, 2005). Storms over Africa and especially over the Sahel and northern Savannah showed high echo tops, high hydrometeor loading aloft and

evidence of low-level evaporation. Storms were most common and deepest in the late afternoon, though weaker shallow systems were relatively more common around noon.

The diurnal variation of outgoing longwave radiation fluxes over Africa for July 2006 was explored by Comer et al. (2007). The majority of the diurnal variation was found to be due to the surface temperature response to solar heating, though the development of convective clouds was also significant in explaining the variance.

And finally a recent study by Chung et al. (2007) investigated the diurnal variation of Upper Tropospheric Humidity (UTH) and its relation to convective activity over tropical Africa. The study made use of a two water vapour and one thermal IR bands from the new Meteosat 8 geostationary satellite for two months (July 2004 and January 2005). Results showed that the diurnal variation of UTH reached a maximum value during the night over the continental region, and that it lagged deep convective and high cloud whose maximums were found in the late afternoon and evening respectively. The study found that cirrus anvil cloud and UTH showed quite similar cycles, particularly in the hours after deep convective cloud reached their maximum, where both tended to increase rapidly reaching their maximum values around 0300 LST over land. These results provided support to the view that the decay of deep convective clouds provides the main source of moisture to the upper troposphere as well as being the source of moisture for the formation of cirrus anvil clouds. The study also suggested that the diurnal cycle over regions of the African continent were likely due to continental-scale daytime solar heating, with topographic features being the next most important control, while the advection of clouds only produced negligible differences to the diurnal variations.

On reviewing all of the above-mentioned literature, it becomes evident that there are some notable gaps in our knowledge of the diurnal variation of cloud cover over southern and central Africa. The global or large-scale studies only provide basic information on the regional or seasonal differences found in the diurnal cycle of cloud cover over the African region. This study provides a baseline seasonal climatology of the diurnal cycle of cloud cover using the most recent version of the ISCCP data which has been found to

have a number of improvements over the previous version (Rossow and Schiffer 1996). More detailed studies in other regions (most notably Central America) highlighted smaller-scale variations in diurnal cloudiness and the importance of using a range of data types to fully investigate the type and lifecycle of clouds. The majority of cloud studies over Africa have focussed on the tropical and western parts, therefore this study focuses more on the central and southern regions. The more recent studies were all of short duration and concerned with slightly different questions, but provide valuable insight into the convective processes and underlying mechanisms responsible for the results shown in this study.

2.5. Convective Cloud Development

This chapter has discussed the role of clouds in the climate system and has provided a short description on the geographic and vertical distribution of clouds, with specific emphasis on the diurnal periodicity. The focus now shifts to a description of the development and life-cycle of clouds over low-latitude continental locations such as southern and central Africa. A summary of the foremost published mechanisms explaining the diurnal variability of precipitation / cloud cover (Yang and Smith, 2006) are provided in Appendix B.

Tropical Africa is a region of pronounced convective activity. When viewed on an annual or seasonal basis, the ITCZ appears to be a well defined region of steady convergence and uplift. At a day-to-day scale, it becomes apparent that the ITCZ is made up of smaller mesoscale disturbances. Mesoscale Convective Systems (MCSs) are treated as a single entity but consist of individual convective cells and thunderstorms, with clouds joining and breaking away from the main complex as they grow and decay (Hodges and Thorncroft, 1997). There are two types: Mesoscale Convective Complexes (MCCs) which are nearly circular clusters of convective cells, and Squall Lines, which consist of a narrow line of thunderstorm cells that move in unison. African MCSs are generally triggered in association with orography and elevated daytime heating, or through synoptic

weather systems such as easterly waves. MCCs usually have lifecycles of around 12 hours, forming in the afternoon and decaying during the night, while Squall Lines have a lifecycle of around 2 days (Hodges and Thorncroft, 1997). Most of southern African rainfall is associated with these MCCs, whereas Squall Lines are most common over West Africa and are relatively rare over the southern and central African study area.

Shallow convection is initiated through the heating of the earth's surface, which creates thermals of warm air that rise and expand. These upward fluxes of both sensible and latent energy result in the surface boundary layer becoming well mixed and conditionally unstable. The boundary layer slowly deepens through the morning, both by the continual heating from below and by the entrainment of air from the layer aloft. Small cloud elements form once the tops of the thermal towers extend above the Lifting Condensation Level. These cloud elements thicken and expand across the top of the boundary layer. These low-level clouds reach their maximum extent just after midday and then decline through the afternoon. This is partly due to decreasing angle of incident shortwave radiation reaching the surface and the increasing shading from clouds. The cloud-base also rises through the afternoon because of the decrease in near-surface relative humidity (Grabowski et al., 2006).

Deep convection only occurs once dry convective overturning has penetrated above the boundary layer. The transition from shallow to deep convection allows clouds to extend vertically into the mid- and upper-troposphere. Clouds need to be of significant size and depth for cloud droplets to grow to the size required for precipitation. Precipitation is usually associated with the cloud top reaching freezing level. This results in widespread glaciation. Large amounts of super-cooled water vapour rapidly freeze, resulting in a corresponding release of latent heat. This energy tends to enhance buoyancy and further growth, allowing clouds to expand upwards towards the top of the troposphere (McIlveen, 1992).

The tops of deep convective clouds are laden with ice which may decay into cirriform anvil clouds, bounded by stable layers both above and below. These cirriform clouds can

last long after the deep convection since the ice particles, with their low saturation vapour pressure, are slow to sublimate. The anvil clouds decay through the night. However, in some deep convective locations the radiative cooling of the cloud top destabilizes the cloud layer, facilitating turbulence within the cloud layer. This can lead to the regeneration of high-level cloud in the early morning (Houze, 1993).

The ISCCP data used in this study are not able to distinguish between convective or cirriform cloud and it are poor at detecting thin cirrus cloud. However, the lifecycle of convective clouds described above may help in the interpreting the results. Also, the three-hourly native resolution of the data may be sufficient to detect this early morning regeneration of high-level cloud and identify the spatial extent of this phenomenon over the deep convective locations.

2.6. Relevance of this study to climate model simulations

While this thesis does not explore the modelling of clouds, the observational understanding of clouds directly informs model development. Moreover, as clouds are such a critical parameter in energy budgets, a brief review of the ability of three-dimensional climate models to simulate cloud fields is considered useful for contextual information.

The accuracy or skill with which climate models are able to simulate the present climate is normally verified by comparing spatially/temporally averaged model fields against those obtained from observations. A review of the results obtained from the Atmospheric Model Inter-comparison Project (AMIP), indicated that whilst models were able to provide a credible simulation of the large-scale distribution of the primary climate variables, outstanding problems were the parameterisation of clouds and their radiative interactions, convection and precipitation, and the representation of the interactions between the land-surface and hydrologic processes (Gates et al., 1999).

A regional study (Hudson and Jones, 2002) of the present and future climate of southern Africa using the HadAM3H GCM, demonstrated that the model was generally able to capture the circulation dynamics of the present-day climate. However, during summer the representation of the convergence associated with the Inter-tropical Convergence Zone (ITCZ) and Zaire Air Boundary was too strong, producing a positive rainfall bias over much of southern Africa. The positive precipitation bias resulted in greater evaporative cooling at the surface and the simulation of too much cloud amount at all levels; especially as thick clouds further attenuated shortwave radiation, thereby reducing the SW radiation reaching the surface. Both of these errors contributed to negative surface temperature biases (Hudson and Jones, 2002).

Such problems across all GCMs have motivated an improvement of the parameterization of convection, cloud-radiation interactions, moist processes and land surface processes in GCM simulations and which has been the focus of a broad body of work in the past few decades. However, the majority of these studies continue to evaluate the skill of the models by focussing on the spatially averaged fields at large temporal time scales (annual, seasonal or monthly scale). The weakness of this is that it is possible for models to produce realistic climate states for the wrong reasons (Tian et al., 2004). It is therefore necessary to evaluate a model's skill at simulating the variability of climates at shorter (such as diurnal) temporal scales. This enables the models to be tested at a timescale much closer to that of many important atmospheric physical processes, such as clouds and convection (Slingo et al., 2004).

The external forcing, large amplitude, consistent phase, and short time scale of the diurnal cycle make it a valuable periodicity at which to test model parameterisation and physics. The diurnal cycle is also useful in the assessment of the interactions between the surface, the boundary layer and the free atmosphere (Yang and Slingo, 2001; Dai and Trenberth, 2004).

A number of studies which compared model results and observations at the diurnal timescale found that generally the model's timing of convective clouds and precipitation

over land peaked far too early in the day (Morcrette, 1991; Lin et al., 2000; Yang and Slingo, 2001). These studies indicated that the timing of tropical convection and precipitation was particularly sensitive to details of a model's formulation and that models often failed to reproduce the observed evening maximum in cloudiness and precipitation (Slingo et al., 2004)

The study by Yang and Slingo (2001) discussed in a previous section, compared satellite-derived results to those of the HadAM3. They found that the model was able to capture the amplitude of the diurnal cycle of precipitation over continental convective locations, though it proved to be poor at simulating the phase of the diurnal harmonic of equivalent T_b and precipitation in the Tropics, with the most significant differences occurring over convective regions. The model showed a maximum in the simulated precipitation occurring before noon, instead of during the late afternoon to early evening as found in the CLAUS data and other observations.

A subsequent study by Slingo et al. (2004) built on the analysis of HadAM3, used a version of the model's radiation scheme which could simulate the radiances observed by Meteosat 7 geostationary satellite. They compared the model results to that of the satellite's infrared window channel and water vapour channel to determine the skill of the model at the diurnal temporal resolution. The study found that the model was able to simulate the geographic distribution of the mean radiances and amplitude of the diurnal variation with some skill. However the model was not able to reproduce the correct timing of maximum and minimum radiances. They found that the timing of minimum radiances over central Africa could be improved by increasing the number of vertical levels and by calling the radiation scheme at every model time step (every half hour) instead of every 3 hours. This improvement was due to the creation of upper-level layer-cloud by detrainment from the convective scheme. This layer cloud reached its maximum much later than that of maximum convective rainfall and persisted long after the convection itself has dissipated. The increase in both vertical resolution and temporal sampling did not improve the models representation of convective precipitation which

still occurred before noon. This suggests that the diurnal errors were almost certainly the result of deficiencies in the model's convective scheme (Slingo et al., 2004).

Dai and Trenberth (2004) used data from available surface observations, mostly derived from 3-hourly synoptic reports, to test the skill of the Community Climate Model (CCSM2) in simulating the diurnal cycle. They found that the model underestimated cloud amount by 10%-30% in the subtropics. They found that over continents, moist convection was simulated prematurely and for an extended duration, which resulted in precipitation occurring too frequently and being at a reduced intensity. The timing of maximum precipitation was also found to be inaccurate; the model produced a morning or near-noon peak in precipitation, which was much earlier than the late afternoon to evening peak known from observational studies (Dai, 2001; Dai and Trenberth, 2004).

Tadross et al. (2005) demonstrated that the diurnal cycle of the regional climate model MM5 over southern Africa was dependent on the choice of convective parameterisation scheme. The Kain Fritsch scheme, like other model simulations, suffered a peak rainfall too early in the day (around 1200 LST). However the Betts Miller scheme resulted in a more realistic diurnal cycle with the peak rainfall occurring later in the day (1800-2000 LST).

Thus, in general it may be concluded that clouds are poorly represented in climate models. Many of these studies also identified the diurnal cycle as being a valuable periodicity at which to test model parameterization and physics. The model studies also indicated the need for accurate cloud observations against which these clouds can be tested and evaluated.

2.7. Summary

This chapter has provided some background information on the physical setting and climate of the study area. It reviews the literature on cloud cover with particular emphasis on the diurnal cycle of cloud cover over the southern and central African region. It is readily apparent that there are significant gaps in our understanding of cloud diurnal variation over southern and central Africa due to the paucity of studies assessing cloud variability at this frequency. There is also a strong need to remedy this deficiency in order to provide support for the broad body of work on climate variability and climate change.

CHAPTER 3

DATA & METHODOLOGY

3.1. Introduction

This chapter describes the data and methodology used in this study. The first section (section 3.2) provides a brief description of the International Satellite Cloud Climatology Project (ISCCP) and discusses the cloud variable used in this thesis. Section 3.3 gives a short description of the climate data obtained the NCEP/NCAR Reanalysis Project. This is then followed by a brief description of the Self-Organising Map tool, since it is used in the second analysis section. The focus of the chapter then progresses onto the methodology used in the thesis (Section 3.5). This includes a discussion on the methods used to reformat the data and a short description of the different analysis methods used in each of the data chapters which follow.

3.2. ISCCP D1 Cloud Data

The primary data used for this project are satellite-derived cloud data obtained from the most recent D-series of the International Satellite Cloud Climatology Project (ISCCP) (Rossow and Schiffer, 1999). This dataset was chosen since it provides a long record of cloud observations at a short (3-hourly) temporal resolution both during the day and night. The 2.5 ° latitude-longitude spatial resolutions of the data are coarse, but sufficient for the scale of this study. The ISCCP-D series data have the most complete and self-consistent set of calibrations available for all the weather satellite imaging radiometers (Rossow and Schiffer, 1999) and the results have been successfully used by numerous other cloud diurnal studies. Many of which were mentioned in the previous chapter.

The International Satellite Cloud Climatology Project (ISCCP) was established in 1982 as part of the World Climate Research Program. The first global radiance dataset was released in 1984, followed by the first cloud dataset in 1988. Numerous assessment studies have investigated the ISCCP analysis methods (e.g. Rossow and Garder, 1993; Rossow et al., 1996a; Rossow et al., 1996b; Rossow and Schiffer, 1999), while the cloud physical properties have been evaluated against those obtained by other remote and surface observation datasets (Rossow et al., 1993; Doutriaux-Boucher and Sèze, 1998; Rossow et al., 2005; Gang and Heygster, 2005). These studies helped identify shortcomings in the data and led to improvements in the analysis methods. It also motivated more detailed results being reported in the most recent D-series of the data.

3.2.1. ISCCP Data Analysis Procedure

The ISCCP cloud detection method employs the cloud's influence on both the shortwave and longwave radiation fluxes leaving the top of Earth's atmosphere. This was achieved by comparing the observed values to that expected from clear-sky conditions for that same location and time.

Radiance measurements were obtained from a global set of imaging radiometers flown on board weather satellites. At least 5 geostationary and two polar orbiting satellites were used to obtain global coverage at any given time. The imaging radiometers on board these satellites captured radiance values in discrete spectral bands. ISCCP made use of two bands common to all these satellites; one visible band near the peak of the solar spectrum (VIS $\approx 0.65 \pm 0.15$ μm), and one thermal emitted band located in the infrared opacity "window" (IR $\approx 11 \pm 1$ μm) (Rossow and Garder, 1993). The original satellite images were sampled in both resolution (30-km) and time (3-hourly). The results were then calibrated (Rossow et al., 1996a; Rossow et al., 1996b), navigated (Rossow et al., 1996c), and placed into a common format to produce the radiance dataset known as the B3 dataset.

The pixel-level cloud analysis used the B3 radiance data, along with geographic, surface and atmospheric data, to produce the DX pixel-level cloud data (Rossow et al., 1996a; Rossow et al., 1996b). The final step in the analysis was to create the D1 dataset, produced by summarizing the pixel-level results (Stage DX data) onto a 280 km equal-area map grid. A schematic of ISCCP cloud analysis can be found in Figure 3.1 below. Further literature on the ISCCP datasets and analysis methods can be found in the documentation by Rossow (Rossow and Schiffer, 1991: Rossow et al., 1991; Rossow et al., 1996a; Rossow et al., 1996b; Rossow et al., 1996c; Rossow and Schiffer, 1999).

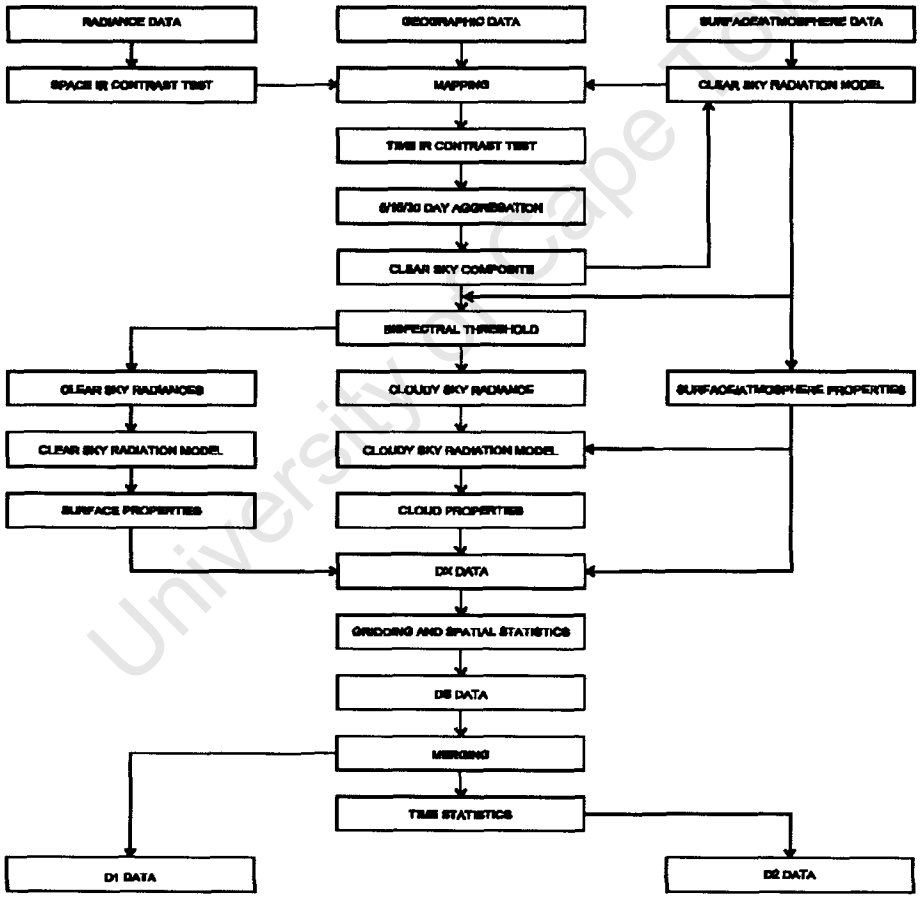

Figure 3.1 Schematic of ISCCP cloud analysis (source ISCCP DX/D1/D2 New Cloud Data Documentation[1])

[1] http://isccp.giss.nasa.gov/docs/D-toc.html

3.2.2. Cloud Variable: Cloud Amount at Seven Pressure Levels

The variable used in this study is the ISCCP Cloud Amount or more correctly, the number of cloudy pixels, with cloud-tops located in each of seven pressure levels. ISCCP computes these pressure levels from the inferred cloud-top temperatures using an atmospheric temperature profile from the Television Infrared Observing Satellite (TIROS) Operations Vertical Sounder (Rossow and Schiffer, 1999). The Cloud Amount variable is calculated exclusively using the IR-channel radiances in order to keep the results consistent both through the day and night hours. The "top down" view of satellites means that only the highest cloud-top in each atmospheric column can be detected. ISCCP makes no statistical assumption on the frequency of cloud overlap and, therefore cloud amount should not be interpreted as *actual* Cloud Amount but rather as *observed* cloud fractional area covered by cloud at this pressure level, which were not obscured by clouds at higher levels.

This cloud amount variable was used in this study to characterise the seasonal average diurnal variations of low-level, mid-level and high-level clouds over the southern and central African subcontinent. The cloud data were also used to train the Self-Organising Map that was used to "upscale" or regionalise the study area into non-discrete and overlapping regions.

3.2.3. Assessment of the ISCCP Cloud Data

3.2.3.1. Cloud Detection and Spatial Coverage

The accuracy with which ISCCP was able to determine cloud amount depended on three factors: the validity of cloud detection, the sensitivity of the cloud detection and the

accuracy with which it was able to estimate cloud cover fraction from counting cloudy pixels of a finite resolution (Rossow and Schiffer, 1999).

Rossow and Schiffer (1999) compared the ISCCP D-series cloud amounts to those from three other cloud datasets. They found that detection errors (validity and sensitivity of cloud detection) accounted for the largest amount of systematic errors. The comparison suggested that the earlier C-series version of ISCCP total cloud amounts were too low over land by 10%, with the error being higher in winter than summer. The improvements in the D-series resulted in an increase in total cloud amount by about 5%, with a pronounced increase of about 9% - 13% over land and a smaller 2% - 4% over oceans. This increase in cloud amount meant that the dataset matched the cloud climatologies determined by surface observations (Doutriaux-Boucher and Sèze, 1998). The increase in cloud amount over land was due to larger increases of low and high cloudiness and a smaller increase in mid-level cloudiness (Doutriaux-Boucher and Sèze, 1998). The ISCCP under-reported low-cloud at night since broken low-clouds do not always exhibit enough contrast in IR to be detected (Rossow and Schiffer, 1999).

When the ISCCP high-cloud amount was compared to that determined by the Stratospheric Aerosol and Gas Experiments (Rind and Liao, 1997) using two different analyses of High-Resolution Infrared Sounder data, ISCCP was found to underestimate upper-level cloudiness by at least 0.05-0.10 (Liao et al., 1995). Most of this was due to the missed detection of very thin cirrus cloud (Rossow and Schiffer, 1999). This problem was most severe during the night hours, or when only the IR channel was employed, since cloud optical depth could not be determined.

A comparative study between ISCCP and C. J. Hahn et al. surface-derived observations found that the magnitudes of annual-mean ISCCP and Hahn observations of low cloud fraction differed by up to 0.4 for a number of locations, and that the spatial patterns of variability were qualitatively different from one another (Weare, 2000). This was found to be largely due to ISCCP only observing low cloud not obstructed by higher cloud. The

Climate Atlas of Clouds over Land and Ocean[2] suggested that the DJF daytime cloud cover was relatively uniform over the southern and central African study area, with slightly lower values over the far north-western and south-western parts. These results suggest that the obscuration effect of ISCCP could be quite severe and that the data may be less skilful at detecting the diurnal amplitude of these clouds.

The interplay between the size and time distribution of cloud, and that of the reported results, is important in determining the accuracy of ISCCP data (Rossow and Schiffer, 1999). Generally, cloud cover fraction is overestimated if the sensor resolution is larger than the most frequent cloud element size (Rossow and Schiffer, 1999). However the size of the area in which cloud fraction is estimated can offset this overestimation. Therefore the precise balance between these offsetting effects depends on the size distribution and properties of clouds. A comparison between ISCCP and surface-observed cloud fraction showed that broken cloudiness displayed roughly the same mean values, but with a root mean square difference of about 0.25. The RMS uncertainly in individual ISCCP cloud amounts appeared to be about 0.15 over all cloud types (Rossow and Schiffer, 1999).

3.2.3.2. Cloud Physical Properties

The ISCCP data agreed very well with surface weather observations on the presence of low-level and thicker mid-level clouds, when upper-level clouds did not obscure them. However it showed three important biases. Firstly ISCCP had a tendency to overestimate the physical cloud-top pressure for high clouds, especially at low latitudes (Liam et al., 1995, Rossow and Schiffer, 1999; Meinke, 2006). Secondly, it tended to under-detect isolated, optically-thin cirrus clouds resulted in cirrus cloud being misclassified as middle-level cloud with moderate optical thickness. Thirdly, it misclassified multi-layer clouds if the upper layer was optically thin (Rossow et al., 2005).

[2] http://www.atmos.washington.edu/~ignatius/CloudMap/

Satellite infrared sensors can only provide an indirect estimate of the properties of the cloud. They only observe the cloud-top temperature and do not directly sense the radiation from their interiors (Hong and Heygster, 2005). Therefore infrared data alone are unable to distinguish between deep convective clouds and cirrus clouds since they often have the same cloud-top temperature. This has important implications for convection studies since cirrus cloud tightly connected with deep convective clouds can extend and persist for some hours after the deep convective clouds have themselves dissipated. This results in a misrepresentation of the hour of maximum convection. The study by Hong et al. (2007) investigated the diurnal cycle of tropical deep convective clouds and the influence cirrus clouds had on the results. They found that cirrus clouds generated by deep convective clouds could result in a 2-hour time lag in the timing of maximum deep convective cloudiness.

3.2.3.3. Diurnal Variations

As stated above, a weakness of the ISCCP cloud data, and all datasets produced using passive remote sensing techniques, are an under-reporting of mid- and low-level cloud amounts. However this under-reporting is not constant through time. The diurnal cycle of the higher and middle clouds can introduce a diurnal variation to the obscuration of lower clouds from the satellite's view. However Rossow and Schiffer (1999) showed that the diurnal variations in low-level cloudiness did not appear to be caused simply by changing high-level obscuration and was in good agreement with surface observations.

A second source of systematic error occurs over locations that experienced large diurnal fluctuation in surface temperature. These fluctuations can result in a large diurnal variation in the temperature contrast between surface and cloud top. The fixed cloud detection threshold may introduce a spurious diurnal component into the low-cloud amount from IR measurements. Bergman and Salby (1996) analyzed the older, monthly-averaged ISCCP-C2 dataset and found that approximately 50% of the observed low-cloud diurnal variation over continental location was due to the surface temperature bias.

3.3. NCEP/NCAR Reanalysis Data

NCEP/NCAR Reanalysis Project climate variables datasets are used in this study to describe the general synoptic conditions and the vertical distribution of humidity over the study area.

The NCEP/NCAR Reanalysis Project was formed as a cooperative undertaking between the National Center for Environmental Prediction (NCEP) and the National Center for Atmospheric Research (NCAR). The aim of the project was to produce a retroactive record of global analysis of atmospheric fields and to provide data on current atmospheric states. This was in order to support of the needs of the research and climate monitoring communities (Kistler et al., 2001). Details on the quality of the reanalysis data and the methods used to obtain the data can be found in Kalnay et al. (1996) and Kistler et al. (2001), while further information on the NCEP/NCAR Reanalysis Project can be found on the NOAA website[3].

The monthly average specific humidity data were used to produce 10-year seasonal climatologies of humidity within the three vertical pressure levels which most closely match that of the ISCCP cloud levels (1000 – 700 hPa, 600 – 500 hPa, and 400 – 300 hPa). NCEP/NCAR output variables are classified into four classes, depending on the degree to which they are influenced by the observations and/or the model. Specific humidity (shum) is classified as a 'B' variable. This indicated that, although there were observational data that directly affect the values of the variable, the model also had a strong influence on the analysis values and therefore caution should be used when interpreting the results (Kalnay *et al* 1996).

[3] http://www.cpc.ncep.noaa.gov/products/wesley/reanalysis.html

3.4. Self-Organising Map

Self-Organising Maps (SOMs) were used in the second data analysis sections of this thesis. SOMs are a relatively new data analysis technique in the climate field and therefore a short description of SOMs is provided below.

A Self Organizing Map (SOM) is a type of Artificial Neural Network (ANN). It is a tool that is able to extract and visualize the important characteristics of the multidimensional data distribution function while still retaining the continuous nature of the data (Hewitson and Crane, 2006). SOMs can be thought of as a dimension reduction tool, or as being similar to traditional clustering techniques. They "seek to place an arbitrary number of nodes within the data space such that the distribution of nodes are representative of the multi-dimensional distribution function, with the nodes being more closely spaced in regions of high data density" (Hewitson and Crane, 2002, p14). SOMs differ from other clustering techniques in that they do not aim to identify clusters in the data; instead they try to find archetypal points that represent the area of data surrounding them. They also differ in that there are no distinct boundaries between groups, and individual data points can contribute to the definition of more than one group (Hewitson and Crane, 2006).

SOMs make use of an iterative training procedure, which is represented diagrammatically in Figure 3.2 below. The input data are provided as a matrix of n variables and m observations. The output layer of the SOM is laid out as a two-dimensional XY array of nodes (though 1 or 3 dimensions are also possible). Each node in the array is described by a $(1, n)$ reference vector. The reference vectors are initially assigned random values, or values based on the loading of the first two eigenvalues of the input data (Crane and Hewitson, 2003).

The SOM is trained by presenting input vectors $(1,n)$ to the network one at a time. The input vector is compared to each of the SOM node reference vectors. The node which most closely matches the input vector is termed the *winning* node. The reference vector

of this node is then updated by adjusting it slightly to better match the input data vector. The amount of adjustment is determined by the user and termed the *learning rate*. Not only is the *winning* node updated, but the surrounding nodes (within a user-defined *update neighbourhood*) are also adjusted in proportion to their distance away from this node. This process is repeated for each data record, and continues through a number of iterations of the full dataset. The *learning rate* and size of the *update neighbourhood* are reduced with successive passes through the dataset. This allows the training to initially determine the broad patterns, but to then slowly uncover the finer-scale variability. The training procedure continues until there is no further change in the SOM reference vectors (Main, 1997; Crane and Hewitson, 2003).

The SOM used in the second data analysis section were created using SOM-PAK 3.1 software (Kohonen et al., 1996) (See Section 3.4.4. for description of the analysis methods, and Chapter 5 for results). It was randomly initialized with a rectangular lattice-type topology and the *update neighbourhood* defined as a step function. The training was done in four passes. The initial pass roughly ordered the reference vectors, while the subsequent stages fine-tuned them. The first training pass was kept short with the initial neighbourhood radius set to the full width of the map (4 units), after which it was linearly reduced to one. The *learning rate* was also initially set quite large (0.1) and decreased to zero during training. The subsequent training phases were of longer duration, with each successive phase employing shorter training lengths (400 000, 100 000, 40 000), learning rates (0.05, 0.025, 0.01) and neighbourhoods (3, 2, 1) (See Kohonen et al. (1996) for further details on running the SOM).

Once the training is complete, each node is a vector that describes the mean value of the nearby cloud of observations in the multi-dimensional data space. The location of the nodes is organised so that they span the data space but are concentrated in regions of higher data density (Crane and Hewitson, 2003). The characteristics of each node can be visualised in the same form as that of the input data. If these archetypes are laid out in the same two-dimensional format of the array, the topological characteristics of the data become discernable. The original input dataset, or new but compatible dataset, can then

be presented to the SOM once again. It will then map each observation to a node in the two-dimensional node space.

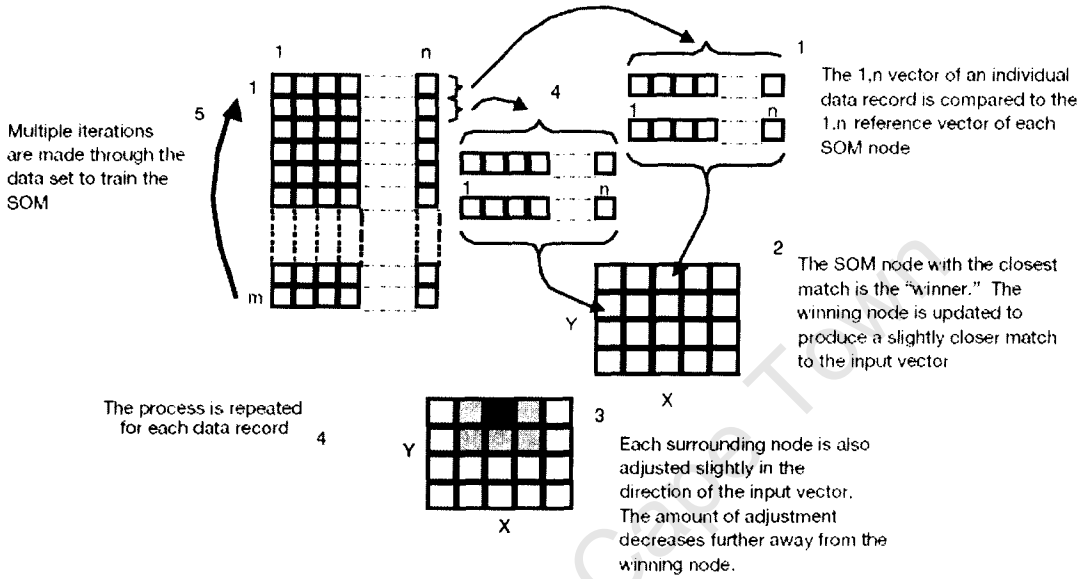

Figure 3.2 The Iterative Self-Organising Map (SOM) training procedure (source: Crane and Hewitson 2003)

A number of further analyses can be done on the output from the SOM. The error with which the observations are mapped to the nodes can be explored. The frequency of data mapping to each node, or the progression from one node to the next can then easily be visualised and interpreted (Main, 1997; Hewitson and Crane, 2002). For further details on SOMs, the reader is referred to the work by Teuvo Kohonen (Kohonen, 1990 and 1995). There are also a number of useful online references which provide good descriptions on the SOM procedures[4]. There are also a growing body of climate literature which makes use of SOMs (Main, 1997; Hudson, 1998; Ambroise et al., 2000; Cavazos, 2000; Crain and Hewitson, 2003; Hewitson and Crane, 2002 and 2006).

[4] Self-Organising Maps http://davis.wpi.edu/~matt/courses/soms/
SOM Toolbox: Intro to SOM by Teuvo Kohonen
http://www.cis.hut.fi/projects/somtoolbox/theory/somalgorithm.shtml

3.5. Methodology

The study is separated into two parts. The first section provides a simple qualitative assessment of the spatial variability of cloud cover and the diurnal variation of cloud cover at the seasonal time-scale (Results are discussed in Chapter 4). While the second section (results of which can be found in Chapter 5) provides more detail on the diurnal variation of clouds and interpreted these results in terms of the life-cycle and the interaction between clouds at these different vertical levels. This section required the data to be averaged over region that show coherent cloud variations.

This study is limited by the coarse 2.5° spatial resolution of the data and can only provide information on the large-scale cloud features. The cloud cover variable used in this study is not identical to that used in surface, or model simulation, studies. The results in this study are presented each hour at local solar time, interpolated from the original satellite derived data at three-hourly resolution and which were reported at Coordinated Universal Time (UTC). Therefore the exact hour of maximum or minimum cloudiness may not always be discernable. The study does not delve into a detailed discussion on cloud physics or the convective processes responsible for the spatial and temporal variation found in the data since this is beyond the scope of the study.

In light of the broad objectives discussed in Chapter One, the methodologies used in this study can be summarised as follows:

- The reformatting of the ISCCP-D1 cloud data to create a 10-year regional cloud record where results are reported for three broad vertical levels at local solar time.

- The summarising of the 10-year record into concise seasonal diurnal climatologies using the long-term median value at each hour.

- The calculation of statistics to describe the diurnal variation, including the mean, the diurnal amplitude and the hours at which maximum and minimum cloud cover is reached.

- The clustering or up-scaling of the gridcell cloud records to determine the regional patterns over the study area using a Self-Organising Map

3.5.1. Cloud Data Pre-Processing

The D1 cloud data from the International Satellite Cloud Climatology Project (ISCCP) required substantial pre-processing before they were suitable for analysis. These steps are detailed below, but in general included; the extraction of the required variables from the full global data files (using ISCCP supplied extraction software); the selection and extraction of the study area from the global domain; the summarization of the seven vertical pressure levels into three vertical cloud levels; and the concatenation of all the daily, single-level data files and into one large three-level datafile.

A simple quality control analysis was then used to identify and remove obvious erroneous time steps from the dataset. The ocean gridcells were also removed from the dataset, since the study was only concerned with cloud cover over land. Finally, the data were then interpolated from the reported three-hour Coordinated Universal Time (UTC) intervals to create one-hourly Local Solar Time (LST) values, the importance of this conversion to local solar time will be explained in detail in Section 3.5.1.4 below.

3.5.1.1. Reformatting of the Cloud Data

The data were supplied in daily data files containing all variables and supplementary data for the full global domain. A programme supplied with the data was edited and used to extract the Cloud Amount variable. The data over the southern and central African region, including Madagascar (10° N - 40° S and 0° E - 50° E) were extracted from the

global domain. The regions further north were not included since they have been the focus of a number of previous studies (Machado et al., 1993; Mathon and Laurent, 2001; Fink and Reiner, 2003). The choice of 50° E as the eastern boundary was to exclude the swath of less reliable data over the central Indian Ocean, arising from the lack of geostationary satellite coverage [5].

ISCCP reported Cloud Amount at seven vertical pressure levels. Cloud cover has been found to show clear vertical distribution patterns. Dessler et al. (2006) investigated the vertical distribution of tropical clouds and found that there were two main peaks in the cloud-top distribution. One maximum in the upper troposphere (12-17 km) and the other in the lower troposphere (generally below 4 km). A less prominent peak was also found between 6 and 8 km. The majority of the cloud studies discussed in the previous section distinguished between clouds located in only three broad pressure levels, which correspond to the vertical levels mentioned above. Therefore this thesis chose to combine the seven pressure levels into three broad cloud levels.

The values for the three upper pressure levels ($10 \leq PC \leq 180$ hPa; $180 \leq PC \leq 310$ hPa; $310 \leq PC \leq 440$ hPa) were summed to create a broad upper-level class called High-Level Cloud Amount (HLCA). Values in the next two levels ($440 \leq PC \leq 560$ hPa; $560 \leq PC \leq 680$ hPa) were combined to create a variable called Mid-Level Cloud Amount (MLCA). The values within the two pressure levels closest to the surface ($680 \leq PC \leq 800$ hPa; $800 \leq PC \leq 1000$ hPa) were combined to create a new variable called Low-Level Cloud Amount (LLCA). Table 3.1 below, provides a summary of the ISCCP-D1 data available, and that used for this study.

[5] ISCCP DX/D1/D2 New Cloud Data Documentation http://isccp.giss.nasa.gov/docs/D-toc.html

Table 3. 1 Specifications of Data used in this project

Dataset Name	**ISCCP D1**	
Variable Name	**Cloud Amount in 7 pressure categories**	
Dimensions	**Available**	**Used**
Period	Jul. 1983 - Sep. 2001	Jan. 1984 - Dec. 1993
Temporal Resolution	3-hourly	1-hourly (interpolated)
Spatial Resolution	280-km equal area grid	2.5° equal angle grid
Spatial Domain	Global	40°S - 10°N; 0°E - 50°E
Vertical Resolution	7 vertical pressure levels	3 vertical cloud levels
	10 < PC ≤ 180 mb	
	180 < PC ≤ 310 mb	High Cloud
	310 < PC ≤ 440 mb	(10 ≤ PC ≤ 440 mb)
	440 < PC ≤ 560 mb	Middle Cloud
	560 < PC ≤ 680 mb	(440 ≤ PC ≤ 680 mb)
	680 < PC ≤ 800 mb	Low Cloud
	800 < PC ≤ 1000 mb	(680 ≤ PC ≤ 1000 mb)

3.5.1.2. Removal of Missing Data

Low-level cloud is common and geographically extensive, especially over the oceanic regions. A simple visual exploration of the LLCA data identified a number of images which showed large areas of no LLCA extending in a swath north to south over the Africa Continent (Figure 3.3 illustrates). These areas do not appear to be natural in origin, but rather due to misdetection by the satellites. These same areas of missing data were also evident, though less clearly, in the two higher cloud levels and so data for all three levels were removed from the dataset. 602 Time steps (roughly 2% of all scenes) were set to undefined.

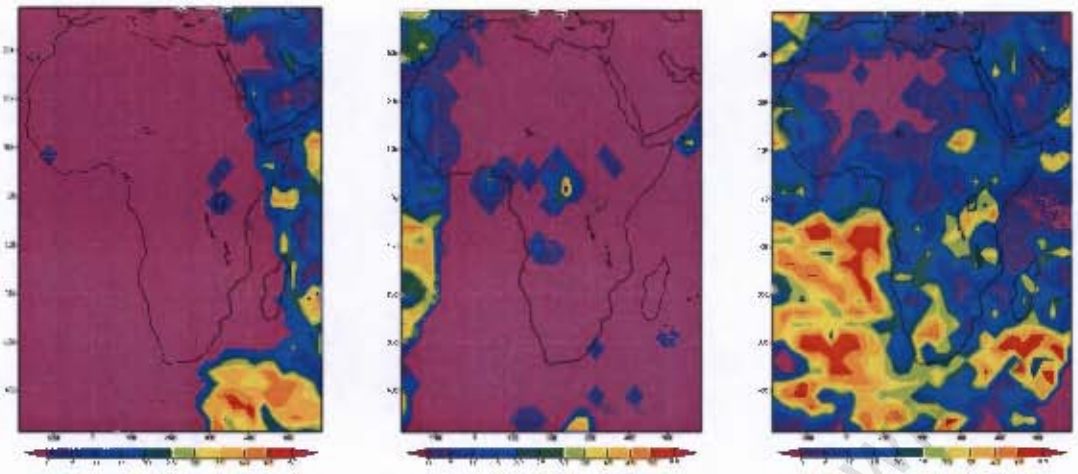

Figure 3.3 Examples of erroneous time steps. Erroneous low-level Cloud Amount (left and centre), a normal image directly following the centre image (right)

3.5.1.3. Masking out of Ocean Grid Cells

The diurnal cycle of cloudiness is found to be very different over the marine versus continental locations. The focus of the study is on terrestrial areas, and accordingly the ocean gridcells were removed from the analysis. This was achieved using a simple land mask, which made use of the elevation of a gridcell to set all ocean grid cells to 'undefined'.

3.5.1.4. Temporal Modifications

The ISCCP results are reported at three-hour intervals at 0000, 0300, 0600 ... 2100 Coordinated Universal Time (UTC). The large African domain of this study extends across a number of time-zones. The midnight or 0000 UTC time step corresponds to 0100 local solar time (LST) over Cameroon and 0300 LST over Madagascar. The diurnal cycle of clouds is strongly influenced by the incident angle of solar radiation. Therefore the data needed to be converted from being reported at UTC to being reported at local solar time.

A natural cubic spline was used to interpolate the data to hourly intervals and to shift the hour of reporting to local solar time based on the longitude of each grid cell. The data were then written out in such a way that all grid cell values for a specific local solar hour were written out to the same time step (0000 LST, 0100 LST, 0200 LST ... 2300 LST).

The natural spline was run over the full 10-year dataset but it had difficulty dealing with missing data (like those created by the removal of erroneous time steps). Therefore these gaps in the data were flagged. Single missing timesteps were ignored, since the spline was believed to be robust enough to interpolate across the 5-hour gap in the data. Longer periods of missing data showed clear errors. These longer periods, as well as the time steps directly before and after them (12 hours on either side), were incorrectly interpolated by the spline and needed to be removed. This resulted in 64 chunks of data, of varying length, being set to 'undefined'. A less significant problem produced by the spline was that it introduced a very low amplitude sine wave into periods where no cloud amount was reported and inserted very small negative values into the dataset. The problem was partially remedied by reassigning all negative values back to zero.

The three-hour difference between the Greenwich meridian and the far eastern boundary of the study area resulted in the first recorded time step common to the full domain being 03z01jan1984 and the last time step being 20z31dec1993. Therefore the first and the last day of the time series were incomplete and were discarded from the dataset.

Once all these reformatting steps were complete, the cloud information was concatenated into one large data file. This contained Cloud Amount (CA) at three vertical levels being high-level (10 hPa – 440 hPa), mid-level (440 hPa – 680 hPa) and low-level (680 hPa – 1000 hPa). The file covered 10 years of hourly data (00z02jan1984 - 23z30dec1993) for the domain 10° N - 40° S, 0° E - 50° E at 2.5° latitude-longitude spatial resolution.

3.5.2. Data Summarisation

This large datafile was separated according to season. This created four 10-year seasonal datafiles: December-February (DJF), March-May (MAM), June-August (JJA) and September-November (SON).

These four seasonal datafiles were then used to generate seasonal climatologies of the 24-hour diurnal cycle. These summaries were determined by averaging all the values for a given hour of the day through time. For example, all midnight values for the December-February seasons were averaged together to obtain a single midnight value for DJF. The median value rather than the mean was chosen to ensure that extreme values did not skew the results. The datafiles reflect a seasonal climatological 24-hour period where each hour is given in a timestep. Each timestep includes cloudiness at the three vertical levels over southern and central Africa domain.

3.5.3. Qualitative Assessment of the Spatial Cloud Diurnal Variability

The first stage of analysis (see Chapter 4 for results) provided a simple qualitative assessment of the spatial distribution of the cloud diurnal variations over southern and central Africa. Much of the spatial variability was due to seasonal differences. Therefore the diurnal variations of cloud cover were averaged over each season. The association between the vertical and horizontal distribution of cloud cover and humidity was also briefly referred to in this section.

The cloud data used in this analysis were taken from the four short seasonal summaries which represent seasonal diurnal climatologies (see section 3.5.2 above for further details). Four variables were used to describe the diurnal cycle of cloud cover for each of the cloud levels.

They were:

- The seasonal mean cloud amount – the mean value for each gridcell

- The trough-to-peak amplitude of the diurnal cycle – the difference between the largest and smallest value in the 24-hour diurnal cycle.

- The hour of maximum cloud cover – the timestep which had the highest value (where there were two or more maximum values, the first time step was recorded).

- The hour of minimum cloud cover – the timestep which had the lowest value (where there were two or more minimum values, the first time step was recorded).

The variables were displayed as spatial plots over the southern and central African region. The grid cell values of the daily mean cloudiness and the peak-to-trough amplitude were shown simply as the Cloud Amount values (or number of cloudy pixels within the grid cell). The phase was displayed as the hour of maximum and hour of minimum Cloud Amount ranging from 0 (2400 LST) to 23 (2300 LST). A continuous colour palette was used so that no discontinuity around midnight was evident.

Seasonal climatologies of specific humidity (kg/kg) were obtained from NCEP/NCAR datasets (see Section 3.3 for further details) The horizontal and vertical distribution of specific humidity was displayed as total tropospheric humidity and as a proportion of humidity found in the lower (1000 hPa - 700 hPa), mid (600 hPa – 500 hPa) and upper (400 hPa – 300 hPa) troposphere.

3.5.4. Regionally Averaged Cloud Diurnal Cycle

The second analysis section of the study investigated the diurnal variation of clouds in more detail (see Chapter 5 for results). It looked at the spatially-averaged diurnal variations of cloud cover. This allowed the diurnal variations to be described by the rate of cloud growth and decay, as well as the diurnal amplitude and phase of the cycle. It also enabled the diurnal variations of the three cloud levels to be investigated together. This information was then used to interpret the cloud results in terms of the life-cycle of convective cloudiness.

Regions are often determined arbitrarily or according to external factors such as political or geographic boundaries. This study chose to separate the study area according to the long-term variations in cloud cover over each location. A Self-Organising Map (SOM), discussed above in Section 3.4, was used to divide the southern and central African study areas into regions of coherent cloud climatologies.

The SOM was used in a similar manner to that of other traditional clustering techniques to regionalise or 'upscale' the cloud data from the grid-cell resolution to a coarser spatial resolution. The methodology used in this section closely followed that described in the paper by Crane and Hewitson (2003).

In this instance, the SOM was trained using similarity matrices, where each line or observation was the covariance between one gridcell and every other gridcell in the study area.

3.5.4.1. Input Data: Covariance Matrix

The original cloud data were not directly used to train the SOM. Instead a measure of similarity between each gridcell and every other gridcell was calculated for each of the three vertical levels. The resultant similarity matrices were used to train the SOM. Any measure of similarity could have been chosen, but covariance, which is the tendency for two datasets to vary together (co-vary) was used. It allowed the magnitude of the common variance to be a factor in determining the similarity of the datasets.

A covariance matrix is simply a collection of many covariance in the form of an n-1 x n matrix, where n is the number of gridcells.

Given n sets of samples, the covariance of two samples r_1 and r_2 is given by:

$$\text{Cov}(r_1, r_2) = 1/n * \Sigma (r_{1\,i} - r_{1\,ave}) * (r_{2\,i} - r_{2\,ave}) \quad (1)$$

The covariance was determined in two steps. First the data were standardised (mean and standard deviations provided in Appendix C) and secondly the covariance of two samples r_1 and r_2 was given by:

$$\text{Cov}(r_1, r_2) = 1/n * \Sigma (r_{1\,i} * r_{2\,i}) \quad (2)$$

A covariance matrix was created for each of the three vertical cloud levels. Each of the resultant covariance matrices for all the gridcells within this southern and central African study area (20 x 20 gridcell array) were used to produce a 399 x 400 covariance matrix with each line representing the convariances for a single gridcell or observation.

Of these gridcells, just under half (195) were located over oceans. Therefore all rows representing the covariance for these undefined ocean gridcells with all the other

locations were removed. The columns that represented the covariance of continental gridcells with these undefined ocean gridcells were also removed from the matrix. This produced a much smaller similarity matrix of 204 x 205 values.

The three covariance matrices representing the three cloud levels were then concatenated to create a 612 x 205 value matrix. The data were then converted from binary to ASCII and the number of samples was inserted in the first line.

3.5.4.2. Self-Organizing Map Routine

A number of different size SOM arrays were trained in order to subjectively determine the best balance between producing a small enough number of archetypes to facilitate ease of analysis, while avoiding too much generalization. It should be noted that the results were stable across these different SOM array sizes and therefore the larger SOM arrays were not more accurate, only more detailed (See Crane and Hewitson, 2003).

The results from a 2x4, 3x4, 3x5, 4x5, 4x6 and a 5x6 node SOM array were compared and the 4x6 node array was chosen to cluster the gridcells into 24 coherent cloud regions. This size array was chosen since it not only identified the main climate regions, but also the more transitional regions. The SOM also identified a few small regions which showed quite unique cloud climatologies. The larger 5x6 node SOM was not selected, even though it provided 30 nodes and therefore more regional detail, because in spite of the increased detail, the SOM still mapped the remote north-eastern and south-western parts to the same archetype.

3.5.4.3. Self-Organising Map Outputs

Once the SOM training was complete, the mapping of the nodes was visually inspected using a Sammon Map. A Sammon Map is an iterative technique where the n-dimensional input vectors are mapped to 2-dimensional points on a plane. The distance between the image vectors tends to approximate to Euclidian distance of the input vectors. The Sammon Map provided an indication of the similarity between nodes in the data-space. This information, along with other information discussed later, was be used to determine the distribution of the nodes in the data-space and to identify regions of high and low data density.

The SOM also generated a list of coordinates corresponding to the best-matching node in the map for each input observation. It also provided the individual quantisation error of the node (Kohonen et al., 1995). The node coordinates were converted to a single number ranging from 1 to 24. These numbers were used to identify the gridcells which mapped to each of the nodes. This created a template showing the location and extent of each cloud climatology region.

This regional template was then used as a mask to extract the cloud data for each of the 24 separate regions from the four seasonal datafile summaries, producing 96 small regional summary files (4 seasonal files for each of the 24 regions). The individual quantisation errors were average for each node in order to infer the within-group variability.

The diurnal cycle of Cloud Amount at each of the three vertical cloud levels and for total cloud amount (the sum of Cloud Amount at all three levels), was calculated for each region. The results were displayed as simple line-graphs showing area-average cloud amount values across the 24 hours of the day.

3.6. Summary

This chapter has described the data and methodology used in this study. It first provided a brief description of the International Satellite Cloud Climatology Project (ISCCP) and discussed the cloud variable used in this thesis. It also provided a short description of the climate data obtained from the NCEP/NCAR Reanalysis Project. A brief description of the Self-Organising Map tool was then given, since it was used to regionalise the study area.

The focus of the chapter then moved on to the methodology employed in the thesis. It discussed the methods used to reformat and summarise the data. A short description of the different analysis methods utilized to assess the spatial and regional cloud diurnal variability. The thesis now moves on to present the results from each of these analyses in the next two chapters.

CHAPTER 4

QUALITATIVE ASSESSMENT OF THE SPATIAL CLOUD DIURNAL VARIABILITY

4.1. Introduction

This chapter explores the general characteristics of the diurnal cycle of cloud cover over southern and central Africa. The seasonal average horizontal distribution of diurnal variability is investigated for each of the three vertical cloud levels using, the mean cloud amount, the peak-to-trough amplitude and phase of the diurnal cycle. More information on the method used to calculate these data can be found in the preceding Data and Methodology Chapter (Chapter 3).

The focus of this study is the diurnal variation of cloud cover. However, it is first useful to determine the mean seasonal variation of cloud cover at each of the levels, and to relate these patterns to the distribution of specific humidity and circulation patterns. The chapter will then assess the broad spatial cloud diurnal variability.

4.2. Seasonally Averaged Cloud Distribution

Figure 4.1 displays the seasonal climatologies of mean cloud amount. The seasonal climatologies are (DJF, MAM, JJA and SON from left to right) for high-level cloud amount (top row), mid-level cloud amount (middle row) and low-level cloud amount (bottom row). The variables are reported as cloud amount or number of cloudy pixels located in each level.

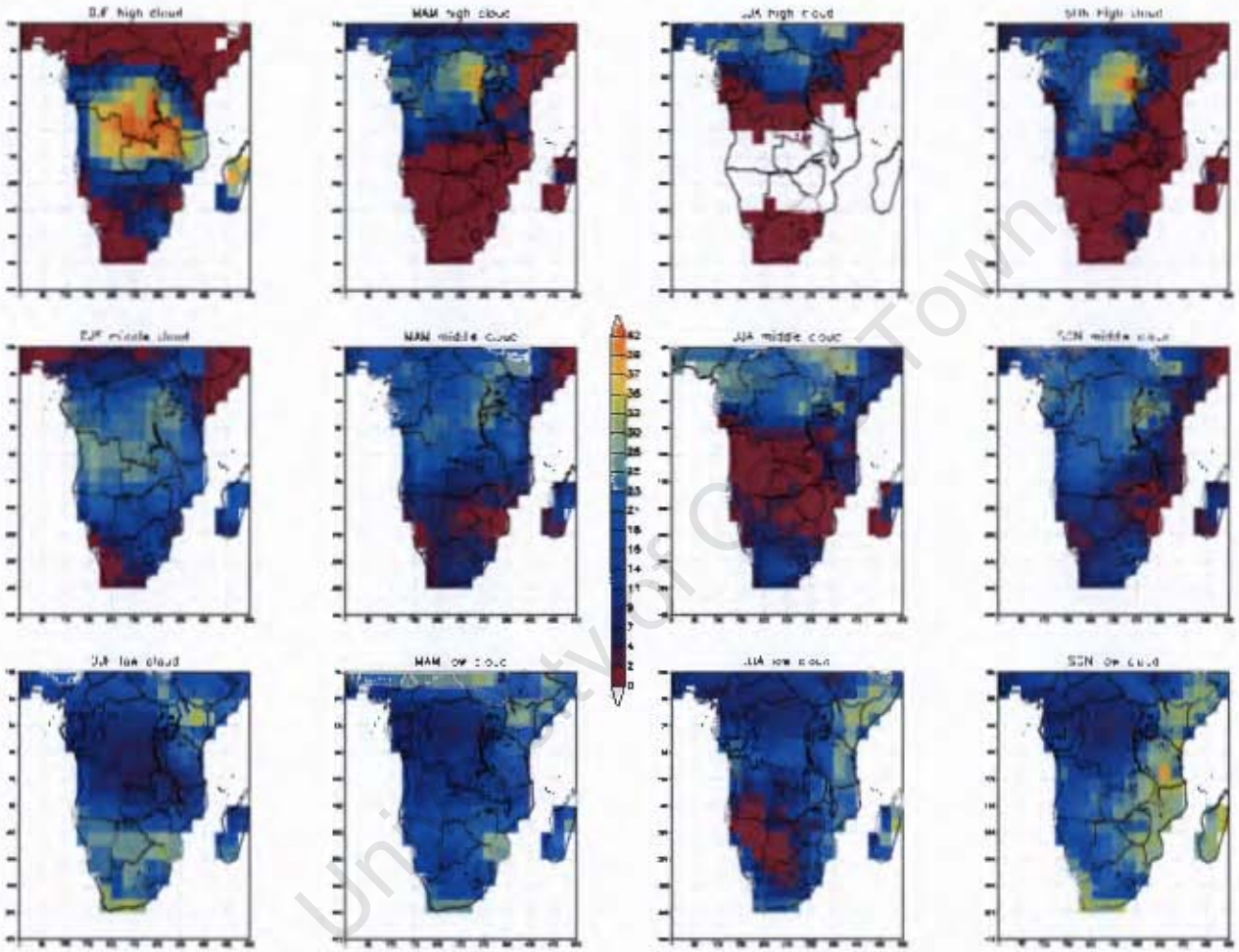

Figure 4.1 Ten-year Seasonal Climatologies of Mean Cloud Amount (number of cloudy pixels) - HLCA (top row), MLCA (middle row) and LLCA (bottom row) for DJF, MAM, JJA and SON (left to right) 1984 – 1993

4.2.1. Seasonal Mean High-Level Cloud Amount

Figure 4.1 shows that the seasonal mean High-Level Cloud Amount (HLCA) follows the seasonal migration of the ITCZ, being centred over the equator during MAM and SON and over 10° North (South) during the boreal (austral) summer. Large values occur over the Congo Basin, but the maximum cloud cover is found over the mountains along the Western Rift in East Africa and other mountainous regions. No HLCA, or very little, appears outside the deep convective regions with large parts of southern and east Africa experiencing very little high-level cloudiness outside of the austral summer season.

During the austral summer season (DJF) the thermal heating of the surface drives strong convection which moistens the upper troposphere and results in substantial high-level cloud over interior of the continent centred on 10° S. The highest values of HLCA occur along the southern and eastern boundary of the Congo Basin. Considerable cloudiness extends over the southern parts of the rift valley to northern Mozambique and across to the mountains of Madagascar. High-level cloud cover is also found over the central parts of southern Africa with a slight increase in cloudiness over the Highveld and eastern escarpment of South Africa.

Mean high-level cloud is reduced and spatially less extensive during austral autumn (MAM) than in it was during DJF. It is restricted to the low latitudes, occurring almost exclusively between 10° north and south and away from the east coast. Maximum values are again associated with the high mountains of the Western Rift on the border between the DRC, Uganda and Rwanda. Small secondary maximums of cloudiness occur over the Cameroon Mountains, Gabon and around Kinshasa, and over the Ethiopian Highlands.

During the austral winter season (JJA) mean HLCA is found almost exclusively in the low latitude of the northern hemisphere, since the location of the ITCZ has shifted to the northern hemisphere. The highest values are found over the mountains of Cameroon and western parts of the Ethiopian Highlands. Virtually no high-level cloud is found between

10° and 25° S. This is the result of the low thermal heating of the surface which inhibits convection and reduces the vertical transport of moisture up into the higher troposphere.

Austral spring (SON) shows a similar distribution pattern of HLCA to that found during MAM. Maximum values are again found along the border of the DRC, Uganda and Rwanda, with cloud cover decreasing slowly westward of this mountainous area. The most obvious difference in the distribution of HLCA between these two seasons is that cloudiness extends further south into Angola, and over the Highveld of South Africa. This could be due the majority of the SON season falling after the spring equinox when the solar angle is more directly over the southern parts. Another clear difference is that very little high-level cloud is found to occur along the east coast northward of South Africa.

4.2.2. Mean Mid-Level Cloud Amount

The mean mid-level cloudiness (middle row of Figure 4.1) shows similar spatial organization to that of HLCA, but coverage is more extensive over southern and eastern Africa. MLCA is generally more uniform than HLCA with smaller maximum values over deep convective regions. These results need to be interpreted in light of the severe obscuration effect from higher level cloud.

The strong surface heating during austral summer enhances convection which results in most of the study areas experiencing mid-level cloud cover. Only the far southwest, north and northeast parts of the study area show little mid-level cloudiness. Maximum daily mean values are generally found over the same locations as that of high-level clouds, but large values are also present along the coast of Angola and Gabon.

During the transition seasons (MAM and SON) the region of largest daily mean MLCA is found roughly in the same locations as that of maximum HLCA, though slightly towards the east, especially over the western rift valley and Lake Victoria. MLCA extends across

to the east coast during both of these seasons (though the values are lower during SON than MAM). It also extends in a band down from the tropics across northern Namibia and Botswana with a small increase in cloudiness over the Eastern Cape and Kwazulu Natal provinces of South Africa. The Limpopo River Valley has very little mid-level cloudiness during either of these seasons.

During austral winter (JJA) the largest mean MLCA occurs over the northern parts of the study area with maximum MLCA associated with the mountains around Lake Victoria, the Ethiopian Highlands and the Cameroon Mountains. Very little mid-level cloud occurs over the subtropics. However the region did not match that of zero HLCA, instead it stretched from Angola in the west to southern Mozambique in the east. Mid-level cloudiness still occurs over the far south; the west coast and the southern interior of South Africa experience their maximum mid-level cloudiness during this season.

4.2.3. Mean Low-Level Cloud Amount

The mean low-level cloud amount is displayed in bottom row of Figure 4.1. The most obvious feature of these figures is the large region of reduced cloudiness which follows the seasonal migration of the ITCZ. This feature is spurious and the result of the severe obscuration by the clouds above, very little can therefore be said about the cloud cover over the tropical region.

A subtle seasonal variation can be discerned over southern Africa which does not appear to be due to the obscuration effect. The western interior of the subcontinent experiences maximum LLCA during austral summer but is relatively free of clouds during the other seasons and especially during JJA, due to the stable high-pressure conditions. The southern and western coasts of South Africa show maximum low-level cloudiness during both DJF and SON. This may be due to stronger orographic uplift associated with the large-scale anticyclonic circulation over the west coast found during these seasons. The

low-lying Limpopo River area displays consistent levels of LLCA during all seasons other than austral winter when slightly less cloudiness occurs.

The countries along the east coast display maximum low-level cloud during austral spring associated with the easterly onshore winds. High values occur along the border between Ethiopia and Somalia, over Kenya, central Tanzania and Mozambique as well as extending inland into eastern Zambia. The values are lower during DJF, but this may be a function of the increased obscuration by higher-level clouds during the austral summer season.

4.2.4. Summary

Thus, in general we see at a purely descriptive level that mid- and high-level clouds show very similar seasonal distributions, moving north and southwards with the migration of the ITCZ. The most obvious difference between these two levels is that HLCA coverage is restricted to the central parts which experience the most intense convection. The seasonal distribution of low-level clouds is less easily discernable, since the true cloudiness is obscured by higher-level clouds. This being said, the coverage of LLCA appeared to be quite extensive along the east coast during SON, while the western half of southern Africa experienced maximum LLCA during austral summer.

4.3. Tropospheric Moisture

Following the above discussion, one can develop a general assessment of cloud distribution in relations to the tropospheric moisture. We first recognize that the life cycle of low-latitude continental cloud has a large diurnal variation and is strongly influenced by convection (Soden, 2000). Furthermore, Cloud growth is driven primarily from below with convection transporting moisture vertically from the surface up through the troposphere. Figure 4.2 (top row) shows seasonal climatologies of total tropospheric

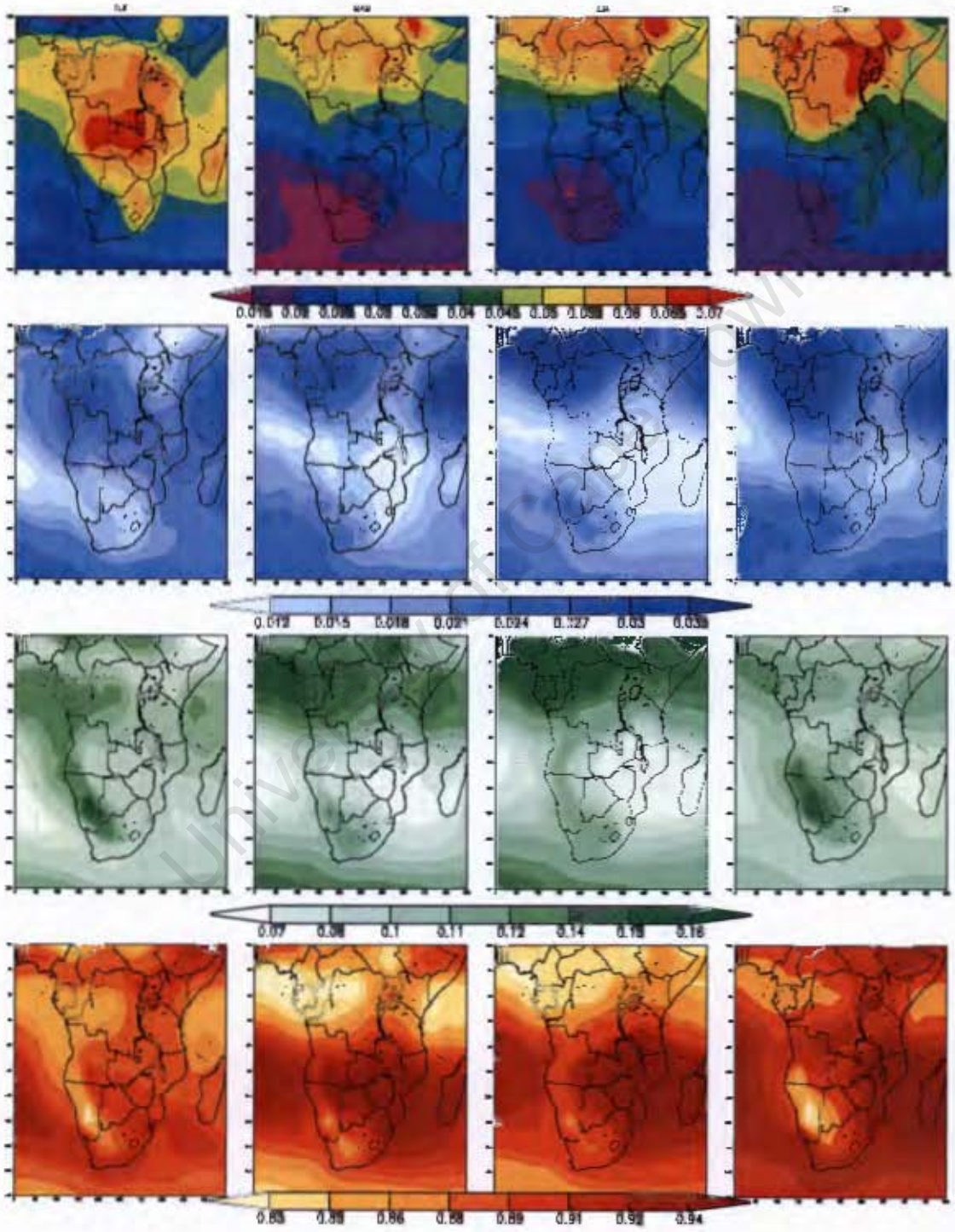

Figure 4. 2 Ten-year Climatologies of Tropospheric Humidity – Total Tropospheric Specific Humidity (kg/kg) (top row), and proportion of total humidity found in the upper-level (second row), mid-level (third row) and low-level (bottom row) troposphere for DJF, MAM, JJA and SON (left to right) 1984 – 1993

specific humidity (kg/kg) from NCEP/NCAR Reanalysis (see section 3.3 in the previous chapter for more details). It shows that the spatial distribution of humidity closely follows that of high-level cloud amount shown above.

Along with total tropospheric specific humidity, Figure 4.2 also displays the proportion of moisture found in the upper-troposphere (second row), mid-troposphere (third row) and lower-troposphere (bottom row). The majority of this moisture (80% – 94%) is found in the lower troposphere, with roughly 5% – 15% in the mid-troposphere and only 1% – 4% located in the upper troposphere.

The western tropics have significant total tropospheric humidity, but also show a larger proportion of moisture in the mid- and upper-troposphere. This suggests that large quantities of moisture are transported upwards by strong convection and that a relatively high proportion of this moisture remains aloft. The subtropics on the other hand have lower total tropospheric humidity and show that the proportion of moisture found in the upper- and mid-troposphere is much smaller, especially during austral winter. This implies that less moisture is transported to the upper-troposphere and that of this small amount of moisture, very little remains aloft.

The relative proportion of moisture found within the mid-troposphere displays clear spatial variations. Over Namibia and the Kalahari regions, total tropospheric humidity is quite low during SON and DJF, but the proportion of mid-tropospheric humidity is high (up to 15%). The eastern interior of South Africa appears as a secondary peak in both high-level cloudiness and total tropospheric humidity during DJF. However, this location is associated with a low proportion of upper-tropospheric humidity and a high proportion of lower-tropospheric humidity. So one can assume that even through there is significant high level cloud, the moisture does not remain in the upper-troposphere, instead the clouds are produced and sustained by moisture from below.

These results provide some insight into the spatial organisation of moisture at different vertical levels. The results can be interpreted in conjunction with the finding from Chung

et al (2007) which suggests that the main source of moisture to the upper troposphere is from below, transported aloft by deep convective clouds which decay into cirrus anvil clouds. Therefore the location of maximum upper-tropospheric humidity probably corresponds to the location of maximum deep convection. It can also be expected that these location of increased upper-tropospheric humidity display the early morning redevelopment of high-level cloud.

4.4. Diurnal Amplitude of Cloudiness

This next section uses the peak-to-trough diurnal amplitude to explore the spatial variability found in the seasonally averaged diurnal cycle of cloud cover (Figure 4.3) The amplitude of a periodic signal provides a measure of the strength of the variation around the mean. However, the diurnal variation of cloud is not perfectly sinusoidal and so the difference between the lowest and highest values within the diurnal period is used to characterise the strength of the diurnal variation.

4.4.1. Diurnal Amplitude of High-Level Cloud Amount

The spatial distribution of the diurnal amplitude closely follows the mean value of high-level cloud amount. The diurnal amplitude also appears to be enhanced over orographic features and where differential solar heating across land-water boundaries (or inland surface thermal boundaries) produces enhanced meso- or synoptic scale circulations.

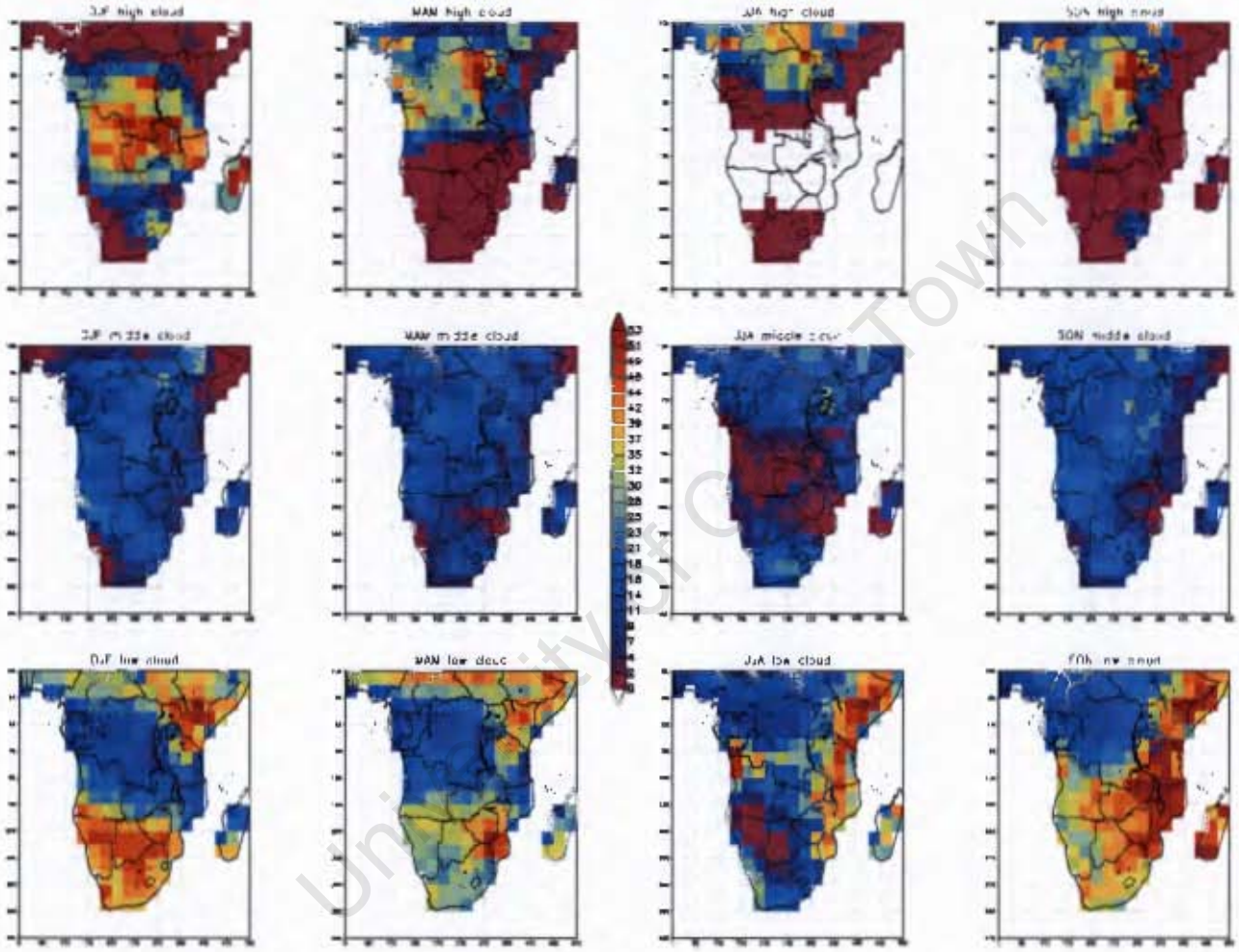

Figure 4.3 Diurnal Peak-to-Trough Amplitude of Cloud Amount (number of cloudy pixels) – HLCA (top row), MLCA (middle row) LLCA (bottom row) for DJF, MAM, JJA and SON (left to right) 1984 – 1993.

In Austral summer (DJF) the largest diurnal amplitudes of HLCA are centred over the same locations which display maximum mean cloudiness, but extend over a wider area to include Angola, Zambia and northern Mozambique (top row of Figure 4.3). The high topography of Madagascar also exhibits very large diurnal variations, even though the mean cloudiness was lower. A small regional maximum in the diurnal amplitude of high-level CA occurs over the eastern escarpment of South Africa which also seems to be enhanced by the orography.

During the transitional seasons, MAM and SON, the amplitude of the diurnal cycle of high-level cloud amount is smaller, with the largest diurnal amplitudes located over the steep topography of the Ruwenzori Mountains. Only the far northern tropics show significant diurnal amplitude of HLCA during JJA. The subtropics, having no high cloud, cannot show any diurnal variations.

4.4.2. Diurnal Amplitude of Mid-Level Cloud Amount

Mid-level Cloud (middle row of Figure 4.3) displays very small diurnal variations and the amplitude is less clearly associated with the magnitude of the mean cloudiness. Instead the amplitude remained fairly constant over the region covered by mid-level cloud. The amplitude of the diurnal cycle of MLCA shows no clear seasonal variations, remaining quite consistent in all locations where mid-level cloud occurs.

4.4.3. Diurnal Amplitude of Low-Level Cloud Amount

Low-level cloud amount has strong diurnal variations of the same magnitude as that of high-level cloud amount (bottom row of Figure 4.3) and the amplitude is again closely correlated with the mean value.

Strong seasonal variations in the amplitude are visible. During austral summer, the maximum amplitude is located over the interior of southern and far-eastern Africa.

During MAM the amplitude of the diurnal variation is generally smaller, except over the Limpopo River Basin which increased slightly. During austral winter, there is very little low-level cloud over the western interior of southern Africa, and therefore the diurnal variation is also low. The region of maximum amplitude is located just inland along the African east coast north of South Africa, and over the Congo River mouth on the west coast. The austral spring season (SON) produces maximum diurnal amplitude in all the east-coast countries north of South Africa, as well as over southern Zambia and Madagascar. The diurnal amplitude is also largest in Angola, Zambia and Zimbabwe during this season, while Namibia, Botswana and South Africa experience largest diurnal variations during austral summer.

4.5. Diurnal Phase of Cloudiness

The phase of the diurnal variation identifies the time of day (or night) at which cloud reaches its maximum and minimum extent or amount. The time of maximum and minimum cloudiness, along with the amplitude, allow the basic cloud diurnal life-cycle to be inferred.

4.5.1. Diurnal Phase of High-Level Cloud Amount

The phase of the diurnal cycle of high-level cloud amount exhibits some clear spatial differences (Figure 4.4 and 4.5). Maximum HLCA is found to occur during the late afternoon / early evening over most convective locations, except over the low-lying parts of the Congo Basin where maximum cloudiness occurs in the early hours of the morning. This delay in the timing of maximum HLCA does not strictly match the locations of highest mean cloudiness or maximum diurnal variations; instead it seems to be associated with the location of maximum upper troposphere specific humidity (see second row of Figure 4.2).

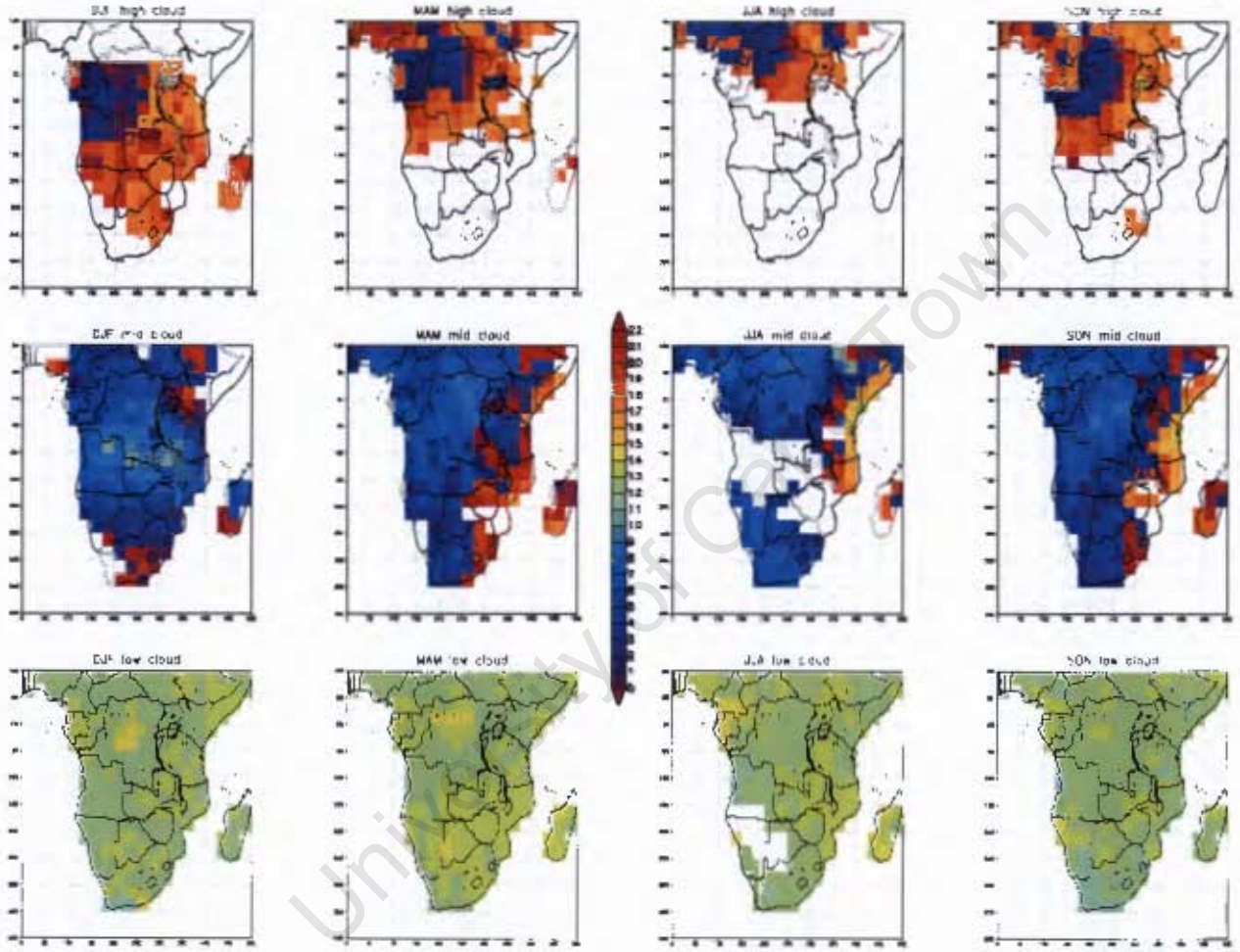

Figure 4.4 Phase of the Diurnal Cycle of Cloud Cover - Hour of Maximum Cloud Amount – HLCA (top row), MLCA (middle row), and LLCA (bottom row) for DJF, MAM, JJA and SON (left to right) 1984 – 1993. The hour is displayed as 0 - 23 (2400 LST- 2300 LST). A continuous colour pallete is used so that no discontinuity around midnight is evident.

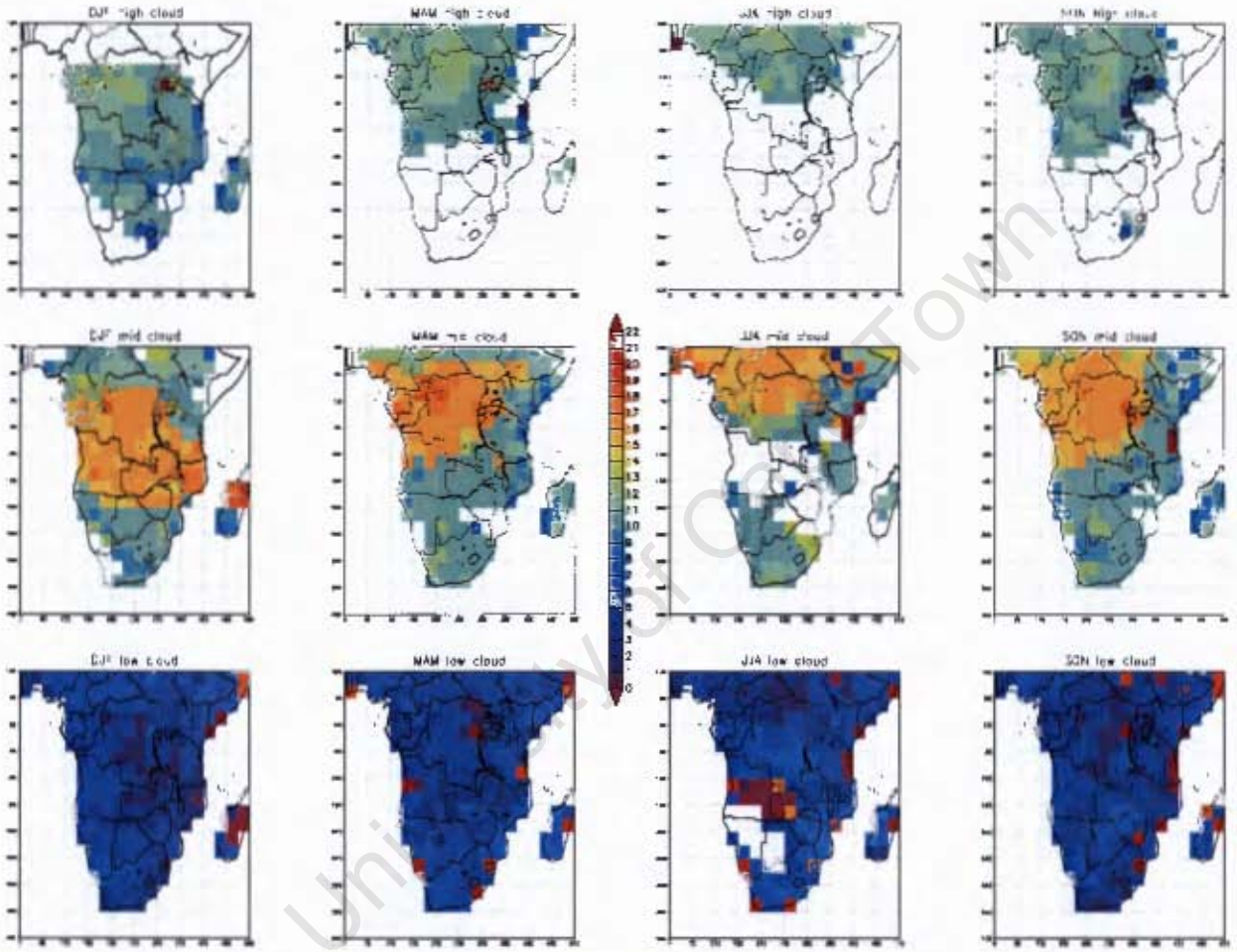

Figure 4.5 Phase of the Diurnal Cycle of Cloud Cover - Hour of Minimum Cloud Amount - HLCA (top row), MLCA (middle row) and LLCA (bottom row) for DJF, MAM, JJA and SON (left to right) 1984 – 1993. The hour is displayed as 0 - 23 (2400 LST - 2300 LST). A continuous colour pallete is used so that no discontinuity around midnight is evident.

The hour of minimum high-level cloud amount is reached within an hour of 1100 LST over almost the whole subcontinent though later in the western tropical (Figure 4.5). A very subtle exception occurs along the edge of the convective area where the minimum is reached a few hours earlier, possibly due to the smaller amount or size of high-level cloud in these boundary locations being eroded at a more rapid rate.

The western half of Lake Victoria stands out as exhibiting significant differences in the phase of HLCA in comparison to the rest of the study area; Maximum (minimum) cloudiness is found at 1300 (2300) LST, 0700 (2000) LST, 1200 (0300) LST and 1500 (0600) LST for DJF, MAM, JJA and SON respectively. These differences in phase are due to the strong mesoscale circulations over this lake basin. This region will be discussed in more detail in Chapter 5.

4.5.2. Diurnal Phase of Mid-Level Cloud Amount

Mid-level cloud reaches its diurnal maximum in the first few hours of the morning over the majority of the study area (Figure 4.4). However the hour of maximum cloudiness is delayed over regions which exhibit large diurnal variations of HLCA (Figure 4.3). An important shift in the timing of maximum cloudiness is found along the East Coast during the transitional seasons and to a lesser extent in JJA. Maximum mid-level cloudiness is found in the late afternoon to evening along the coast and is found slightly later inland. This coastal region lacks high-level cloud during these seasons which suggests that in the absence of high-level cloud, the phase of the diurnal cycle of MLCA may follow that of convection.

Minimum mid-level cloudiness is found to occur at one of two distinct periods (Figure 4.4). Over regions which do not show considerable mean HLCA, the mid-level cloudiness decreased to a minimum around 1100 LST (the same hour as minimum HLCA), while over the regions which have considerable daily mean HLCA, the minimum MLCA is found to be delayed until late afternoon (around 1600 LST) (Figure

4.5). This relationship between the timing of mid- and high-level cloud will be discussed in more detail in Chapter 5.

4.5.3. Diurnal Phase of Low-Level Cloud Amount

The phase of the diurnal cycle of low-level cloud amount displays very little regional or seasonal differences (Figure 4.3 and 4.4). In all locations, maximum LLCA is reached around 1300 LST, and minimum cloudiness occurs in the early hours of the morning before dawn. A few locations, mostly along the coast, show minimum cloud cover in the evening. This may be due to local sea breeze effects or marine influences. Minimum LLCA is found around midnight over central Angolan and western Zambian during local winter, though this may be the result of the way the minimum values were calculated; it may be that in reality there is no low-level cloud from midnight until early morning at this location.

4.6. Summary

To summarise the finding of this chapter: High-level cloud amount is associated with deep convection and therefore its spatial distribution follows the seasonal migration of the ITCZ. Mean HLCA is large over convective locations and the diurnal amplitude closely follows that of the mean. The orographic influence on the diurnal cycle of low HLCA is evident even in this low-resolution data. Maximum cloudiness if found over the steep topography around the Congo Basin. High-level cloud is found to develop from a minimum just before noon and to reach a maximum in the early evening over most locations. However, in locations which have high values of upper tropospheric humidity, the timing of diurnal maximum HLCA is delayed until roughly 0300 LST the following morning, this early morning maximum in HLCA cannot be explain through deep convective processes. Instead it may be the result of destabilization of the upper troposphere due to radiative cooling. This will be explored further in the following chapters.

Mid-level cloud amount is also associated with deep convection and high-level cloud cover. The results show that MLCA has relatively high daily mean values and is spatially extensive, but that the amplitude of the diurnal cycle is small. Most locations report maximum mid-level cloud in the early morning, or slightly later in regions associated with intense convection. This can be explained by the sinking or erosion of the high-level cloud-top through the night. However, in locations where high-level cloud is not prevalent, such as along the east coast, mid-level cloud amount peaks in the early evening suggesting that in these locations shallower convection predominate. MLCA displays an interesting variation in the timing of minimum cloudiness; in the absence of HLCA, it decreases to a minimum at the same time as LCCA (1100 LST), while in locations which have high-level cloud; it only reaches its minimum in the mid-afternoon. This minimum in the mid-afternoon is hard to explain in terms of convection and will be discussed further in the following chapters.

Low-level cloudiness exhibits quite dissimilar spatial patterns to that of the two higher levels. It shows strong diurnal variation, which is clearly associated with the diurnal cycle of surface heating, advection and orographic influences. It increases from a minimum in the early morning to peak just after noon over the whole study area. The low-level cloud amount over much of the study areas suffers from the obscuration by higher level clouds and therefore little can be said about the magnitude of the mean or the amplitude of the diurnal cycle. However the phase of the cycle appears to be accurately recorded and matches that of surface observation (Rossow et al., 1993).

CHAPTER 5

REGIONAL DIFFERENCES IN CLOUD DIURNAL CYCLE

5.1. Introduction

The previous chapter provided a summary of the seasonal average cloud diurnal cycle for different cloud levels. It focussed on the mean values, and the diurnal amplitude and phase (hour of maximum and minimum cloud amount) of upper-, mid- and low-level cloud amount. This chapter provides a more detailed exploration of the data by investigating the diurnal variations within smaller geographic regions.

The chapter first discusses the results from the regionalization procedure. A Self-Organising Map was used to classify the study area into smaller regions according the similarity of each location's cloud variation. The diurnal cycle of cloudiness is then investigated within selected regions. The life-cycle of shallow and deep convective cloudiness is inferred from the results and the regional differences discussed in relation to possible driving mechanisms.

5.2. Regionalisation

The clear spatial differences in the diurnal cycle of cloud amount found in the previous chapter justified the subdivision of the African continent into smaller geographic regions. We employed a Self Organizing Map (SOM) to regionalize or 'up-scale' the data from the grid-cell resolution to a coarser regional-scale resolution following the procedure of Crane and Hewitson (2003) (The methodology was outlined in Section 3.7.1). This regionalisation was performed using a measure of similarity of the gridcells' long-term mean cloud variation. Each continental gridcell was assigned to an archetype which most

closely matched its own climatological cloud variability. Therefore all the grid cells which mapped to the same archetype are effectively clustered as members of the same cloud climatology group since they all have similar cloud variations through time.

5.2.1. Self-Organizing Map Up-Scaling

A number of different size SOMs were trained using the covariance of cloud record at each of the three cloud levels for each gridcell with every other gridcell in the study area. Of these, the 4×6 array SOM (24 nodes) was found to provide the most appropriate level of generalisation. Therefore the following section will focus on the results from the training of this SOM size.

The SOM represents the full range of cloud histories (represented by the covariances) found across the study area, as 24 archetypes. Similar archetypes are located close to each other and very different ones are placed far apart in the array. A Sammon Map or distortion surface (Figure 5.1a) displays the similarity (or dissimilarity) as a measure of distance in data space between each archetype and its neighbouring archetypes.

The Sammon Map shows that the array is not strictly rectangular in shape; the top left to bottom right diagonal is shorter than the top right to bottom left diagonal. This indicates that Node 6 and 19 represent more dissimilar states than Nodes 1 and 24 (refer to figure 5.1b for node numbering and colour convention). The nodes in the left half of the SOM are relatively evenly spaced, but a significant difference exists between the nodes on the left and right side of the array. The nodes on the right are less closely or evenly spaced, especially in the horizontal direction. Node 15, and to a lesser extent Node 16, stands out as being the most dissimilar to the nodes around it.

In effect the node distribution across data space reflects that more nodes are required to capture the variation in some regions of the data space, where as in other regions of data space the variation is more homogenous (see discussion in Hewitson and Crane, 2003).

(a) (b)

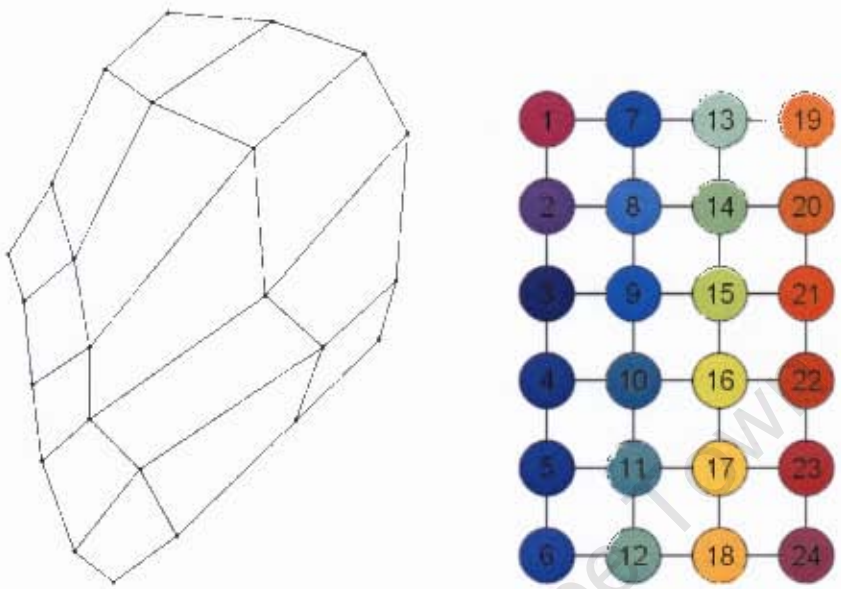

Figure 5.1 **(a) SOM node distortion surface (b) a stylised representation of the SOM node numbering and colouring convention used to associate the SOM node distorted surface (Figure 5.1a) and the SOM node average error plot (Figure 5.3) with the regions displayed in Figure 5.2**

Each of the 205 continental gridcells making up the study area was associated with the archetype that most closely matched its own 10-year cloud climatology. This is displayed as a spatial map (Figure 5.2), where each gridcell is numbered according to the archetype of long-term cloud climatology to which it mapped. The map shows that the SOM nodes are clearly geographically arrange across the study area. Grid cells which map to the same archetype are, for the most part, spatially contiguous and form discrete geographic regions. However, some distant locations do map to the same archetype due to similarities in their long-term cloud climatologies. These remote areas may share similar cloud variations, but the underlying mechanisms responsible for these similar variations may be very different.

These spatially coherent groupings, allows for amalgamating of the gridcells into geographic regions which allows the regional attributes of the cloud diurnal variations to be explored.

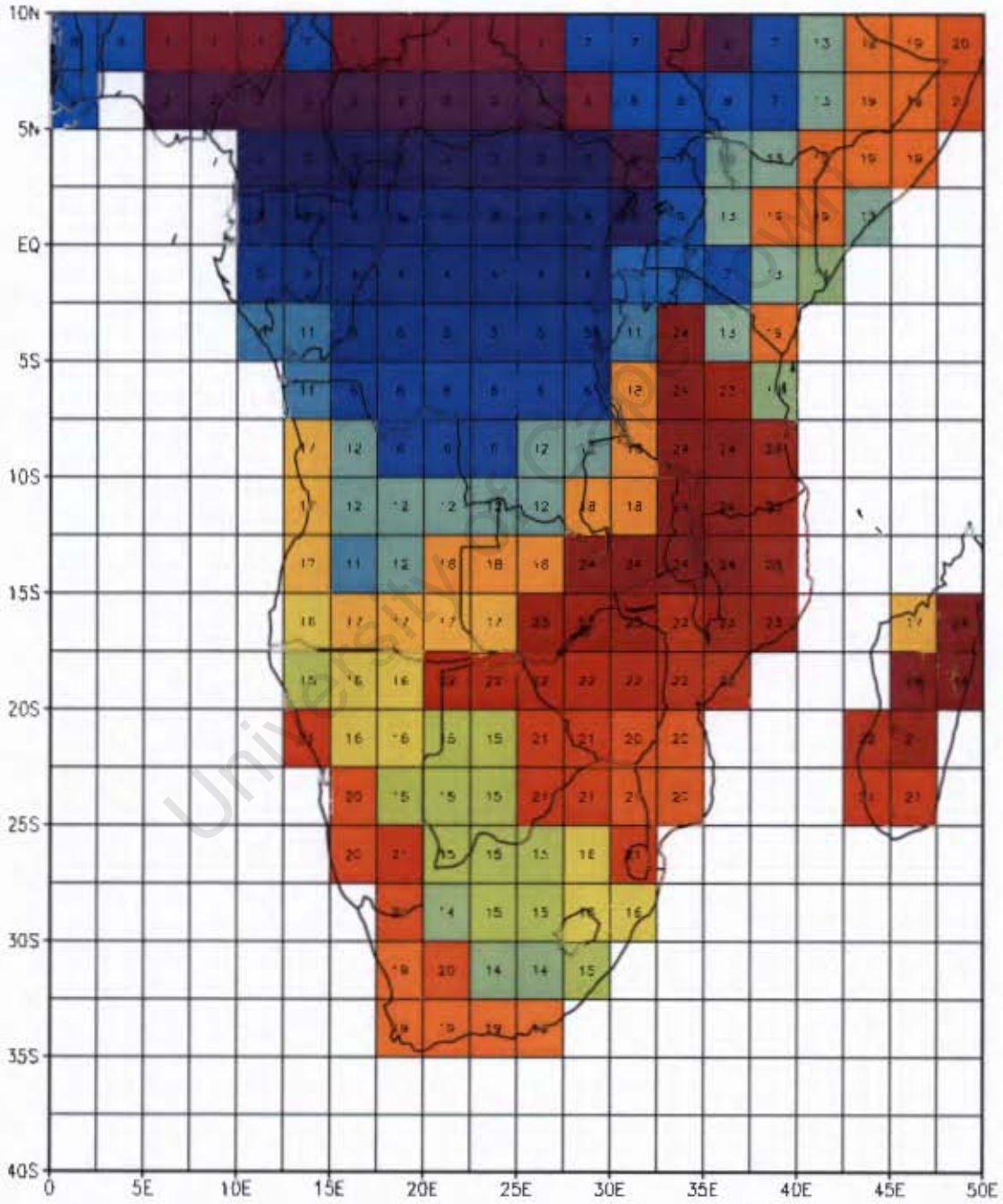

Figure 5.2 **Results of the 4 x 6 node SOM Regionalization. The numbers and colours refer to the SOM node to which the gridcell mapped.**

5.2.2. Geographic Regions

Figure 5.2 shows the spatial map of geographic regions determined through the up-scaling procedure. The nodes within the left half of the node array are quite clearly geographically organized from north to south as one moves down through the SOM array. The first column of nodes represent the deep convection locations (Regions 1 – 6), while those in the second column are associated with the transitional regions on the edge of these deep tropical locations (Region 7 – 12). The central Congo Basin (Region 4) is placed halfway down the one side of the node array, with the far northern (Region 1) and southern (Region 6) extensions of deep convective cloud cover assigned to the top-left and bottom-left corner nodes respectively. The relatively even spacing of the nodes in the first two columns suggests that they may capture the seasonal migration of the ITCZ.

The bottom row of the node array is associated with the regions along the south-eastern extension of tropical convection found during austral summer (Region 6, 12, 18 and 24), while the top row is associated with the far northern regions from west to east (Region 1, 7, 13 and 19).

The spatial organisation of the geographic regions associated with the archetypes in the right half of the SOM array are roughly organised from north to south as one moves upwards through the array from region 24. Regions in the far right column are generally located to the east of those in the next column. Both the regions in the far southwest and northeast of the study areas mapped to the nodes in the top right of the array.

Figure 5.3 displays the average error with which the samples mapped to the nodes – in effect a measure of the within-group variance of the clustered cells. The results show interesting differences between the cloud climatology archetypes. The node with the highest average error is Node 10 found over Lake Victoria. This node is similar to the more tropical archetypes (see small distance in Figure 5.1a), but only two gridcells mapped to this archetype. This suggests that the two gridcells have very distinct

climatologies and that neither of them is well represented by the archetype. As the SOM generalises, such grouping is not unexpected where there are strong spatial gradients in the cloud attributes. A larger SOM could separate these out, but for the purposes of this study the intention is to retain a greater degree of generalization. As noted by Hewitson and Crane (2003), nodes in the centre of the node array are indicative of intermediate states. In this instance it implies that climatology of Node 10 represents a boundary spatial state.

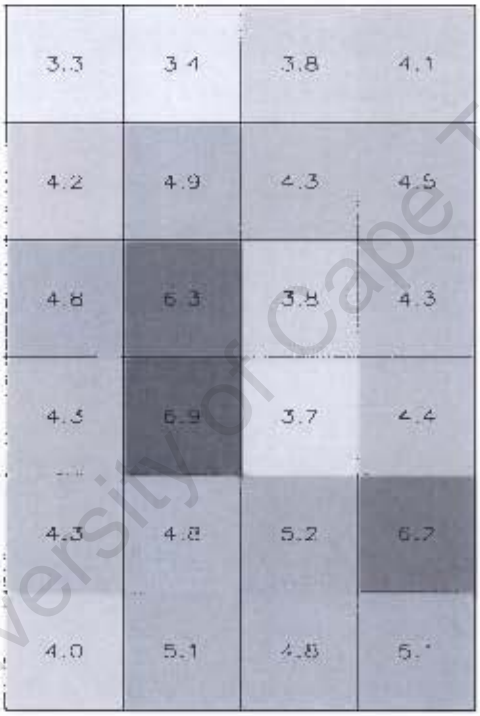

Figure 5.3 Average Error (covariance) of all grid cells mapping to each node in 4×6 SOM. The corner nodes of the SOM array are: 1 (top left corner), 6 (bottom left corner), 19 (top right corner) and 24 (bottom right corner).

The average error with which the gridcells mapped to Node 23 is also large, indicative of large within group variance. This suggests that the archetype represents a grouping of cells dissimilar to each other and also not well accommodated in other groups. As such they are representative of locations where there are strong local controls on the cloud. The gridcells which map to this archetype are located in diverse location; along the southern Tanzanian and northern Mozambique coast and inland over the Zambezi River

as well as over the mountains of southern Madagascar. It is therefore not surprising that this node has such a large average error.

The lowest average errors are found for the nodes associated with locations in the far north of the study area (node 1 and 7), followed by the Kalahari (node 15), northern Namibia and Highveld of South Africa (node 16). This implies that the cloud climatology's over these regions are quite uniform even over significant geographic areas.

5.2.3. Geographic Regions identified in smaller SOM arrays

In addition to the 4×6 node SOM array chosen to upscale the cloud data, SOMs with other dimensions (different degrees of generalizations) can provide additional insight. Figure 5.4a – d displays a selection of geographic plots of the grouping of gridcells as determined by different size SOMs, all these SOMs happen to be smaller than the 4×6 node, however larger SOMs were also created. The orientation by the SOM of up-scaled regions across the node array can be flipped depending on the training of the SOM, which in the mapping scheme used changes the colours and number assigned to the cells. This is illustrated by comparing two of the size SOMs: in the 2×4 SOM (5.4a) the region associated with the far southwest is found in the bottom left corner node (node 4) while in the 3×4 SOM (5.4b) the region is found in the top left node (node 1). The different SOM sizes still capture the regional climate, merely generalising to a greater or lesser degree which indicates that the method is robust (as found by Crane and Hewitson, 2003). It is interesting to see that the larger SOM arrays identify more linear structures in some groups, indicative of the SOM disaggregating some of the larger groups identified in the smaller SOM into boundary zones as discussed earlier.

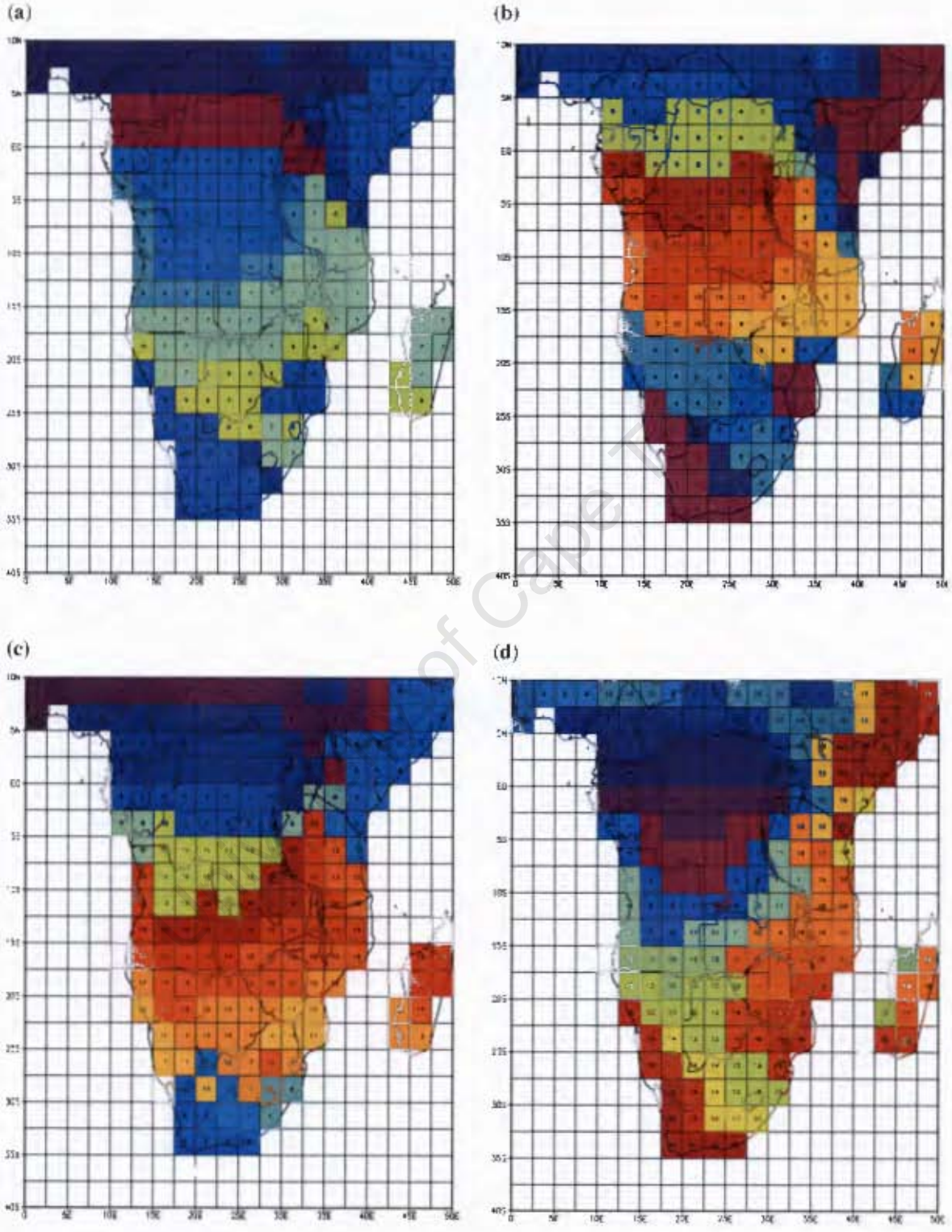

Figure 5. 1 **Results of the (a) 2×4 SOM, (b) 3×4 SOM, (c) 3×5 SOM and (d) 4×5 SOM regionalisation. The number and colour shows the SOM node to which each gridcell maps, however the numbers are not consistent across different size SOMs.**

5.2.4. Summary of Cloud Regions over Southern and Central Africa

The results from the different SOMs provide information on the broad regionality of cloud cover over the southern and central African region, but at different levels of generalisation. A comparison between these SOMs (Figure 5.4a-d) and the seasonal mean cloud amounts (Figure 4.1 in the previous chapter), show that the majority of the divisions follow the seasonal distribution of high-level cloud amount. This is especially true over the tropical regions, where the regional divisions are orientated with latitude (especially in the more detailed SOMs). The more southern regions appear to be more strongly controlled by the distribution of HLCA during DJF. It is hard to separate out the influence of high- and mid-level cloud since they show relatively similar spatial organisations.

The seasonal variations of mean low-level cloud, excluding those due to the obscuration effect, do not seem to have had a strong influence on determining the regions. The east coast, which shows significant LLCA, and very strong diurnal variations (Figure 4.3), is not grouped together into a coherent region. The far southern and western coasts also show significant mean LLCA right throughout the year (Figure 4.1), though less significant diurnal variations (Figure 4.3), and is only separated out from the surrounding regions in the more detailed 4×5 node array (Figure 5.4d).

These results provide some justification for continuing to separate the diurnal variation of cloud amount according to seasons. It also suggests that the regional divisions are more appropriate for determining the variations of high-level cloud, but may be less appropriate divisions for low-level cloud.

5.3. Regional Cloud Diurnal Cycle

Now returning to the results obtained by the 4×6 node array. The seasonal average diurnal variation for each vertical cloud level is averaged for each node (region) and displayed as line graphs. This allows the amplitude and phase of the diurnal variations, as well as the rate of cloud development and decay and any sub-diurnal variations to be exposed.

The results are presented as an array of plots, where each plot corresponds to a SOM node representing a geographic region. The layout of the plots mimics the relative location of the nodes in the SOM array, with most different regions positioned at opposite corners of the array. The diurnal variations for each of the three cloud levels, and that of total cloud amount, are displayed as line graphs for DJF (Figure 5.5a), MAM (Figure 5.5b), JJA (Figure 5.5c) and SON (Figure 5.5d).

This section does not aim to provide a full description of all the results; instead it gives a brief description of the spatial variations found during the austral summer season since the HLCA is most extensive during this season, before focussing on the results from some key regions and discussing the important or interesting variations found within one or more of the cloud levels.

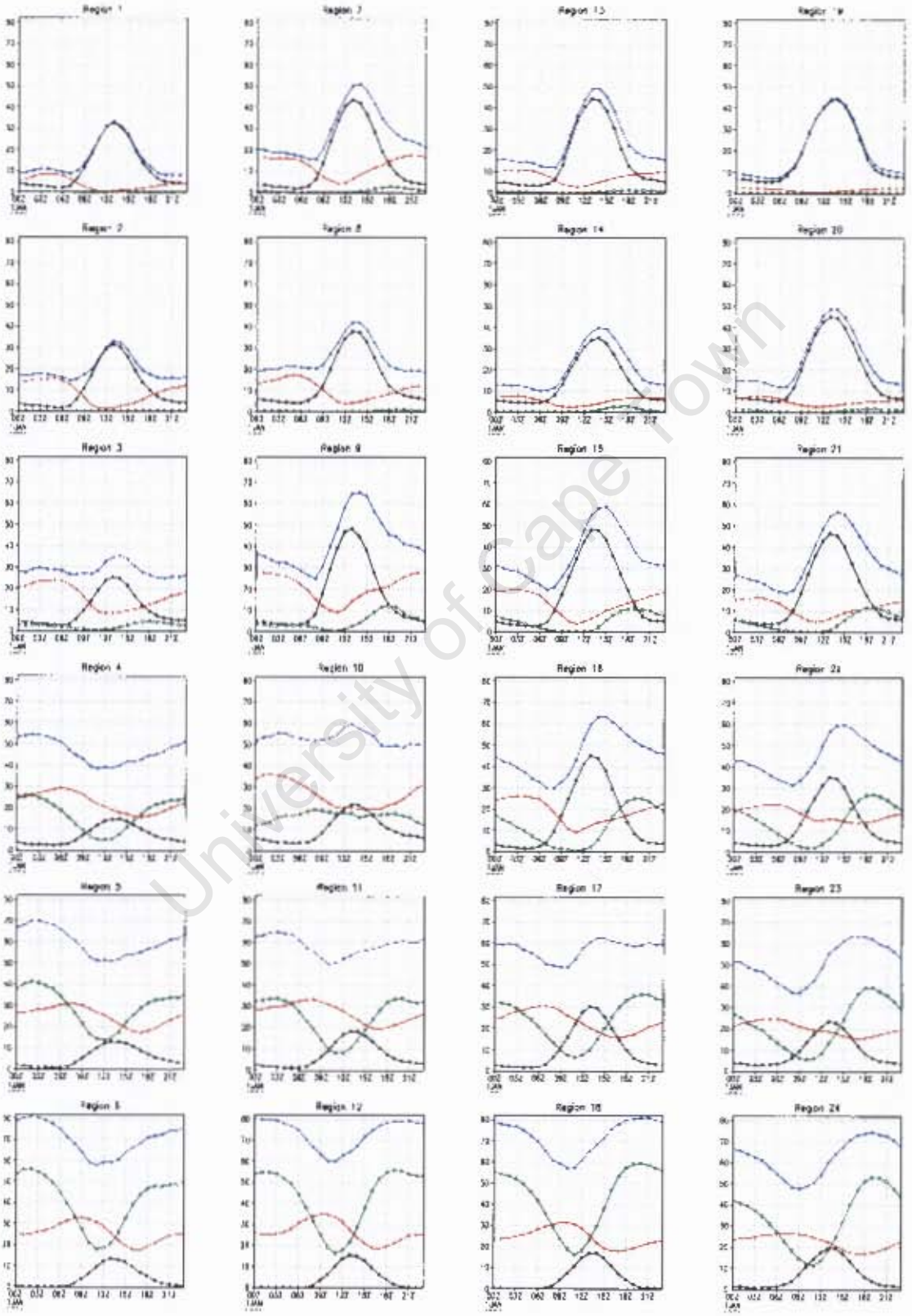

Figure 5.5a Regional average diurnal variation for the DJF season. LLCA - black, MLCA - red, HLCA - green and Total Cloud amount – blue.

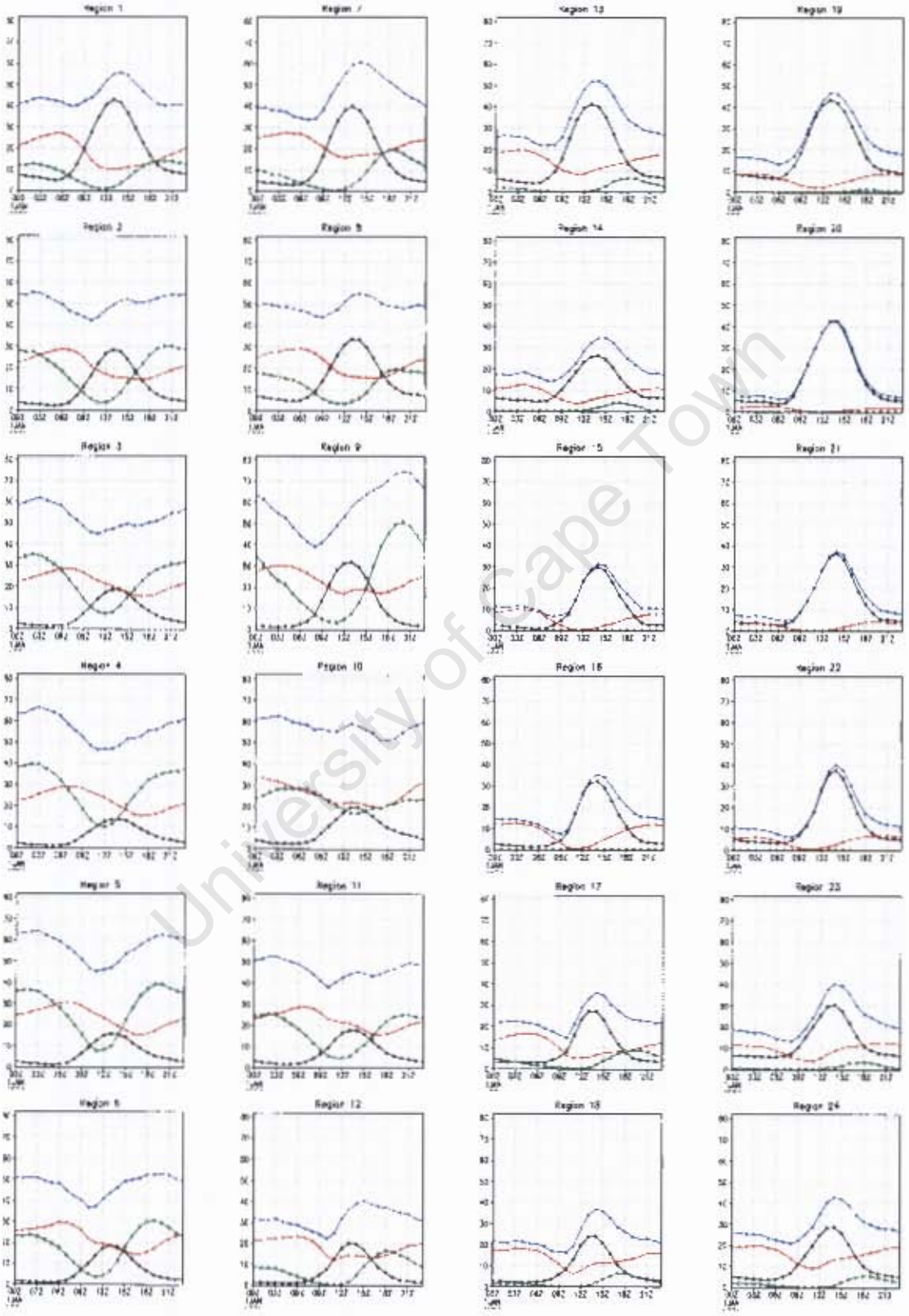

Figure 5.5b Regional average diurnal variation for the MAM season. LLCA - black, MLCA - red, HLCA - green and Total Cloud amount - blue.

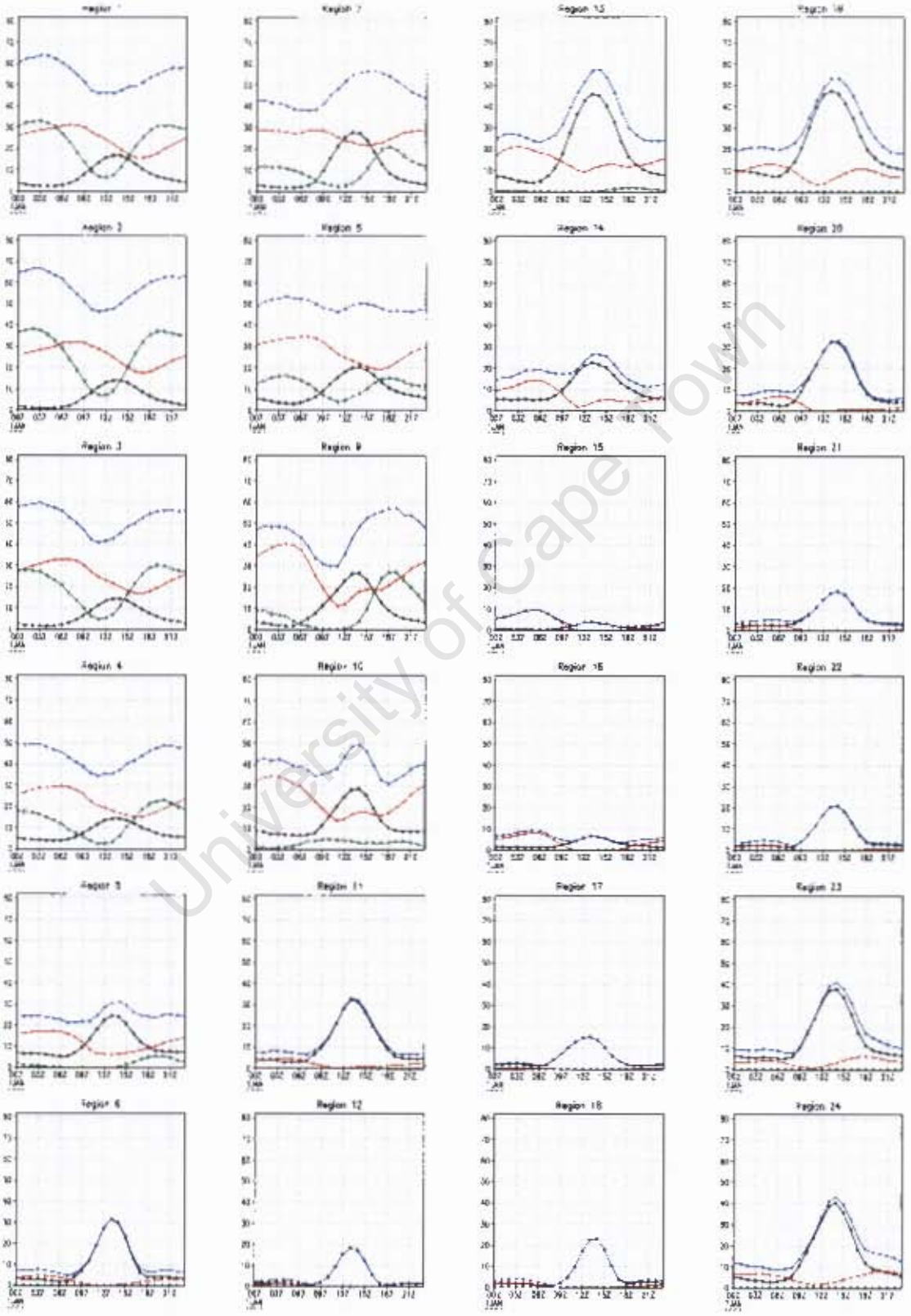

Figure 5.5c Regional average diurnal variation for the JJA season. LLCA - black, MLCA - red, HLCA - green and Total Cloud amount - blue.

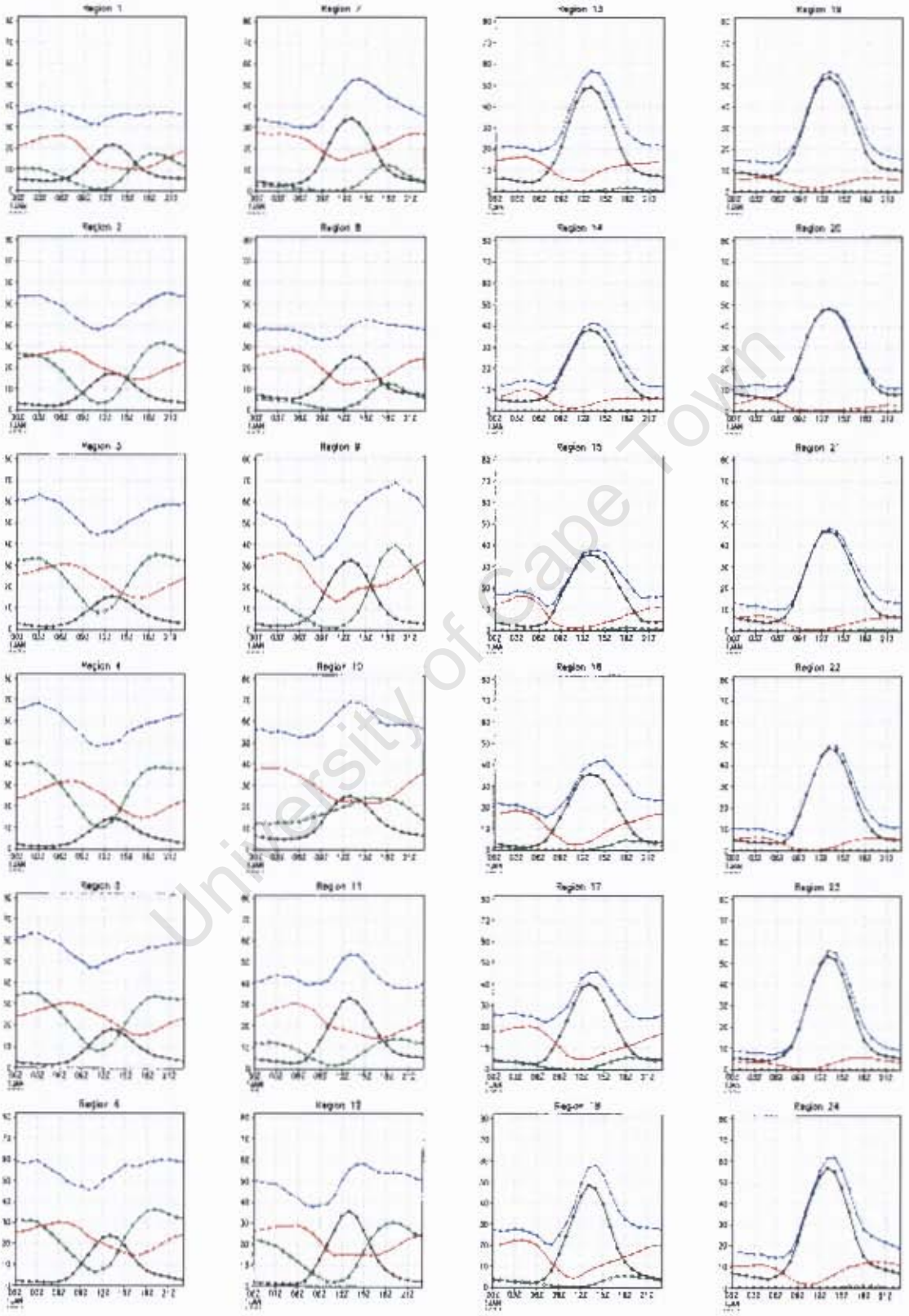

Figure 5.5d Regional average diurnal variation for the SON season. LLCA - black, MLCA - red, HLCA - green and Total Cloud amount - blue.

Figure 5.5a displays an array of regional plots showing the diurnal variations for high-level cloud amount (green), mid-level cloud amount (red), low-level cloud amount (black and total cloud amount (blue). The largest diurnal variations of HLCA are found in the regions along the bottom of the array (Region 6, 12, 18 and 24, refer back to Figure 5.2 for the geographic location of these regions) and the magnitude and amplitude of the cycle decreases as one moves upwards through the array. No HLCA is found in the regions displayed in the top row of the array, which correspond to the regions in the far north and extreme southwest. Within the lower half of the array, the timing of maximum HLCA is found in the early evening for regions on the right side of the array corresponding to regions around Malawi, while it is found to increase through the night and reach a maximum extent around 0300 LST for the more tropical regions on the left side of the array.

Mid-level cloud is more extensive over the regions in the bottom half of the array. The diurnal amplitude is also larger over these regions, with maximum cloud cover occurring between 0600 – 0900 LST and minimum coverage at 1700 LST. The regions represented in the top half of the array have maximum mid-level cloudiness slightly earlier than those in the bottom half of the array, and minimum cloudiness much earlier in the day at 1100 LST.

The largest diurnal variation of low-level cloud amount during DJF is found in Region 19 displayed in the top right corner of the array (geographically located in the far southwest and northeast of the study area). The diurnal amplitude decreases away from this region, with the smallest diurnal variations being found over Region 6 which is shown in the bottom left corner of the array (southern part of the Congo Basin).

Total cloud amount shows similar or smaller diurnal variations to that of the individual cloud levels. This is largely due to HLCA and LLCA being out of phase with one another. The phase of the diurnal variation for regions found in the top half of the array

generally follow that of LLCA, while the regions in the bottom half of the array track that of HLCA.

Figure 5.5b – 5.5d display the regional plots for the other three seasons. Differences in the broad distribution of cloud cover at the three vertical levels are clearly apparent. This is especially clear for HLCA which is only found in the regions represented in the left half of the array in MAM (Figure 5.5b) and SON (Figure 5.5d) and exhibited in even fewer regions in JJA (Figure 5.5c).

The next section explores the diurnal variations over a select number of regions. It does not attempt to fully describe all the detail, but rather uses these regions to describe the observed diurnal variability in terms of convective cloud development and decay.

5.3.1. Malawian Region (Region 24)

The region centred over Malawi is discussed since it was located in one of the corner nodes in the SOM array and therefore represents one of the most extreme cloud climatologies of the study area. Region 24 is shaped like a reversed 'L' extending down through central Tanzania, over Malawi and westward across central Zambia. The northern parts of Madagascar form a satellite sub-area of Region 24. This region is associated with the southern extension of the ITCZ during austral summer. It shows a very strong diurnal variation of HLCA during this season, but almost no HLCA during the rest of the year, therefore this discussion is restricted to the DJF season.

Figure 5.5a (bottom right plot) shows that low-level cloud (black) begins to form from dawn (0600 LST) over this region. The heating of the surface produces upward fluxes of both sensible and latent energy. This instigates convective overturning which deepens the boundary layer through the morning. LLCA increases through the morning as the number of clouds, and the size of the clouds increase. Maximum LLCA is achieved just after mid-day (1300 LST) after which it decreases through the afternoon. This is due to the

reduction of surface convection; both because the angle of insolation becomes more oblique, and also because the surface becomes shaded by increasing cloudiness. The warming of the lower-troposphere decreases the relative humidity and causes the cloud base to rise. By evening there is little low-level cloud and the small amount that is present, decreases slowly through the night hours. LLCA is probably severely underestimated over this deep convective location due to the significant amount of mid- and high-level clouds. Therefore little can be said about the amplitude of the diurnal variations.

Mean high-level cloudiness is relatively large over this region during austral summer. Cloudiness increases from 1100 LST as convection begins to penetrate the planetary boundary layer. Deep moist convective overturning reach as high as the tropopause and are associated with the rapid increase observed in HLCA. These clouds peak in the evening between 1800 - 2100 LST which is approximately two hours after maximum convection (Dai et al., 2007) since the convective clouds decay into anvil clouds which have a larger lateral extent. The diurnal amplitude of these clouds may also be influenced by the topography of the region. The differential heating due to variations in elevation, as well as across land-lake boundaries, can result in mesoscale circulations intensifying convective uplift and cloud development (Yang and Smith, 2006). High-level cloud cover decreases during the night through four main factors: precipitation, large-scale subsidence, radiative cooling, and turbulent mixing with air outside the cloud. The rate of decay accelerates after 0300 LST which corresponds to the time at which relative upper-tropospheric humidity begins to fall (Chung et al., 2007). The clouds are then eroded away from the upper levels as the sun warms their upper surface through the morning hours.

Mean mid-level cloud amount is quite large over this region, but the diurnal variation is small. This suggests that either cloud at this level is not strongly influenced by the diurnal cycle, or that the ISCCP data are not able to observe the true amplitude of this cloud. Maximum MLCA is found between 0600 - 0900 LST, which is the time at which HLCA.

Coverage is a minimum. Minimum mid-level cloud cover is found around 1800 LST which corresponds to the hour at which HLCA peaks.

These seasonal average diurnal variations remove most of the shorter-temporal variability or 'weather noise' leaving the variability which is most closely associated with convective cloudiness. Therefore it can reasonably be assumed that mid-level clouds are convective in origin and that they increase from just before noon in association with deep convective cloudiness. This increase in MLCA is assumed to be undetected by satellites in this location of intense deep convection. The maximum MLCA in the early morning is the result of the sedimentation and general sinking of higher level clouds to this level, but also due to the increased detection of mid-level cloud as the higher level cloud is eroded away. The deep convective cloud cover takes many hours to decay down to the mid-level, and these clouds may themselves take time to dissipate through the morning and afternoon of the day following deep convection. Deep convective clouds have been found to show 'diurnal dancing' (Chen and Houze, 1997), which is a mechanism whereby convection is not found in the same location on consecutive days. Instead, convection is found to alternate between neighbouring areas. This suggests that over this region, the initial growth of MLCA associated deep convective clouds was severely obscured by HLCA and is therefore absent in this data. It also suggests that deep convective clouds may require more than the 24-hours to develop and decay and that ISCCP data only observed the decaying stage of MLCA.

This result highlights a significant limitation of the ISCCP data. Where the changing obscuration of this cloud level by higher clouds introduces an artificial factor into the diurnal variation. This emphasises the value of using other types of data to validate results and also shows the value in interpreting the results in terms of the physical processes which drive them.

5.3.2. East Coast (Region 23)

Region 23 is found to the southeast of Region 24. It runs down the coast of southern Tanzania and northern Mozambique and inland along the Zambezi River. The SOM suggested that this region is representative of locations where there are strong local controls on the cloud (see Section 5.2.2 above). Region 23 was shown to correspond to the areas which displayed a late afternoon peak in mid-level cloud amount in chapter 4.

This region is dominated by low-level cloud, with the diurnal amplitudes being largest in JJA (Figure 5.5c) and SON (Figure 5.5d). During these two seasons there is no high-level cloud and only a small diurnal variation of mid-level cloud amount. During SON, the low-level winds are light easterlies which may be a factor in explaining the lack of higher level clouds. MLCA increases during the afternoon and reaches a maximum around 1600 LST. It decreases through the first half of the night remaining relatively constant between midnight and 0400 LST before decreasing again though the morning. The magnitude and amplitude of this mid-level cloud is not large, but its diurnal variation follows the general pattern of HLCA in other locations. Much of this region is found along the coast of southern Tanzania and northern Mozambique. This region may experience land-sea breeze circulations, which focus the energy of afternoon heating into convective storms located along a narrow mesoscale frontal line (Yang and Smith, 2006). This could help explain the increased amplitude of LLCA found in a band just inland from the coast. These regions of lifting tend to be too shallow (there is less surface heating during these winter months) to initiate deep convection and therefore only barely penetrate the mid-level.

5.3.3. Congo Basin (Region 4)

This section focuses on results for Region 4 which is located directly over the equator in the Congo Basin. As stated above and in the previous chapter, the Congo Basin area

shows strong diurnal variations of high-level cloudiness through all or most of the year but especially during MAM and SON when the sun is most directly overhead.

Figure 5.5b and 5.5d display the results for MAM and SON respectively; HLCA is shown in green, MLCA in red, LLCA in black and total observed Cloud Amount (TCA) in blue. Region 4 is found in the first column, fourth plot down. The diurnal variations over Region 4 during MAM and SON are almost identical for each of the three cloud levels and will therefore be discussed together.

Low-level clouds show relatively small diurnal variations probably due to the severe obscuration by higher-level clouds. Mean high-level cloud amount is relatively large over this location and displays strong diurnal fluctuations, though smaller than that found over more southern regions during DJF. Minimum HLCA is found at mid-day with cloud cover increasing rapidly through the afternoon due to the intense convection found in this tropical location. Unlike Region 24 which reached maximum HLCA in the early evening this region shows cloudiness remaining high through the night and reaching a maximum in the early morning. During MAM, HLCA expansion slows after 1800 LST but still increases gradually right up until 0200 LST. During SON HLCA decreases very slightly from 1900 to 2300 LST before increasing again to reach a maximum at 0200 LST. The first peak in cloudiness is associated with the deep convection, while the second peak corresponds to the timing of maximum upper-tropospheric relative humidity (Chung et al., 2007).

Moisture is transported upward by convection. Much of it returns to the surface through precipitation, but a small proportion dissipates into the upper-troposphere from decaying convective clouds. In this deep convective location, a relatively high proportion of moisture remains in the upper-troposphere, this reduces the rate of cloud decay, but cannot explain the redevelopment of clouds in the early morning. The only widely accepted explanation for this feature is that the enhanced nighttime cloud-top radiative cooling thermally destabilises the upper atmosphere, allowing condensation to occur and resulting in a small redevelopment of high-clouds (Dai, 2001; Yang and Smith, 2007).

Region 4 shows clear diurnal cycles of total observed cloud amount (blue) during MAM and SON. The diurnal variations of high- and low-level clouds are almost perfectly out of phase, which dampens the diurnal amplitude of total cloudiness. Total cloudiness is lowest just before noon. It increases steadily through the afternoon and night, reaching a maximum at 0300 LST before decreasing more rapidly through the morning. The phase of total cloudiness would result in a net warming effect on the radiative balance at the top of the atmosphere, since maximum cloudiness is found at night and for high-level clouds.

5.3.4. Lake Victoria (Region 10)

The results for the Lake Victoria area (Region 10) need to be explained in light of the complicated local climates found in this relatively small area. Lake Victoria is situated within a shallow continental depression bounded by steep mountains along the two arms of the East Africa Rift Valley system. The region experiences complex interactions between large-scale monsoonal circulation and regional topographic and lake-induced circulations. The Indian Ocean monsoon flow transports maritime moisture into the interior of East Africa. The humid Congo air mass also boosts convection and overall rainfall amount over the western and north-western parts of the lake. However a quasi-permanent trough lingers over the Lake throughout much of the year (Ba and Nicholson, 1998).

Strong convergence over the western sector of the lake occurs at night and over land areas east of the lake during the day. These circulation patterns were found to be linked to the interactions between diurnal land-lake breeze circulations, mountain-valley slope winds and the prevailing synoptic circulations (Anyah et al., 2006).

The two gridcells making up Region 10 each cover half of Lake Victoria and half of the mountainous region to the east or west of the lake. The regionalization procedure determined that the cloud climatology of the region is quite similar to that of the more tropical regions (shown by the short distance between the two nodes in Figure 5.1a) and

some of the smaller SOM arrays included these locations with the more tropical locations. However, the average error with which the two gridcells mapped to this archetype is large and suggests that their cloud variations do not often match the archetype precisely.

Figure 5.5a-d show that Region 10 has small diurnal variations of HLCA and significant phase scatter between seasons. The previous chapter noted that these two grid cells display quite clear differences in their diurnal phase of HLCA (Figure 4.3 and 4.4), both when compared with each other and with the grid cells around them. Therefore the group is disbanded and the diurnal cycle is determined for each gridcell separately.

Figure 5.6 verifies that both halves of the region experience large diurnal variations of HLCA but that the variations are out of phase with one another. The western half has a single peak during the day, while the eastern half displays a peak both in the evening and again in the morning.

This section focuses exclusively on the diurnal variations of high-level cloud amount, specifically for MAM and SON seasons, since these seasons show the most diverse phase variations and the lower levels show less variability. Cloud cover over the western half of the region displays a phase shift, with the peak in cloudiness occurring in the morning during MAM and in the afternoon during SON. Minimum cloud cover occurs around 2000 LST during MAM while during SON it remains low from midnight until 0900 LST. Over the eastern half of the region, maximum HLCA is maintained through the night during MAM and minimum cloudiness occurs at 1400 LST, while two distinct peaks are found during SON; the first at 1100 LST, and the second at 2000 LST. Minimum cloud cover is reached during the first few hours of the day and a secondary minimum is found around 1400 LST.

The study of Ba and Nicholson (1998) can be used to better understand these results. Their study used the ISCCP-B2 monthly data for the period April 1983 through December 1990. The 30-km resolution of the data allowed more local differences to be

determined. Figure 5.7 displays the phase of the diurnal variation of cold cloud occurrences during (a) April and (b) November found in that study.

For April, the central part of the lake has maximum cloudiness in the early morning due to the confluence of the land breezes. The north-western lake and shore areas reach maximum cloudiness around 0900 LST and the phase shifts later to just after noon towards the west. These finer-scale results help to explain the broad peak around noon found in this study's MAM results. It shows that it is due to the averaging of locations which have different phases. During November, the central part of the lake does not show the early morning maximum, suggesting weaker land breezes. The whole of the western half of the lake has maximum high-level cloudiness in the late morning. The same progression from late morning to early afternoon is found west of the Lake. The merging of these less varied results produces the narrower peak in HLCA during the SON season.

The diurnal cycle for HLCA for the eastern half of the lake is also clearly the result of averaging very different diurnal variations. During MAM, the first peak is the result of the early morning maximum found over the lake shown in figure 5.7a. The second peak is due to the early evening maximum found over the high-lying area to the east of the lake. During SON, the early morning maximum over the lake is replaced by generally late-morning maximums, shifting the first peak in the SON high-level cloudiness to later in the morning. The secondary peak, due to the intense surface heating, remains in the early evening.

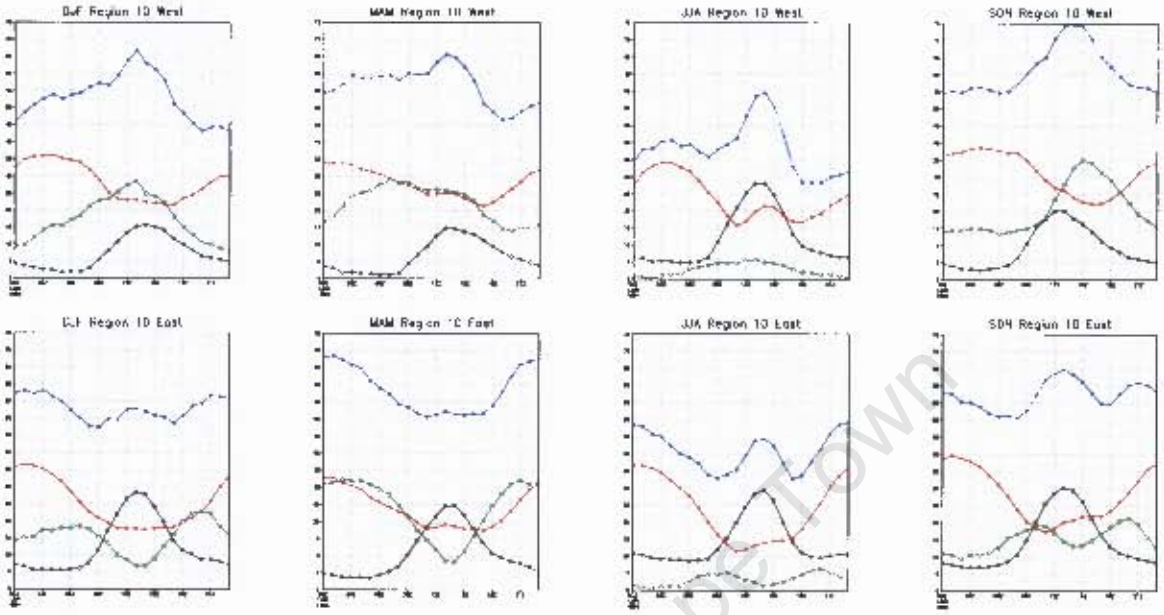

Figure 5.6 Seasonal diurnal variation for HLCA (green), MLCA (red), LLCA (black) and Total Cloud Amount (blue) for (a) western half of Region 10 (top row) and (b) eastern half of Region 10 (bottom row) .

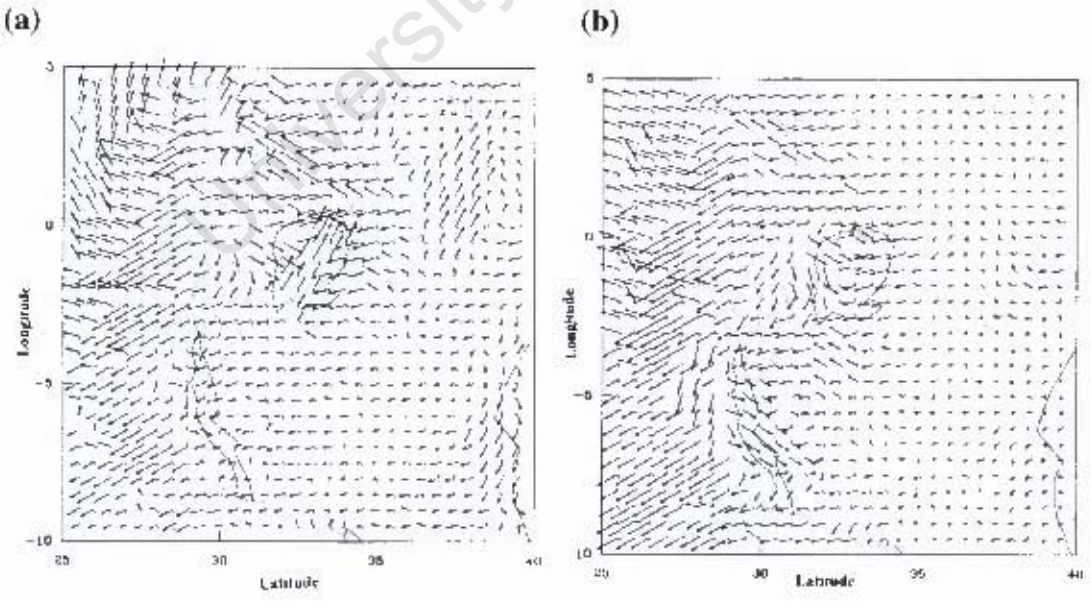

Figure 5.7 Phase of diurnal variations of cold cloud occurrences for (a) April 1983-90, (b) November 1983-90 (From Ba and Nicholson, 1998). The tail of the arrow points to the LST of the minimum occurrence, and the head points to the LST of the maximum. The head (tail) of arrow pointing northward indicates that the maximum (minimum) of occurrence of cold clouds occurs at local midnight.

5.3.5. Kalahari (Region 15)

The results from the up-scaling analysis suggests that the cloud climatology of this region fitted in the middle of the continuum of cloud climatologies since it was located near the centre of the array. The Sammon map shows that it represents a state quite different to the nodes around it, but that the gridcells mapping to node 15 all show a relatively constant pattern (see figure 5.1 and 5.3).

High-level cloud amount (green) is only found during DJF (Figure 5.5a). Mid-level cloud amount (red) is found during all seasons, though the variation is largest in DJF and smallest in JJA (Figure 5.5a-d). Low-level cloudiness (black) is interesting in that it shows very strong diurnal variation, except during JJA where it shows almost none.

During JJA (Figure 5.5c) MLCA is small, but it shows the largest diurnal variation of any of the levels. It also shows a slightly larger variation than over the surrounding regions (For example Region 17, 20 and 21). This result does not make sense in terms of convective cloud cover, since the thermal heating of the surface is small during this season. One explanation could be that this is thin cirrus associated with the equator-ward edge of mid-latitude cyclones which ISCCP misclassified as thick midlevel cloud.

5.3.6. Southwest Coast (Region 19)

Locations mapping to Node 19 are located both in the far southwest and northeast of the study area. These two locations may show similar diurnal variations of cloud cover. However, the mechanisms behind their cloud climatologies are different. This section focuses on the southern part.

The southern part of Region 19 is located along the southern and western coast of South Africa which has a Mediterranean Climate. Figure 5.8 shows that no diurnal variation of high-level cloud is found over this region during any season. The diurnal cycle of mid-

level cloud amount is largest during JJA, MLCA is not present during the afternoon, only begins to increase from 1900 LST reaching a maximum around 0600 LST and decreasing to almost zero by 1100 LST.

During SON the base-level from which low-level cloud increases is higher than for any other location or season. The peak is also broader extending later into the afternoon. This suggests that low-level clouds over this location show a larger variation in phase. The southwestestern parts of South Africa are influenced by mid-latitude cyclones. These systems are less diurnally regulated than tropical systems which may help to explain the large base value. The diurnal variation superimposed on this may be due to the orographic uplift along the coast.

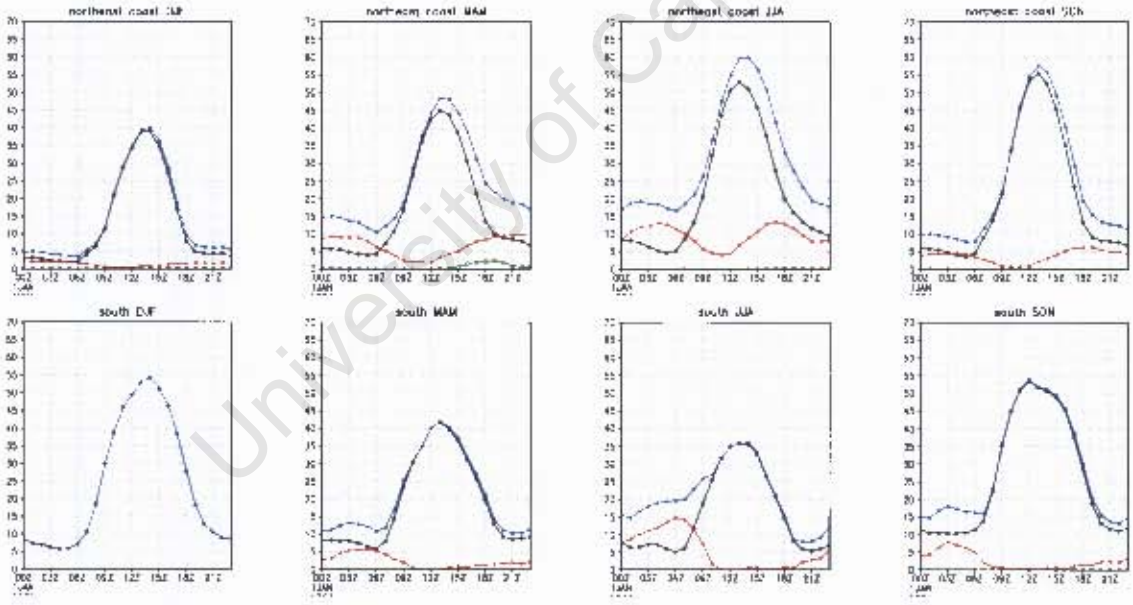

Figure 5.8 Seasonal diurnal variation for HLCA (green), MLCA (red), LLCA (black) and Total Cloud Amount (blue) for the north-eastern (top row) and southern (bottom row) parts of Region 19.

5.4. Summary

This chapter discussed the results from a regionalisation process using Self-Organising Maps. Stable results were produced across the range of different sized maps only the level of generalisation changed. The 4×6 array was chosen to regionalise the study area since it distinguished between broad climatic regions, but also identified some boundary or distinctive climate regions.

The regional analysis showed that clouds displayed broad spatial differences in the diurnal variations of cloud amount. These differences were most clearly associated with the seasonal migration of the Inter-tropical Convergence Zone. The regional analysis showed that the diurnal variations were not strictly sinusoidal in nature and therefore the diurnal amplitude and phase is not sufficient to resolve these variations in the diurnal cycle of cloud.

Low-level clouds showed very symmetrical rate of growth and decay centred on 1300 LST and were almost completely absent through the night. This feature was consistent over the whole of the study area and only the amplitude of the diurnal variation differed. These differences in diurnal amplitude may be real feature, but also may be partly the result of obscuration by higher-level clouds, especially in deep convective regions.

Chapter 4 found a clear difference in the timing of maximum high-level cloud over the deep convective regions versus the less convective locations. This section showed that this was due to the maintenance of HLCA through the night and a secondary reinvigoration of high-level clouds in the early morning.

The regional analysis found that mid-level clouds in this dataset showed smaller diurnal variations than the other two levels, and that they mostly represented decaying convective systems. MLCA began to increase at the same time as high-level clouds (1100 LST) but reached their maximum a few hours after HLCA. The timing of maximum and minimum MLCA over the deep convective locations is later than that found over other areas. The

extensive coverage and longevity of high-level clouds in these deep convective locations resulted in mid-level clouds only becoming viewable (from the satellite's vantage point) slightly later the morning following the deep convection, and mid-level clouds continued to decline right through the afternoon.

CHAPTER 6

DISCUSSION & CONCLUSION

6.1. Overview and Summary

This thesis stands against a background of key knowledge gaps, namely the limited availability of the climatology of spatial and temporal distribution of clouds, and recognises the important need for this in order to further our understanding of the regional climate dynamics, and to support the development of climate models.

The aim of this study was to improve the current understanding of the cloud diurnal variability over southern and central African. The diurnal cycle is a key periodicity found in a number of important climatic variables, including clouds and plays a crucial role in governing the radiation budget. Clouds have a long history of being studied; however, the information on the distribution of clouds over the southern and central African region is poor, especially at the diurnal frequency. This study sought to fill some of these gaps by evaluating a base-line climatology of low-level, mid-level and high-level cloud cover over this region.

Sections 6.1 and 6.2 and their associated sub-sections provide an overview of the main findings of the thesis. Section 6.3 discusses some constraints and caveats and Section 6.4 provides recommendations for further extensions of this work.

6.1.1. Spatial Organisation

6.1.1.1. Seasonal Variations of Cloud Cover

The cloud data for the southern and central African region showed clear spatial organisation. Much of this variation is due to large-scale regional differences in climate processes and spatial positioning of synoptic circulation features, but topographic features are also notably important. The distribution of mid- and high-level cloud amount displayed strong annual variations following the seasonal migration of the ITCZ over the African continent. Maximum HLCA was found during DJF and was often associated with orographic features along the southern and eastern boundary of the Congo Basin. No HLCA, or very little, was found outside the deep convective regions with large parts of southern and east Africa only experiencing high-level cloudiness during the austral summer season.

Mid-level cloudiness showed similar spatial organization to that of HLCA. However, the coverage was more extensive and uniform than that of HLCA and the maximum values were smaller and less clearly associated with topographic features.

The seasonal variation of low-level cloud was less apparent, with much of the observed variability being due to changes in the obscuring higher level clouds. Even so, a small seasonal maximum was discernable over the eastern parts of the continent and Madagascar during SON and over the western half of southern Africa during DJF.

6.1.1.2. Diurnal Variation of Cloud Amount

The diurnal variation of high-level cloud cover was shown to be closely related to the mean high-level cloud amount and to total tropospheric specific humidity. Large diurnal amplitudes appeared to be associated with orographic features which is in support of

previous higher-resolution studies. HLCA increased rapidly from just before midday and reached maximum extent in the early evening. In most locations HLCA was found to decrease through the night. However, the rate of decay appeared to be inversely related to total tropospheric specific humidity. High-level cloud decreased more gradually in regions of high humidity, and the regions associated with maximum humidity actually experienced an increase in HLCA in the early hours of the morning. These locations were clearly identified in Chapter 4 by the timing of maximum cloudiness (Figure 4.4). All regions experienced a rapid decrease in HLCA through the morning hours.

Mean mid-level cloud amount was shown to be high in most regions, though the diurnal variation about the mean was relatively small. The phase of the diurnal variation displayed some clear regional differences. In locations not dominated by high-level cloud, the results showed minimum MLCA just before noon, cloudiness increased right through the afternoon and night, peaking in the early hours of the morning before decreasing quite rapidly through the morning hours. A clear exception occurred along the east coast where the diurnal amplitude of MLCA was small. In these locations the maximum cloudiness was found to occur in a broad peak from afternoon to evening. This suggests that over these coastal locations, convection is relatively shallow and clouds only extend as high as the mid-troposphere. Regions which displayed large values of HLCA displayed maximum MLCA occurring slightly later in the morning than over other locations and cloudiness decaying right through to the next evening. The extensive coverage and longevity of high-level clouds in these deep convective locations may have resulted in mid-level clouds only becoming viewable (from the satellite's vantage point) slightly later the morning following the deep convection, with mid-level clouds continuing to decline right through the afternoon.

Low-level cloud displayed very strong diurnal variations, which closely tracked the diurnal variation of incoming solar radiation. Very little low-level cloud occurred just before daybreak. Cloudiness increased rapidly through the morning to reach a peak just after midday. LLCA then decreased swiftly through the afternoon and continued to decrease after dusk, though at a very gradual rate. The amplitude of LLCA diurnal cycle

was severely reduced over locations of extensive higher level cloud, but was found to be large over the eastern countries (e.g. northern Mozambique, central Tanzania and the border between Ethiopia and Somalia), especially during SON and over the far southern countries during DJF (e.g. Namibia and Botswana). Interestingly, neither the diurnal amplitude, nor the obscuration effect by high- or mid-level cloud appeared to affect the phase of the diurnal cycle. It remained consistent over the whole study area and showed little seasonal variation. This confirms how strongly the diurnal variation of low-level cloud is controlled by the daily cycle of insolation.

6.2. Regionalisation of the Study Area

A regionalisation of the southern and central African study area was used to determine regions of homogenous cloud variance for further examination. The grid-cell cloud data could then be averaged over each of these regions to better assess the characteristic diurnal variations of clouds at each of the three vertical levels. Furthermore, the regionalisation methodology also provided valuable insights into broad contiguous regions of cloudiness, irrespective of periodicity in the diurnal cycle.

The regions appeared to be most strongly defined by the seasonal variations of mean high-level cloud cover. This was illustrated by the zonal orientation of the regions over the deep tropical areas. The seasonal migration of HLCA therefore appears to be a greater influence on these regions than necessarily the diurnal (also a function of seasonality) or orographic influences. For example, even though maximum diurnal variations of HLCA were consistently found west of the Ruwenzori Mountains, these gridcells were not grouped together. The large 4×6 array SOM did identify the Lake Victoria Region as a wholly separate region. However, the two gridcells making up this region experienced quite different diurnal variations of HLCA which suggests that the two gridcells have very distinct climatologies and that neither of them are well represented by the archetype.

Regions over the southern and eastern parts of the continent appeared to have been determined solely by the distribution of HLCA during DJF. This was clearly the case for the regions extending from southern DRC to the coast of northern Mozambique, and for the band of increased cloudiness linking northern Namibia to the east coast of South Africa. The large values of low-level cloud along the eastern coast during SON did not seem to have had much of an influence in determining the regions. LLCA only appeared to have been responsible for determining the regions in the far south-west and north-east. The grouping together of these two very remote geographic areas could not be explained in terms of similar synoptic circulations. However, both regions were dominated by low-level cloud of similar diurnal amplitudes. These locations only had small amounts of mid-level cloud and almost no high-level cloud cover to disassociate themselves from each other.

To summarise, the geographic arrangement of these regions appears to be most strongly influenced by the seasonal variation of high-level cloud over the deep convective locations, while the southern and eastern parts were most strongly controlled by the mean distribution of high-level cloud during austral summer. Only the far southwestern and northeastern regions appear to have been significantly determined by the diurnal cycle of low-level cloud. This implies that the strongest variations over the study areas were found in the seasonal cycle of high-level cloud, which in turn validates using seasonal means for regionalisation, but also implies that regions most appropriate for identifying homogenous regions of HLCA may not be as well suited for the two lower cloud levels.

6.2.1. Regional Average Cloud Diurnal Cycle

The results from the second data analysis (Chapter 5) provided information on the rate of growth and decay of clouds, along with the amplitude and phase of the diurnal variation. This information was useful in understanding the life-cycle of continental convective clouds. The regional variations in the cloud diurnal cycle could then be interpreted in relation to other diurnally forced meteorological variables and continental or synoptic

scale forcing mechanisms. These results were investigated within a number of specific regions to illustrate the general life-cycle of convective cloud cover and to highlight some interesting regional differences.

6.2.1.1. Life-Cycle of Low-level Clouds

The life-cycle of low-level cloud followed the diurnal variation of shortwave radiation (with a small time lag) and was very consistent across all of the regions. The only differences were found in the diurnal amplitude and the base-level from which cloud increased. It was not possible to determine the severity of the obscuration effect of higher-level clouds on the diurnal amplitude of LLCA. However, from the results of comparative studies it can be assumed to be significant (Weare, 2000).

6.2.1.2. Life-Cycle of Deep Convective Clouds

The life-cycles of high- and mid-level cloud are discussed together since over the majority of the study area (and for the main summer season), except for the far southwest, these clouds are likely to be convective in origin. The late afternoon to early evening maximum in high cloud cover is generally accepted to be due to the land surface heating cycle. Our results showed that high-level clouds began to develop from 1100 LST, which would generally correspond to the time at which dry convective overturning penetrates the planetary boundary layer. Cloud cover then rapidly increases through the afternoon as deep moist convective overturning reaches to the upper troposphere.

Deep convection can be initiated by diurnally regulated thermally driven mesoscale circulations. These circulations fall into two main categories. The first is due to differential heating of the atmosphere by the surface, while the second is forced by variations in elevation (Yang and Smith, 2006). The complicated diurnal variations of high-level cloud amount over the Lake Victoria Region are likely driven by both of these mechanisms. The differential heating of the lake and coastal areas produces sea and land

breezes, while the differential heating of the elevated terrain both to the east and west of the lake results in diurnally modulated slope breezes. Unfortunately, the coarse spatial resolution of the ISCCP data were not able to resolve these mesoscale variations, though they have been in a higher resolution study by Ba and Nicholson (1998) who used the 30-km pixel-resolution radiances from ISCCP.

Another example of high diurnal variations due to these mechanisms was found over the southern and eastern boundary of the Congo Basin, which was the location of maximum mean high-level cloud amount and significant diurnal amplitudes during the DJF season. The steep topography, especially at the eastern boundary, can induce thermally-driven slope flow, enhancing the development of convective clouds over, and down wind off these mountains. The thermal and latent energy differences between the tropical rainforest vegetation of the Congo Basin and the deciduous and African Montane vegetation to the east and south respectively could also contribute to diurnally-induced circulations over these boundaries.

Our study reported maximum high-level cloudiness being reached between 1800 – 2100 LST over much of the study area, but was not able to distinguish between deep convective cloud and cirrus anvil cloud. However, the work by Chung et al.(2007) showed that over continental Africa (30° N - 30° S, 50° E – 50° W) during January 2005, deep convective clouds reached their maximum around 1700 LST, total high cloud peaked at 1900 LST, and cirrus anvil cloud only reached their maximum coverage around 0200 LST. This implies that once surface convection ceased at nightfall, the deep convective clouds decayed into cirrus anvil clouds. These anvil clouds have larger spatial coverage than deep convective clouds, so our results probably represent a mixture of both deep convective and cirrus anvil clouds.

HLCA showed quite clear regional variations in the rate of decay. These differences did not appear to be strongly linked to the diurnal amplitude of these clouds. Instead they appeared to be more closely associated with the magnitude of total tropospheric humidity. Regions 6 and 24 both showed similar diurnal amplitudes during DJF, but

displayed very different values of cloud during the night. Over the Malawian Region (Region 24), HLCA reached a maximum at 1900 LST and decreased steadily through the night and morning hours. In contrast, the southern boundary of the Congo Basin (Region 6), displayed HLCA increasing relatively slowly from 1800 – 2200 LST, and then more rapidly thereafter, reaching a maximum at 0200 LST. It then decreased through the morning to reach a minimum at 1100 LST.

Conversely, the Congo Basin had higher values of specific humidity and also showed higher proportion of this humidity within the upper-troposphere. One would assume that the upper level humidity was transported to this level through the same convective mechanisms responsible for the high-level cloud, and that the humidity was in fact due to the decay of these clouds. This was supported by Chung et al. (2007) who found that cirrus anvil cloud and upper tropospheric relative humidity both increased after the peak in convection reaching their maximums around 0200 LST. This suggested that deep convective clouds were responsible for these increases, presumably through the spreading of anvil clouds and the decay and evaporation of convective clouds.

Two mechanisms may help to explain the continued increase in HLCA over the Congo Basin. Firstly, the differential heating across the vegetative and topographic boundary can induce down-slope circulations during the night. The surface convergence and latent energy release over the tropical forest may also result in continued convection and cloud development after dark. The high upper-tropospheric humidity reduces the rate of cloud decay through evaporation, but this cannot explain the clear peak in HLCA in the early morning, Another mechanism for this feature may be enhanced nighttime cloud-top cooling (Dai, 2001). This may thermally destabilise the upper atmosphere, resulting in shallow overturning of the cloud. This cooling (in association with the increase in relative upper-tropospheric humidity) would increase nighttime condensation, and could lead to an early morning maximum in upper-level cloud cover. This regeneration of upper-level cloud found has been corroborated by Yang and Smith (2007) who found a secondary early morning maximum for the incidence of drizzle and light rain over tropical Africa. All regions showed HLCA decreasing rapidly through the morning hours as the sun

warmed the cloud-tops and eroded the clouds from above. This warming of the top-layer enhances stability within the cloud and shuts off any further convective overturning.

The diurnal variation of mid-level cloud in this study needs to be interpreted in relation to high-level cloud over most of the region. However, no diurnal variation of HLCA was found over the east coast during SON. This location (represented by Region 23) was dominated by low-level cloud and specific humidity and showed only small diurnal variations of MLCA. The results showed that MLCA increased from 1100 LST and reached a broad maximum in the later afternoon. It decreased slightly through the evening but remained relatively stable through the night before decreasing during the morning to almost zero. This suggests that in this 'coastal' location, sea-breeze type circulation may have resulted in convective uplift in the afternoon, but that this circulation barely penetrates the mid-troposphere and dissipates through the night.

Over the western half of southern Africa, MLCA increased from 1100 LST right through the afternoon and night, reaching a maximum around 0300 LST. Deep convective cloud peaks in the early evening, but mid-level cloud continues to increase as the relatively small deep convective clouds decay into larger anvil clouds. This explains the maximum coverage found in the early morning.

Over more intense convective locations MLCA was found to increase from around 1700 LST, and reach a maximum between 0600 – 0900 LST. It can reasonably be assumed that in reality MLCA increases from just before noon in all convective locations, and that it was undetected by satellites in those locations of intense deep convection. The maximum MLCA in the early morning was the result of both the sinking of higher level clouds to this level during the night, but also due to the increased detection of mid-level clouds as the higher level clouds are eroded. In deep convective locations the convective cloud cover takes many hours to decay down to the mid-level, and these clouds themselves take time to dissipate. This was discernable in the continual decay of MLCA throughout the afternoon. Deep convective clouds have been found to show 'diurnal dancing' (Chen and Houze, 1997), which is a mechanism whereby convection is not found in the same

location on consecutive days. Instead, convection is found to alternate between neighbouring areas. This suggests that the initial growth of MLCA associated with deep convective clouds is severely obscured by HLCA and therefore absent in the dataset used here. It also suggests that deep convective clouds may show a bi-daily variation, and that ISCCP data only observes the decaying stage of MLCA.

6.3. Constraints and Caveats

The aim of this thesis was to provide a 10-year climatology of the seasonally averaged diurnal variation of cloud cover over southern and central Africa, based on coarse resolution ISCCP data. Clouds are extremely complex features displaying variations at many different spatial and temporal scales. It was beyond the scope of this study to provide a comprehensive or definitive review of the finer details for this region's cloud diurnal variations.

The study was also severely limited by the cloud data available over this region. Surface observations of cloud distributions are inadequate. The gridded cloud data obtained from surface observation found on the Climate Atlas of Clouds over Land and Oceans website[6] determined cloud cover statistics for this study areas using between 1 and 10 observations per 2.5° gridcell. Out of all the available satellite-based cloud data, the ISCCP-D1 dataset provided the most appropriate balance between length of record, temporal sampling, spectral sampling and spatial resolution and coverage. Importantly it also provides coherent results during both the day and night hours.

The ISCCP data may have been the most appropriate data source, but there were a number of constraints associated with this type of data. These can broadly be summarised as:

[6] http://www.atmos.washington.edu/~ignatius/CloudMap/

- The spatial resolution of the data – ISCCP-D1 data were provided on a 2.5° latitude-longitude grid. Many cloud processes happen at the finer mesoscale resolution and were therefore not discernable in this data.
- The temporal resolution of the data – The three-hourly temporal resolution of the data were sufficient to resolve the basic diurnal variations, but was not able to identify the subtle mesoscale variations assumed to exist in regions of complicated topography. This study chose to interpolate the data to hourly intervals. This was done to convert the data from being reported at Coordinated Universal Time (UTC) to Local Solar Time (LST). The interpolation did not add information, and therefore the skill-level of the data remained at the three-hourly resolution. The east-to-west variation in the timing of the original data could introduce some subtle errors into the results, which would be most severe at times when cloud amount changes from increasing to decreasing and vice versa. For example, the 1800 UTC reading corresponds to 1900 LST over the western parts of the study areas (before or at sunset), but to 2100 LST over the far eastern parts (after sunset). As no discernable east-west errors or discontinuities were found in the data, it is assumed that this error is small.
- The spectral resolution of the data - The data made use of radiances from a single broad infrared band. This band of frequencies is able to determine the temperature of the cloud top. However, it is not able to distinguish between clouds of different optical thickness and is insensitive to thin cirrus. This is a significant limitation, firstly because the radiative properties of clouds are very strongly influenced by the depth and phase of the cloud and secondly, because cirrus is a common cloud type in this region.
- The viewing angle of the satellite – The satellite sensor is only able to observe the highest cloud level in each atmospheric column. No cloud-overlap assumptions were used in this dataset and so the mid- and low-level results were underreported and had to be interpreted as 'observable' cloud amount.
- Vertical averaging of results – The seven vertical levels were summed to create three broad levels. The choice of levels followed the historically accepted divisions of the atmosphere and has been used by numerous other cloud studies, yet they may not best

capture the observed dynamics across all seasons and locations, especially in regions of shallow convection e.g. the mid-latitude regions.

- Seasonal averaging of results – The study chose to average the result over four broad seasons. These seasonal boundaries have been widely used in the literature yet may blur seasonal boundaries that do not fall neatly into these categories.
- Horizontal movement of convective clouds – Deep convective clouds are advected downwind from their point of origin over time. This study did not attempt to track cloud clusters, instead it focuses on the diurnal variation at each location. This methodology was supported by the results from Hodges and Thorncroft (1997) who found that most mesoscale convective systems over the southern and central African region were nearly circular clusters of convective clouds. These systems usually have lifecycles of around 12 hours, forming in the afternoon and decaying during the night with little down-wind movement.
- The study averaged the data to create 10-year seasonal climatologies of the diurnal cycle of cloud cover. This was done to expose the underlying diurnal variation and smooth variations resulting from day to day weather. However, daily weather is important since it introduces complexity into the day-to-day variations of clouds at any given location.

6.4. Recommendations

This study has successfully produced a base-line climatology of cloud cover over central and southern Africa, as well as investigated the seasonal and diurnal variations of the cloud cover. As a consequence the study has also highlighted a number of possibilities for further study.

One of the most severe limitations found in this study was the coarse spatial resolution of the data. A future study could make use of the data recorded by the Spinning Enhanced Visible and Infrared Images (SEVIRI) instruments on the new geostationary satellites,

Meteosat-8 (launched in 2002) and Meteosat-9 (launched in 2005)[7]. These imagers provide far superior spatial, temporal and spectral resolution. They are also able to distinguish different types of cloud. Only a relatively short record is presently available and the data sizes are very large, but even now the data could be used to perform a short study on the mesoscale variations found over a specific geographic region.

Furthermore this study could prove very useful in testing climate model simulations of the southern and central African region. As discussed earlier climate models sometimes have difficulty in simulating clouds and moisture, especially at a diurnal resolution. The observations presented here could form a baseline against which both global and regional models could be tested. This work has also identified a number of regions which warrant further exploration. For example, the region of enhanced diurnal variability over the southern and eastern boundary of the Congo Basin is a case in point. Climate models, and specifically Regional Climate models, may prove useful in uncovering the physical mechanisms associated with the enhanced amplitude of the diurnal variations of clouds over these areas. An example of this type of study was given by Anyah et al. (2006) who simulated the physical mechanisms associated with climate variability over the Lake Victoria Basin. The study was able to examine the relative influence of different processes on the lake basin climate. Ultimately it will be necessary for climate models to be able to simulate the observed characteristics of cloud that have been presented in this thesis if they are to accurately simulate the surface energy balance and the response of the regional climate to processes such as anthropogenic climate and land-use change.

[7] ESA – Meteosat Second Generation http://www.esa.int/esaMI/MSG/

REFERENCES

Ambroise, C., C. Seze, F. Badran and S. Thiria, 2000: Hierarchical clustering of self-organizing Maps for cloud classification. *Neurocomputing*, **30**, 47-52.

Anyah, R.O., F.H.M. Semazzi, and L. Xie, 2006: Simulated Physical Mechanisms Associated with Climate Variability over Lake Victoria Basin in East Africa. *Mon. Wea. Rev.,* **134**, 3588-3609.

Arnaud, Y., M. Desbois, and J. Maizi 1992: Automatic tracking and characterization of African convective systems on meteosat pictures. *J. Appl. Meteor.,* **31**(5), 443-451.

Ba, M.B. and S.E. Nicholson, 1998: Analysis of convective activity and its relationship to the rainfall over the rift valley lakes of East Africa during 1983-90 using the meteosat infrared channel. *J. Appl. Meteor.*, **37**(10), 1250-1264.

Bergman, J. and M.L. Salby, 1996: Diurnal variations of cloud cover and their relationship to climatological conditions. *J. Climate*, **9**, 2802-2820.

Cairns, B., 1995: Diurnal variations of cloud from ISCCP data. *Atmos. Res.*, **37**, 133-146.

Cavazos, T. 2000: Using Self-Organizing Maps to Investigate Extreme Climate Events: An Application to Wintertime Precipitation in the Balkans. *J. Climate*, **13**, 1718-1732.

Chen, S.S. and R.A. Houze, 1997: Diurnal variation and life-cycle of deep convective systems over the Tropical Pacific warm pool. *Quart. J. Roy. Meteor. Soc.*, **123**(538), 357-388.

Chung, E.S., B.J. Sohn, J. Schmetz, and M. Koenig, 2007: Diurnal Variation of Upper Tropospheric Humidity and its Relations to Convective Activity over Tropical Africa. *Atmos. Chem. and Phys.,* **7**, 2489-2502.

Comer, R.E., A. Slingo, and R.P. Allan, 2007: Observations of the diurnal cycle of outgoing longwave radiation from the Geostationary Earth Radiation Budget instrument. *Geophys. Res. Lett.,* **34**. L02823.

Crain, R.G. and B.C. Hewitson, 2003: Clustering and upscaling of station precipitation records to regional patterns using self-organizing maps (SOMs). *Clim. Res.*, **25**, 95-107.

Dai, A, 2001: Global precipitation and thunderstorm frequencies. Part II: Diurnal Variations. *J. Climate*, **14**, 1112-1128.

Dai, A, and K.E. Trenberth, 2004: The diurnal cycle and its depiction in the Community Climate System Model. *J. Climate*, **17**, 930-951.

Desbois, M., T. Kayiranga and B. Gnamien, 1989: Diurnal cycle of convective cloudiness over tropical Africa observed from Meteosat: Geographic characterization and interannual variations. *Annales Geophysicae*, **7**, 395-404.

Dessler, A.E., S.P. Palm and J.D. Spinhirme, 2006: Tropical cloud-top height distribution revealed by the Ice, Cloud, and Land Elevation Satellite (ICESat)/ Geoscience Laser Altimeter System (GLAS). *J. Geophys. Res.,* **111** (D12), D12215.

Doutriaux-Boucher, M. and G. Sèze, 1998: Significant changes between the ISCCP C and D cloud climatologies. *Geophys. Res. Letts.*, **25**(22), 4193-4196.

Fink, A.H. and A. Reiner, 2003: Spatiotemporal variability of the relation between African Easterly Waves and West African Squall Lines in 1998 and 1999. *J. Geophys. Res.*, **108**(D11), Art. No. 4332.

Futyan, J.M. J.E. Russell and J.E. Harries, 2004: Cloud radiative forcing in Pacific, Africa, and Atlantic tropical convective regions. *J. Climate*, **17**(16), 3192-3202.

Garreaud, R.D. and J. M. Wallace, 1997: The diurnal march of convective cloudiness over the Americas. *Mon. Wea. Rev.*, **125**, 3157-3171.

Gates, W. L., J.S. Boyle, C. Covey, C.G. Dease, C.M. Doutriaux, R.S. Drach, M. Fiorino, P.J. Gleckler, J.J. Hnilo, S.M. Marlais, T.J. Phillips, G.L. Potter, B.D. Santer, K.R. Sperber, K.E. Taylor and D.N Williams, 1999: An overview of the results of the Atmospheric Model Intercomparison Project (AMIP I). *Bull. Amer. Meteor. Soc.*, **80,** 29–56.

Geerts, B. and R. Dejene, 2005: Regional and Diurnal Variability of the Vertical Structure of Precipitation Systems in Africa Based on Spaceborne Radar Data. *J. Climate*, **18**, 893-916.

Grabowski, W.W, P. Bechtold, A. Cheng, R. Forbes, C. Halliwell, M. Khairoutdinov, S. Lang, T. Nasuno, J. Petch, W.-K. Tao, R. Wong, X. Wu and K.-M Xu, 2006: Daytime convective development over land: A model intercomparison based on LBA observations. *Quart. J. Roy. Meteor. Soc.*, **132**, 317-344.

Hahn, C.J. and S.G. Warren, 1999: Extended edited cloud reports from ships and land stations over the globe, 1952-1996. Tech. Rep. NDP-026C, Carbon Dioxide Information Analysis Center, pp 79.

Hewitson, B.C. and R.G. Crane, 2002: Self-Organizing Maps: Applications to Synoptic Climatology. *Clim. Res.*, **22**, 13-26.

Hewitson, B.C. and R.G. Crane, 2006: Consensus between GCM Climate Change Projections with Empirical Downscaling: precipitation downscaling over South Africa. *International Journal of Climatology*, **26** (10), 1315-1337.

Hodges, K.I. and C.D. Thorncroft, 1997: Distribution ad statistics of African mesoscale convective weather systems based on the ISCCP Meteosat imagery. *Mon. Wea. Rev.*, **125**, 2821-2837.

Hong, G. and G. Heygster, 2005: Intercomparison of Deep Convective Cloud Fraction from Passive Infrared and Microwave Radiance Measurements. *IEEE Geoscience and Remote Sensing Lett.,* **2**(1), 18-22.

Hong, G., P. Yang, B-C Gao, B.A. Baum, Y.X Hu, M.D. King and S. Platnick, 2007: High Cloud Properties from Three Years of MODIS Terra and Aqua Collection-4 Data over the Tropics. *J. Appl. Meteor. Clim.,* **46**, 1840-1856.

Houze, R.A. Jr., 1993: *Cloud Dynamics*. Academic Press. San Diego. 359 pp.

Hudson, D.A., 1998: Antarctic Sea ice extent, southern hemisphere circulation and South African rainfall. PhD thesis, University of Cape Town

Hudson, D.A. and R.G. Jones, 2002: Simulations of Present-Day and Future Climate over Southern Africa Using HadAM3H. *Hadley Centre technical note,* **38**, 1-37.

Kalnay, E., M.Kanamitsu, R. Kister, W. Collins, D. Deaven, L Gandin, M Iredell, S. Saha, G. White, J. Woollen, Y. Zhu, M. Chelliah, W. Ebisuzaki, W. Higgins, J. Janowiak, K.C. Mo, C. Ropelewski, J. Wang, A. Leetmaa, R. Reynolds, R. Jenne, D. Joseph, 1996: The NCEP/NCAR 40-Year Reanalysis Project. *Bull. Am. Meteor. Soc.*, **77** (3), 437-471.

Kistler, R., E. Kalnay, W. Collins, S. Saha, G. White, J. Woollen, M. Chelliah, W. Ebisuzuki, M Kanamitsu, V. Kousky, H. van den Dool, R. Jenne, M Michael, 2001: The NECP-NCAR 50-Year Reanalysis Monthly Means CD-ROM and Documentation. *Bull. Am. Meteor. Soc.*, **82**(2), 247-268.

Kohonen, T., 1990: The self-organizing map, *Proc. IEEE*, **78**, 1464-1480.

Kohonen, T, 1995: Self-organizing maps. Springer-Verlag, Heidelberg.

Kohonen, T., J. Hynninen, J. Kangas, and J. Laaksonen. 1996: SOM_PAK: The Self-Organizing Map Program Package. Technical Report A31, Helsinki University of Technology, Laboratory of Computer and Information Science, FIN-02150 Espoo, Finland.

Kondragunta, C.R. and A. Gruber, 1994: Diurnal variation of the ISCCP cloudiness. *Geophys. Res. Lett.*, **21**(18), 2015-2018.

Kondragunta, C.R. and A. Gruber, 1996: Seasonal and annual variability of the diurnal cycle of clouds. *J. Geophys. Res.*, **101**(D10), 21377-21390.

Kruger, A.C., 2007: Trends in cloud cover from 1960 to 2005 over South Africa. *Water SA.* **33**, 603-608.

Laing, A.G. and J.M. Fritsch. 1993: Mesoscale Convective Complexes in Africa. *Mon. Wea. Rev.,* **121**, 2254-2263.

Laing, A.G., J.M. Fritsch, and A.J. Negri, 1999: Contribution of mesoscale convective complexes to rainfall in Sahelian Africa: estimates from geostationary infrared and passive microwave data. *J. Appl. Meteor.*, **38**(7) 957-964.

Liao, X., W. Rossow, and D. Rind, 1995: Comparison between SAGE II and ISCCP high-level clouds. Part 1: Global and zonal mean cloud amounts. *J. Geophys. Res.,* **100**, 1121-1135.

Lin, X., D.A. Randall and L.D Fowler, 2000: Diurnal Variability of the Hydrologic Cycle and Radiative Fluxes: Comparison between Observed and a GCM. *J. Climate*. **13**, 4159-4179.

Lindesay, J.1998: Present Climates of Southern Africa. In: *Climates of the Southern Continents Present, Past and Future.* [Hobs, J.E., J.A. Lindesay, and H.A. Bridgman (eds.)]. John Wiley and Sons, West Sussex, UK, pp 5-62.

Luo, Z. and W.B. Rossow, 2004: Characterizing tropical cirrus life cycle, evolution, and interaction with upper-tropospheric water vapor using lagrangian trajectory analysis of satellite observations. *J. Climate*, **17**, 4541-4563.

Machado, L.A.T., M. Desbois, and J.-Ph. Duvel, 1992: Structural Characteristics of Deep Convective Systems over Tropical Africa and the Atlantic Ocean. *Mon. Wea. Rev.,* **120**, 392-406.

Machado, L.A.T., J.-Ph. Duvel, and M. Desbois, 1993: Diurnal –Variations and Modulation by Easterly Waves of the Size Distribution of Convective Cloud Clusters over Wes Africa and the Atlantic-Ocean. *Mon. Wea. Rev.,* **121**, 37-49.

Machado, L.A.T., H Laurent, and A.A Lima, 2002: Diurnal march of convection observed during TRMM-WETAMC/LBA. *J. Geophys. Res.*, **107** (20) doi:10.1029/2001JD000338.

Main, J.P.L., 1997: Seasonality of circulation in South Africa using the Kohonen Self Organising Map. MSc thesis, University of Cape Town.

Martin, W.D., and A.J. Schreiner, 1981: Characteristics of West Africa and east Atlantic cloud clusters: A survey from GATE. *Mon. Wea. Rev.*. **109**, 1671-1688.

Mathon, V. and H. Laurent, 2001: Life Cycle of Sahelian Mesoscale Convective Cloud Systems. *Quart. J. Roy. Meteor. Soc.*. **127**, 377-406.

McIlveen, R.F. 1992: *Fundamental of Weather and Climate*. Chapman and Hall, London pp. 497

Meinke, I, 2006: A comparison of simulated clouds to ISCCP data. *Mon. Wea. Rev.*, **134**, 1669-1681.

Meisner, B.N. and P.A. Arkin, 1987: Spatial and Annual Variations in the Diurnal Cycle of Large-Scale Tropical Convective Cloudiness and Precipitation. *Mon. Wea. Rev.*, **115**, 2009-2032.

Nicholson, S. E., 1996: A review of climate dynamics and climate variability in eastern Africa. The Limnology, Climatology and Paleoclimatology of the East African Lakes, T. C. Johnson and E. Odada, Eds., Gordon and Breach, 25–56

Peixoto, J.P. and A.H. Oort, 1992: *Physics of Climate*. American Institute of Physics, New York, pp 520.

Rickenbach, T.M., 2004: Nocturnal cloud systems and the diurnal variation of clouds and rainfall in southwestern Amazonia. *Mon. Wea. Rev.*, **132**, 1201-1219.

Rind, D., and X. Liao, 1997: Statrospheric Aerosol and Gas Experiment II CD-ROM Atlas of Global Monthly Aerosols, Ozone, NO2, Water, Vapor, and Relative Humidity (1985-1993). *Earth Interactions*, **1**(2), 1-15.

Rossow, W.B., and L.C. Garder, 1993b: Validation of ISCCP cloud detection. *J. Climate*, **6**, 2370-2393.

Rossow, W.B. and R.A. Schiffer, 1991: ISCCP cloud data products. *Bull. Am. Meteor. Soc.*, **80**, 2261-2257.

Rossow, W.B. and R.A. Schiffer, 1999: Advances in understanding clouds from ISCCP. *Bull. Am. Meteor. Soc.*, **72**(1), 2-20.

Rossow, W.B., L.C. Garder, P.J. Lu, and A.W. Walker, 1991: International satellite cloud climatology product (ISCCP), documentation of cloud data. WMO/TD-737, World Climate Research Programme (ICSU and WMO), Geneva, Switzerland, 76 pp. plus 3 appendixes.

Rossow, W.B., A.W. Walker and L.C. Garder, 1993: Comparison of ISCCP and Other Cloud Amounts. *J. Climate*, **6**, 394-2418.

Rossow, W.B., C.L Brest, and M.D. Roiter, 1996a: International satellite cloud climatology project (ISCCP) update of radiance calibrations. WMO/TD-No 736. World Meteorological Organization, 79 pp. http://isccp.giss.nasa.gov/docs/documents.html

Rossow, W.B., A Walker, and D.E Beuschel, and M.D. Roiter, 1996b: International satellite cloud climatology project (ISCCP) documentation of new cloud datasets. WMO/TD-No 737. World Meteorological Organization, pp 115 pp. http://isccp.giss.nasa.gov/docs/documents.html

Rossow, W.B., A Walker, and M. Roiter, 1996c (revision): International satellite cloud climatology project (ISCCP) description of reduced resolution radiance data. WMO/TD-No 58. World Meteorological Organization, 163 pp. http://isccp.giss.nasa.gov/docs/documents.html

Rossow, W.B., Y. Zhang and J. Wang, 2005: A statistical model of cloud vertical structure based on reconciling cloud layer amounts inferred from satellites and radiosonde humidity profiles. *J. Climate*, **18**, 3587-3605.

Slingo, A., 2001: Sensitivity of the Earth's radiation budget to changes in low clouds. *Nature*, **343**, 49-51.

Slingo A, K.I Hodges and G.J. Robinson, 2004: Simulation of the diurnal cycle in a climate model and its evaluation using data from Meteosat 7. *Quart. J. Meteor. Soc.*, **130,** 1449-1467.

Soden, B. J., 2000: The diurnal cycle of convection, clouds, and water vapor in the tropical upper troposphere. *Geophys. Res. Lett.*, **27**(15), 2173-2176.

Stephens, G.L., 2005: Cloud feedbacks in the climate system: a critical review. *J. Climate*, **18**, 237-273.

Stubenrauch, C.J., A. Chendin, G. Radel, N.A. Scott, and S. Serrar. 2006: Cloud Properties and their seasonal and diurnal variability from TOVS Path-B. *J. Climate.* **19**, 5531-5553.

Tadross, M.A., C.D. Jack, B.C. Hewitson, 2005: On RCM-based projections of change in southern African summer climate. *Geophys. Res. Lett.*, **28,** 95-107.

Tian, B., B.J. Soden, and X. Wu, 2004: Diurnal cycle of convection, clouds and water vapor in the tropical upper troposphere: Satellites versus a general circulation model, *J. Geophys. Res.*, **109**, D10101, doi: 10.1029/2003JD004117.

Tyson, P.D. and R.A Preston-Whyte, 2000: *The Weather and Climate of Southern Africa* (second edition). Oxford University Press, Cape Town, pp 396.

Wang, J., W.B. Rossow and Y. Zhang, 2000: Cloud vertical structure and its variations from a 20-yr global rawinsonde dataset. *J. Climate*, **13**, 3041-3056.

Warren, S.G, C.J. Hahn, R.M. Chervin, and R.L. Jenne, 1986: Global distribution of total cloud cover and cloud type amount over land. NCAR Tech. Note NCAR/TN-273+STR, 29 pp. and 200 maps.

Warren, S.G, C.J. Hahn, J. London, R.M. Chervin, and R.L. Jenne, 1988: Global distribution of total cloud cover and cloud type amount over ocean. NCAR Tech. Note NCAR/TN-317+STR, 42 pp. and 170 maps.

Warren, S.G., R.M Eastman and C.J Hahn, 2007: A survey of changes in cloud cover and cloud types over land from surface observations, 1971-1996. *J. Climate*. **20**, 717-738.

Weare, B.C., 2000: Near-Global Observations of Low Clouds. *J. Climate*. **13**, 1255-1268.

Wielicki, B.A. R.D. Cess, M.D. King, 1995: Mission to Plantet Earth – Role of Clouds and Radation in Climate. *Bull. Am. Meteor. Soc.*, **76**, 2125-2153.

Wylie, D.P. and H.M. Woolf, 2002: The Diurnal Cycle of Upper-Tropospheric Clouds Measured by GOES-VAS and the ISCCP. *Mon. Wea. Rev.*, **130**, 171-179.

Yang, G. and J. Slingo, 2001: The diurnal cycle in the tropics. *Mon. Wea. Rev.*, **120**, 784-801.

Yang, S. and E.A. Smith, 2006: Mechanisms for Diurnal Variability of Global Tropical Rainfall Observed from TRMM. *J. Climate*, **19**, 5190-5226.

APPENDIX A

Glossary of Acronyms & Abbreviation

AMPI	Atmospheric Model Inter-comparison Project
DJF	December – February
CLAUS	Cloud Archive User Service
EECRA	Extended Edited Cloud Report Archive
EOF	Empirical Orthogonal Function
GCM	General Circulation Model
GLAS	Geoscience Laser Altimeter System
GOES	Geostationary Operational Environmental Satellite
IR	Infrared
ISCCP	International Satellite Cloud Climatology Project
ISCCP-C2	ISCCP-C2 Data (monthly, 280 km equal-area grid, older version)
ISCCP-DX	ISCCP-DX Data (3-hourly, 30 km sampled image pixels)
ISCCP-D1	ISCCP-D1 Data (3-hourly, 280 km equal-area grid, new version)
ISCCP-D2	ISCCP-D2 Data (Monthly, 280 km equal-area grid, new version)
ITCZ	Inter-tropical Convergence Zone
JJA	June - August
LTS	Local Solar Time
LW	Long Wave
MAM	March – May
MCC	Mesoscale Convective Complexes
MCS	Mesoscale Convective Systems
NCAR	National Center for Atmospheric Research, USA
NCEP	National Centers for Environmental Prediction, USA
SON	September – November
SOM	Self-Organising Map
SW	Short Wave

TIROS	Television Infrared Observation Satellite
TOA	Top of the Atmosphere
TOVS	TIROS Observational Vertical Sounder
TRMM	Tropical Rainfall Measuring Mission
TTT	Tropical Temperate Trough
UTC	Coordinated Universal Standard
UTH	Upper Tropospheric Humidity
ZAB	Zaire Air Boundary

APPENDIX B

Principal Mechanisms Responsible for Diurnal Cloud Variability

Yang and Smith (2006) provided a summary of the foremost published mechanisms explaining the diurnal variability of precipitation. Further details can be found in their appendix and references found within. These are the same mechanisms responsible for the diurnal variation of convective cloud cover, therefore a very brief description of the mechanisms applicable to our continental study area is provided below:

- **Boundary Layer Wind Oscillation**: A mesoscale phenomenon where the solar-forced cycle of the convective boundary layer enhances local convergence, mechanical convection, Richardson number instability, and the strength of the near-surface winds. This in turn leads to a maximum in cloud cover and precipitation.

- **Land Surface Heating – Static Destabilisation**: Static destabilisation occurs as a result of both surface sensible and latent heating. The dry and moist static stability variations associated with these diurnal thermal and moisture oscillations lead to the growth of dry and moist convective overturning. Deep moist convective overturning will only take place once dry convective overturning penetrates the boundary layer. Once initiated, this deep moist convective overturning can reach as high as the tropopause.

- **Land Surface Heating – Differential Heating**: Differential solar heating across land-sea boundaries produces daytime circulations with surface flow from the ocean to the land. The land experiences low-level convergence, convective lifting and the formation of clouds and precipitation along a narrow mesoscale front. At night, the circulation is reversed and the land experiences subsidence and suppression of clouds.

- **Large Scale Continent Heating – Propagating**: Continental heating is diurnally regulated by insolation. This diurnal variation in heating modulates the large-scale upper-tropospheric divergence in which a positive divergence anomaly is linked to maximum cloudiness. This divergence anomaly aloft can propagate and produce a downstream phase shift in the cloudiness maximum

- **Nighttime Cloud Radiative Cooling**: Enhanced nighttime cloud-top radiative cooling thermally destabilises the upper atmosphere. This increases nighttime relative humidity and condensation and leads to a late-night maximum in cloudiness, drizzle and light precipitation.

APPENDIX C

Mean & Standard Deviations

The mean and standard deviations determined for each of the cloud levels required for determining the covariance matrix.

High-Level Cloud Amount:	mean = 13.367361	stdev = 13.675054
Mid-Level Cloud Amount:	mean = 7.277088	stdev = 9.890146
Low-Level Cloud Amount:	mean = 3.208896	stdev = 7.066066